UNIVERSIDADE FEDERAL DE SANTA CATARINA
CENTRO TECNOLÓGICO
PROGRAMA DE PÓS-GRADUAÇÃO EM ENGENHARIA DE ALIMENTOS

Diego Alex Mayer

Phase equilibrium data and thermodynamic modeling of ε-caprolactone and poly(ε-caprolactone) systems at high pressures

FLORIANÓPOLIS
2020

Diego Alex Mayer

Phase equilibrium data and thermodynamic modeling of ε-caprolactone and poly(ε-caprolactone) systems at high pressures

Tese submetida ao Programa de Pós-Graduação em Engenharia de Alimentos da Universidade Federal de Santa Catarina para a obtenção do título de doutor em Engenharia de Alimentos.
Orientador: Prof. Dr. José Vladimir de Oliveira
Coorientadora: Prof. Dra. Débora de Oliveira
Coorientadora: Prof. Dra. Selene Maria de Arruda Guelli Ulson de Souza

Florianópolis
2020

Ficha de identificação da obra elaborada pelo autor, através do Programa de Geração Automática da Biblioteca Universitária da UFSC.

Mayer, Diego Alex
Phase equilibrium data and thermodynamic modeling of ε-caprolactone and poly(ε-caprolactone) systems at high pressures / Diego Alex Mayer ; orientador, José Vladimir de Oliveira, coorientadora, Débora de Oliveira, coorientadora, Selene Maria de Arruda Guelli Ulson de Souza, 2020.
132 p.

Tese (doutorado) - Universidade Federal de Santa Catarina, Centro Tecnológico, Programa de Pós-Graduação em Engenharia de Alimentos, Florianópolis, 2020.

Inclui referências.

1. Engenharia de Alimentos. 2. Lactonas. 3. Fluido Supercritico. 4. Equilibrio de Fases. I. de Oliveira, José Vladimir . II. de Oliveira, Débora. III. de Souza, Selene Maria de Arruda Guelli Ulson IV. Universidade Federal de Santa Catarina. Programa de Pós-Graduação em Engenharia de Alimentos. V. Titulo.

Diego Alex Mayer

Phase equilibrium data and thermodynamic modeling of ε-caprolactone and poly(ε-caprolactone) systems at high pressures

O presente trabalho em nível de doutorado foi avaliado e aprovado por banca examinadora composta pelos seguintes membros:

Prof.(o) Papa Matar Ndiaye, Dr(o).
Universidade Federal do Rio de Janeiro

Prof.(a) Claudia Sayer, Dr(a).
Universidade Federal de Santa Catarina

Prof.(o) Marcelo Lanza, Dr(o).
Universidade Federal de Santa Catarina

Certificamos que esta é a **versão original e final** do trabalho de conclusão que foi julgado adequado para obtenção do título de doutor em Engenharia de Alimentos.

Documento assinado digitalmente
Sandra Regina Salvador Ferreira
Data: 27/02/2020 15:06:11-0300
CPF: 564.352.079-68

Prof. Dra. Sandra Regina Salvador Ferreira
Coordenadora do Programa

Documento assinado digitalmente
Jose Vladimir de Oliveira
Data: 27/02/2020 14:17:04-0300
CPF: 025.858.198-09

Prof. Dr. José Vladimir de Oliveira
Orientador

Florianópolis, 17 de fevereiro de 2020.

Este trabalho é dedicado à minha amada esposa, aos meus queridos pais, a Ginger Alda e o Linus Pauling.

AGRADECIMENTOS

À UFSC – Universidade Federal de Santa Catarina e ao PPGEAL - Programa de Pós-graduação em Engenharia de Alimentos, pelo suporte físico e acadêmico para a realização deste trabalho.

Ao LATESC e ao LABSIN/LABMASSA, pela infraestrutura laboratorial disponibilizada para a realização deste trabalho.

Ao meu orientador professor José Vladimir de Oliveira e às minhas coorientadoras professoras Débora de Oliveira e Selene Maria de Arruda Guelli Ulson de Souza, pela confiança em mim depositada, pelas sugestões e conhecimentos compartilhados para a realização deste trabalho.

Ao professor Papa Matar Ndiaye, pela colaboração na realização deste trabalho.

Ao meu grande amigo e colega Evertan Antonio Rebelatto, pela colaboração na realização deste trabalho.

Ao bolsista de Iniciação Científica, Davi Gustavo Lisboa Girardi, pela amizade e colaboração na realização deste trabalho.

A todos colegas do grupo LATESC e do LABSIN/LABMASSA, pela amizade e por sempre se mostrarem prestativos.

E a todos que, embora não citados, de alguma forma contribuíram para a concretização deste trabalho.

“Education is the most powerful weapon we can use to change the world”.

(Nelson Mandela, 2003)

RESUMO

Poli(ε-caprolactona) é um polímero biodegradável, bioabsorvível e biocompatível usado em uma ampla variedade de aplicações biomédicas, farmacêuticas e alimentícias de alto valor agregado. Esse polímero pode ser produzido pela técnica de polimerização por abertura de anel da ε-caprolactona via catálise enzimática em sistema de alta pressão. Porém, ainda é necessária uma melhor compreensão do comportamento termodinâmico das espécies químicas envolvidas durante esse processo de polimerização a alta pressão. Neste contexto, o objetivo deste trabalho foi estudar o comportamento de fases do sistema ternário [dióxido de carbono + diclorometano + ε-caprolactona] e a influência da massa molar da poli(ε-caprolactona) e da quantidade de água inicialmente presente na ε-caprolactona no sistema quaternário [dióxido de carbono + diclorometano + ε-caprolactona + poli(ε-caprolactona)] em alta pressão através de dados experimentais de equilíbrio de fases e modelagem termodinâmica desses sistemas. Todos os experimentos de equilíbrio de fases foram conduzidos em uma célula de volume variável pelo método estático-sintético, numa faixa de temperatura de 323,15 a 353,15 K. No sistema ternário observou-se transições de fases do tipo líquido-vapor (ponto-bolha), líquido-líquido e líquido-líquido-vapor e uma pressão de transição máxima de 25,8 MPa. No sistema quaternário somente transições do tipo líquido-vapor (ponto-bolha) foram observadas. Nesse sistema foi também observado que diferentes massas molares de poli(ε-caprolactona) não alteraram significativamente a pressão de transição do sistema, porém foi observado que com o aumento da quantidade de água inicialmente presente na ε-caprolactona maiores são as pressões necessárias para solubilizar o sistema. Em todos os sistemas estudados foi observado o comportamento LCST (*Lower Critical Solution Temperature*), onde com o aumento da temperatura é necessária uma maior pressão para solubilizar o sistema em uma única fase. Em relação à modelagem termodinâmica foi observada que a equação de estado de Peng-Robinson promoveu um bom ajuste aos dados experimentais do sistema ternário e a equação de estado PC-SAFT promoveu uma boa representação dos dados experimentais do sistema quaternário onde havia a presença de polímero. Os dados apresentados neste trabalho são inéditos e relevantes para o desenvolvimento e otimização da síntese da poli(ε-caprolactona) em meio supercrítico, servindo de base para a determinação das melhores condições experimentais, otimização de processos e modelagem cinética.

Palavras-chave: Lactonas. Fluido Supercrítico. Equilíbrio de Fases.

RESUMO EXPANDIDO

Introdução

Poli(ε-caprolactona) é um polímero biodegradável, bioabsorvível e biocompatível usado em uma ampla variedade de aplicações biomédicas, farmacêuticas e alimentícias de alto valor agregado. Esse polímero pode ser produzido pela técnica de polimerização por abertura de anel da ε-caprolactona via catálise enzimática em sistema de alta pressão. Porém, ainda é necessária uma melhor compreensão do comportamento termodinâmico das espécies químicas envolvidas durante esse processo de polimerização a alta pressão. Até o momento são escassos os trabalhos na literatura sobre o equilíbrio de fases envolvendo sistemas contendo ε-caprolactona e poli(ε-caprolactona). Só existem trabalhos avaliando o comportamento de fases dos sistemas binários [dióxido de carbono + ε-caprolactona] e [dióxido de carbono + poli(ε-caprolactona)] e sistemas ternários [dióxido de carbono + diclorometano + poli(ε-caprolactona)] e [dióxido de carbono + clorofórmio + poli(ε-caprolactona)]. Contudo não existem estudos que avaliam o comportamento de fases do sistema ternário [dióxido de carbono + diclorometano + ε-caprolactona] e do sistema quaternário [dióxido de carbono + diclorometano + ε-caprolactona + poli(ε-caprolactona)].

Objetivos

O objetivo deste trabalho é estudar o comportamento de fases do sistema ternário [dióxido de carbono + diclorometano + ε-caprolactona] e a influência da massa molar da poli(ε-caprolactona) e da quantidade de água inicialmente presente na ε-caprolactona no sistema quaternário [dióxido de carbono + diclorometano + ε-caprolactona + poli(ε-caprolactona)] em alta pressão através de dados experimentais de equilíbrio de fases e modelagem termodinâmica desses sistemas.

Metodologia

O dióxido de carbono foi adquirido da White Martins S.A. (Brasil), diclorometano, ε-caprolactona, poli(ε-caprolactona) ($\overline{M}_n$ (10.000 g.mol^{-1}) e dispersão 1.4) e poli(ε-caprolactona) ($\overline{M}_n$ (80.000 g.mol^{-1}) e dispersão < 2.0) foram adquiridos Sigma-Aldrich (Estados Unidos). A ε-caprolactona foi seca por dois diferentes métodos: (1) 60ºC e 0,01 MP por 72 horas em estufa a vácuo; (2) 100ºC e 0,01 MP por 48 horas em estufa a vácuo. A quantidade de água foi determinada pelo método de titulação Karl Fischer (HI-904 - HANNA®) e os demais reagentes foram usados sem purificação. As medidas experimentais de equilíbrio de fases a altas pressões realizadas neste trabalho foram conduzidas em uma célula de volume variável com visualização, baseada no método estático sintético, numa faixa de temperatura de 50 a 80ºC. No método estático sintético é necessário conhecer a composição global. Assim, diferentes massas de diclorometano, ε-caprolactona e poli(ε-caprolactona) foram pesadas em uma balança analítica (Shimadzu, Modelo AY220 com precisão de 0,0001 g) e inseridas rapidamente na célula de equilíbrio junto com uma barra magnética. Após a inserção de todos os componentes, a célula de equilíbrio foi rapidamente fechada e conectada ao sistema de alta pressão. Posteriormente, um volume conhecido de dióxido de carbono foi adicionado à célula de equilíbrio por uma bomba de seringa (Isco, Modelo 260D), que estava mantida a 10,0 MPa e 7ºC. Durante a adição de dióxido de carbono, nenhuma pressão foi aplicada no sistema de equilíbrio para permitir que o experimento iniciasse com a célula de equilíbrio em seu volume máximo de 27 cm^3. Após a adição completa de dióxido de carbono, a agitação da solução e o aquecimento do sistema

foram iniciados. A partir do momento em que a temperatura de 50ºC foi atingida, a pressão do sistema foi gradualmente aumentada até uma única fase. Após a estabilização da pressão e temperatura, as medidas do equilíbrio de fases (ponto de bolha) foram iniciadas pela redução da pressão (0,15-0,3 $MPa.min^{-1}$) até o aparecimento de uma segunda fase. Este procedimento foi repetido pelo menos três vezes para avaliar a reprodutibilidade da metodologia experimental.

Resultados e Discussão

No sistema ternário [dióxido de carbono + diclorometano + ε-caprolactona] na faixa de temperatura entre 50 a 80ºC observou-se transições de fases do tipo equilíbrio líquido-vapor (ponto-bolha), equilíbrio líquido-líquido e equilíbrio líquido-líquido-vapor e pressão de transição entre 5,1 - 25,8 MPa. No sistema quaternário na faixa de temperatura entre 50 a 80ºC somente transições do tipo equilíbrio líquido-vapor (ponto-bolha) foram observadas e pressão de transição entre 6.4 – 16.5 MPa. No sistema quaternário foi observado que diferentes massas molares de poli(ε-caprolactona) não alteraram significativamente a pressão de transição do sistema, porém foi observado que com o aumento da quantidade de água inicialmente presente na ε-caprolactona são maiores as pressões necessárias para solubilizar o sistema em uma única fase. Em todos os sistemas estudados foi observado o comportamento LCST (*Lower Critical Solution Temperature*), em que com o aumento da temperatura é necessária uma maior pressão para solubilizar o sistema em uma única fase. Em relação à modelagem termodinâmica foi observada que a equação de estado de Peng-Robinson com a regra de mistura de van der Waals promoveu um bom ajuste aos dados experimentais do sistema ternário e a equação de estado PC-SAFT (*Perturbed Chain-Statistical Associating Fluid Theory*) promoveu uma boa representação dos dados experimentais do sistema quaternário onde havia a presença de polímero.

Considerações Finais

Os dados apresentados neste trabalho são inéditos e relevantes para o desenvolvimento e otimização da síntese da poli(ε-caprolactona) em meio supercrítico, servindo como base para a determinação das melhores condições experimentais, otimização de processos e modelagem cinética.

Palavras-chave: Lactonas. Fluido Supercrítico. Equilíbrio de Fases.

ABSTRACT

Poly(ε-caprolactone) is a biodegradable, bioresorbable and biocompatible polymer used in a wide variety of high-value biomedical, pharmaceutical, and food applications. This polymer can be produced by enzymatic ring-opening polymerization of ε-caprolactone in high pressure system. However, it is still necessary better understanding the thermodynamic behavior of the chemical species during the process of polymerization in high pressure. In this context, the objective of this work is to study the phase behavior of the ternary system [carbon dioxide + dichloromethane + ε-caprolactone] and also the influence of the molar mass of poly(ε-caprolactone) and water content in ε-caprolactone in the quaternary system [carbon dioxide + dichloromethane + ε-caprolactone + poly(ε-caprolactone)] in high pressure through of experimental data collection and thermodynamic modeling of the referred systems. All phase equilibrium experiments were conducted employing the static synthetic method in a high pressure variable-volume view cell over the temperature range of 323.15 to 353.15 K. In the ternary system, it was observed vapor-liquid equilibrium with bubble point transition, liquid-liquid, and vapor-liquid-liquid and a phase transition pressure up to 25.8 MPa. In the quaternary system, it was verified only phase transitions of vapor-liquid bubble point type. In this system, it was also noted that different molar mass of poly(ε-caprolactone) does not change significantly the transition pressure of the system; however, it was observed that with the increase of water content present in the ε-caprolactone, higher pressures are required to solubilize the system. In all systems studies, it was observed the lower critical solution temperature (LCST) behavior phase, wherewith the increasing temperature, there is an increase in system pressure. In relation to the thermodynamic modeling, it was observed that the Peng-Robison EoS provided good performance for the ternary system, and the PC-SAFT EoS led to a good representation of the experimental phase equilibrium data for the system with polymers. The data reported in this work are new and relevant for the development and optimization of polymer synthesis in supercritical media, serving as the basis for the determination of the best conditions for the polymerization reactions, process optimization and kinetic modeling.

Keywords: Lactone. Supercritical Fluids. Phase Equilibrium.

LIST OF FIGURES

Figure 1 - Molar mass distribution curve typical of a polymer showing the three main mean values (Mn, Mw, and Mv).....26
Figure 2 - (a) Chemical structure of ε-caprolactone; (b) Chemical structure of the repeating monomeric unit of poly(ε-caprolactone).....27
Figure 3 - Kinetic reactions mechanism of poly(ε-caprolactone) synthesis by enzyme-mediated.....29
Figure 4 - Schematic P-T diagram for a pure component showing the liquid phase region, solid phase region, the vapor phase region, the supercritical fluid (SCF) region, the critical point and triple point.....31
Figure 5 - Variation in density for pure CO_2 at 308.15 K. At this temperature (i.e., close to Tc for CO_2) there is a rapid but continuous increase in density near the critical pressure (Pc).....32
Figure 6 - Classification of *P-T* diagrams of binary systems (Classification of van Konynenburg and Scott (1980)).....36
Figure 7 - Phase diagram (Type I): (a) *P-T-x* surface; (b) *P-T* projection showing vapor-liquid equilibria for a simple binary mixture.....37
Figure 8 - Phase diagram (Type II): (a) *P-x*, *P-T* and *T-x* projections.....38
Figure 9 - Phase diagram (Type III): (a) *P-x*, *P-T* and *T-x* projections.....40
Figure 10 - Phase diagram (Type III): Possible forms of critical lines $l = g$ and $l = l$.
.....40
Figure 11 - Phase diagram (type V): (a) *P-x*, *P-T* and *T-x* projections.....42
Figure 12 - Equilibrium cell. (MB) magnetic bar; (SW) sapphire windows; (TC) thermocouple.....53
Figure 13 - High pressure phase equilibria apparatus. (SR_1) solvent reservoir (CO_2); (RB_1) cold recirculation bath; (RB_2) hot recirculation bath; (SP) syringe pump; (EC) equilibrium cell; (MS) magnetic stirrer; (LS) light source; (SW) sapphire windows; (TI) temperature indicator; (TC) thermocouple; (PI) pressure indicator; (PT) pressure transducer; (V_1, V_3, V_4, V_5, and V_6) ball valve; (V_2) check valve; (V_7 and V_8) micrometric valve.....54
Figure 14 - Pressure−overall composition diagram for the system [CO_2 (1) + CH_2Cl_2 (2) + ε-CL (3)], in CH_2Cl_2 free-basis, at CH_2Cl_2 to ε-CL mass ratio of 0.5:1. Experimental data: 323:15 K: ◨ (BP), ■ (LL) and □ (LLV); 333:15 K: ◑ (BP), ● (LL) and ○ (LLV);

343:15 K: ◭ (BP), ▲ (LL) and △ (LLV); 353:15 K: ◸ (BP), ▼ (LL) and ▽ (LLV). Continuous lines denote calculated values applying the PR EoS model with global temperature fitted parameters. 63
Figure 15 - Pressure−overall composition diagram for the system [CO_2 (1) + CH_2Cl_2 (2) + ε-CL (3)], in CH_2Cl_2 free-basis, at CH_2Cl_2 to ε-CL mass ratio of 1:1. Experimental data: 323:15 K: ◨ (BP), ■ (LL) and □ (LLV); 333:15 K: ◑ (BP), ● (LL) and ○ (LLV); 343:15 K: ◭ (BP), ▲ (LL) and △ (LLV); 353:15 K: ◸ (BP), ▼ (LL) and ▽ (LLV). Continuous lines denote calculated values applying the PR EoS model with global temperature fitted parameters. 64
Figure 16 - Pressure−overall composition diagram for the system [CO_2 (1) + CH_2Cl_2 (2) + ε-CL (3)], in CH_2Cl_2 free-basis, at CH_2Cl_2 to ε-CL mass ratio of 2:1. Experimental data: 323:15 K: ◨ (BP), ■ (LL) and □ (LLV); 333:15 K: ◑ (BP), ● (LL) and ○ (LLV); 343:15 K: ◭ (BP), ▲ (LL) and △ (LLV); 353:15 K: ◸ (BP), ▼ (LL) and ▽ (LLV). Continuous lines denote calculated values applying the PR EoS model with global temperature fitted parameters. 65
Figure 17 - Pressure-temperature diagram for the system [CO_2 (1) + CH_2Cl_2 (2) + ε-CL (3)], in CH_2Cl_2 free-basis, at CH_2Cl_2 to ε-CL mass ratio of 0.5:1. Experimental data: ◨ (BP) – [w_1 = 0.2788; w_2 = 0.2405; w_3 = 0.4807]; ◑ (BP) – [w_1 = 0.4003; w_2 = 0.2004; w_3 = 0.3993]; ▶ (LL) – [w_1 = 0.5482; w_2 = 0.1506; w_3 = 0.3012]; ◀ (LL) – [w_1 = 0.5943; w_2 = 0.1347; w_3 = 0.2711]. Continuous lines denote calculated values applying the PR EoS model with global temperature fitted parameters. 66
Figure 18 - Pressure-temperature diagram for the system [CO_2 (1) + CH_2Cl_2 (2) + ε-CL (3)], in CH_2Cl_2 free-basis, at CH_2Cl_2 to ε-CL mass ratio of 1:1. Experimental data: ◨ (BP) – [w_1 = 0.2255; w_2 = 0.3875; w_3 = 0.3870]; ◑ (BP) – [w_1 = 0.4347; w_2 = 0.2834; w_3 = 0.2819]; ▶ (LL) – [w_1 = 0.5249; w_2 = 0.2362; w_3 = 0.2389]; ◀ (LL) – [w_1 = 0.5764; w_2 = 0.2117; w_3 = 0.2119]. Continuous lines denote calculated values applying the PR EoS model with global temperature fitted parameters. 67
Figure 19 - Pressure-temperature diagram for the system [CO_2 (1) + CH_2Cl_2 (2) + ε-CL (3)], in CH_2Cl_2 free-basis, at CH_2Cl_2 to ε-CL mass ratio of 2:1. Experimental data: ◨ (BP) – [w_1 = 0.2485; w_2 = 0.5042; w_3 = 0.2473]; ◑ (BP) – [w_1 = 0.3664; w_2 = 0.4223; w_3 = 0.2113]; ▶ (LL) – [w_1 = 0.5395; w_2 = 0.3069; w_3 = 0.1536]; ◀ (LL) – [w_1 = 0.5719; w_2 = 0.2861; w_3 = 0.1420]. Continuous lines denote calculated values applying the PR EoS model with global temperature fitted parameters. 68

Figure 20 - Comparison between experimental values obtained in this work for the ternary system [CO_2 (1) + CH_2Cl_2 (2) + ε-CL (3)], on a CH_2Cl_2 free-basis with three different CH_2Cl_2 to ε-CL mass ratios, 0.5:1 [◨ (BP), ■ (LL) and □ (LLV)], 1:1 [◑ (BP), ● (LL) and ○ (LLV)] and 2:1 [◭ (BP), ▲ (LL) and △ (LLV)] with the literature (Bender et al., (2010a)) for the binary system [CO_2 (1) + ε-CL (2)] [+ (BP), ⁎ (DP)] at the temperature of 333.15 K. 70
Figure 21 - Formation of a PC-SAFT molecule according to Gross and Sadowski (2001). 79
Figure 22 - *P*-$w4'$ diagram for VLE-BP for the system [CO_2 (1) + CH_2Cl_2 (2) + ε-CL (3) + PCL (4)] for the mass ratio CO_2: CH_2Cl_2: (H_2O + ε-CL + PCL) of 1:0.5:1 in different number average molar mass (Mn) of the PCL. Experimental data: 323:15 K: □ (10,000 g·mol^{-1}) and ■ (80,000 g·mol^{-1}); 333:15 K: ○ (10,000 g·mol^{-1}) and ● (80,000 g·mol^{-1}); 343:15 K: △ (10,000 g·mol^{-1}) and ▲ (80,000 g·mol^{-1}); 353:15 K: ▽ (10,000 g·mol^{-1}) and ▼ (80,000 g·mol^{-1}). Predicted data by PC-SAFT model: dashed line (10,000 g·mol^{-1}) and solid line (80,000 g·mol^{-1}). 89
Figure 23 - *P*-$w4'$ diagram for VLE-BP for the system [CO_2 (1) + CH_2Cl_2 (2) + ε-CL (3) + PCL (4)] for the mass ratio CO_2: CH_2Cl_2: (H_2O + ε-CL + PCL) of 1:1:1 in different number average molar mass (Mn) of the PCL. Experimental data: 323:15 K: □ (10,000 g·mol^{-1}) and ■ (80,000 g·mol^{-1}); 333:15 K: ○ (10,000 g·mol^{-1}) and ● (80,000 g·mol^{-1}); 343:15 K: △ (10,000 g·mol^{-1}) and ▲ (80,000 g·mol^{-1}); 353:15 K: ▽ (10,000 g·mol^{-1}) and ▼ (80,000 g·mol^{-1}). Predicted data by PC-SAFT model: dashed line (10,000 g·mol^{-1}) and solid line (80,000 g·mol^{-1}). 90
Figure 24 - *P*-*T* diagram for VLE-BP for the system [CO_2 (1) + CH_2Cl_2 (2) + ε-CL (3) + PCL (4)] for the different number average molar mass (Mn) of the PCL to mass ratio CO_2: CH_2Cl_2: (H_2O + ε-Cl + PCL) of 1:0.5:1 and 1:1:1. Experimental data: 1:0.5:1: ◨ (w_4' = 0.00%), □ (w_4' = 15.00% - Mn = 10,000 g·mol^{-1}) and ■ (w_4' = 15.00% - Mn = 80,000 g·mol^{-1}); 1:1:1: ◭ (w_4' = 0.00%), △ (w_4' = 15.00% - Mn = 10,000 g·mol^{-1}) and ▲ (w_4' = 15.00% - Mn = 80,000 g·mol^{-1}). Predicted data by PC-SAFT model: dot line (0.00% PCL), dashed line (10,000 g·mol^{-1}) and solid line (80,000 g·mol^{-1}). 92
Figure 25 - *P*-$w4'$ diagram for VLE-BP for the system [CO_2 (1) + CH_2Cl_2 (2) + ε-CL (3) + PCL (4)] for the mass ratio CO_2: CH_2Cl_2: (H_2O + ε-CL + PCL) of 1:0.5:1 in different H_2O content in ε-CL. Experimental data: 323:15 K: ■ ($wH2O$= 0.040) and □ ($wH2O$= 0.184); 333:15 K: ● ($wH2O$= 0.040) and ○ ($wH2O$= 0.184); 343:15 K: ▲ ($wH2O$=

0.040) and △ ($wH2O$= 0.184); 353:15 K: ▼ ($wH2O$= 0.040) and ▽ ($wH2O$= 0.184). 104
Figure 26 - *P*-$w4'$ diagram for VLE-BP for the system [CO_2 (1) + CH_2Cl_2 (2) + ε-CL (3) + PCL (4)] for the mass ratio CO_2: CH_2Cl_2: (H_2O + ε-CL + PCL) of 1:0.5:1 in different H_2O content in ε-CL. Experimental data: 323:15 K: ■ ($wH2O$= 0.040) and □ ($wH2O$= 0.184); 333:15 K: ● ($wH2O$= 0.040) and ○ ($wH2O$= 0.184); 343:15 K: ▲ ($wH2O$= 0.040) and △ ($wH2O$= 0.184); 353:15 K: ▼ ($wH2O$= 0.040) and ▽ ($wH2O$= 0.184). 105
Figure 27 - *P*-*T* diagram for VLE-BP for the system [CO_2 (1) + CH_2Cl_2 (2) + ε-CL (3) + PCL (4)] for the mass ratio CO_2: CH_2Cl_2: (H_2O + ε-CL + PCL) of 1:0.5:1 and 1:1:1, and $w4'$ = 0.0%. Experimental data: 1:0.5:1: △ ($wH2O$ = 0.040 %) and ▲ ($wH2O$ = 0.184 %); 1:1:1: □ ($wH2O$ = 0.040 %) and ■ ($wH2O$ = 0.184). 106

LIST OF TABLES

Table 1 - Polymers types and applications. 24
Table 2 - An overview of the existing works in the literature about phase equilibrium data of ε-caprolactone and poly(ε-caprolactone) systems at high pressures. 34
Table 3 - Parameters of state equations for use in the generalized equation, Eq. (7). 45
Table 4 - Chemical name, molecular formula, provenance, purification method and purity of the materials used (purity provided by suppliers). 52
Table 5 - Characteristic parameters of pure compounds used in the work. 57
Table 6 - Phase equilibrium results for the ternary system [CO_2 (1) + CH_2Cl_2 (2) + ε-CL (3)], in CH_2Cl_2 free-basis, at CH_2Cl_2 to ε-CL mass ratio of 0.5:1. 59
Table 7 - Phase equilibrium results for the ternary system [CO_2 (1) + CH_2Cl_2 (2) + ε-CL (3)], in CH_2Cl_2 free-basis, at CH_2Cl_2 to ε-CL mass ratio of 1:1. 60
Table 8 - Phase equilibrium results for the ternary system [CO_2 (1) + CH_2Cl_2 (2) + ε-CL (3)], in CH_2Cl_2 free-basis, at CH_2Cl_2 to ε-CL mass ratio of 2:1. 61
Table 9 - Binary interaction parameters of PR EoS model fitted in this work for the ternary system [CO_2 (1) + CH_2Cl_2 (2) + ε-CL (3)]. 69
Table 10 - Molar fractions for the multicomponent system [CO_2 (1) + CH_2Cl_2 (2) + ε-CL (3)] in CH_2Cl_2 free-basis, at CH_2Cl_2 to ε-CL mass ratio of 0.5:1. Molar fractions related to the data presented in Table 6. 72
Table 11 - Molar fractions for the multicomponent system [CO_2 (1) + CH_2Cl_2 (2) + ε-CL (3)] in CH_2Cl_2 free-basis, at CH_2Cl_2 to ε-CL mass ratio of 1:1. Molar fractions related to the data presented in Table 7. 72
Table 12 - Molar fractions for the multicomponent system [CO_2 (1) + CH_2Cl_2 (2) + ε-CL (3)] in CH_2Cl_2 free-basis, at CH_2Cl_2 to ε-CL mass ratio of 1:2. Molar fractions related to the data presented in Table 8. 73
Table 13 - Chemical name, molecular formula, CAS number, supplier and minimum mass fraction purity of the materials used (purity provided by suppliers). 77
Table 14 - PC-SAFT EOS pure component parameters used in this work. 83
Table 15 - Phase equilibrium results for the quaternary system [CO_2 (1) + CH_2Cl_2 (2) + ε-CL (3) + PCL (4)] for the mass ratio CO_2: CH_2Cl_2: (H_2O + ε-CL + PCL) of 1:0.5:1. In this case the H_2O content in the ε-CL was 0.04 + 0.001 % and PCL had number average molar mass (Mn) of 10000 g.mol^{-1} and dispersion (D) of 1.4 85

Table 16 - Phase equilibrium results for the quaternary system [CO_2 (1) + CH_2Cl_2 (2) + ε-CL (3) + PCL (4)] for the mass ratio CO_2: CH_2Cl_2: (H_2O + ε-CL + PCL) of 1:1:1. In this case the H_2O content in the ε-CL was 0.040 + 0.001 % and PCL had number average molar mass (Mn) of 10000 g.mol^{-1} and dispersion (D) of 1.4.....86
Table 17 - Phase equilibrium results for the quaternary system [CO_2 (1) + CH_2Cl_2 (2) + ε-CL (3) + PCL (4)] for the mass ratio CO_2: CH_2Cl_2: (H_2O + ε-CL + PCL) of 1:0.5:1. In this case the H_2O content in the ε-CL was 0.040 + 0.001 % and PCL had number average molar mass (Mn) of 80,000 g.mol^{-1} and dispersion (D) of 1.74.....87
Table 18 - Phase equilibrium results for the quaternary system [CO_2 (1) + CH_2Cl_2 (2) + ε-CL (3) + PCL (4)] for the mass ratio CO_2: CH_2Cl_2: (H_2O + ε-CL + PCL) of 1:1:1. In this case the H_2O content in the ε-CL was 0.040 + 0.001 % and PCL had number average molar mass (Mn) of 80,000 g.mol^{-1} and dispersion (D) of 1.74.....88
Table 19 - Binary interaction parameters of PC-SAFT EOS in this work for the multicomponent system [CO_2 (1) + CH_2Cl_2 (2) + H_2O (3) + ε-CL (4) + PCL (5)]. 93
Table 20 - Molar fractions for the multicomponent system [CO_2 (1) + CH_2Cl_2 (2) + H_2O (3) + ε-CL (4) + PCL (5)] for the mass ratio CO_2: CH_2Cl_2: (H_2O + ε-CL + PCL) of 1:0.5:1. In this case, PCL had number average molar mass (Mn) of 10,000 g·mol^{-1} and dispersion (D) of 1.40. Molar fractions related to the data presented in Table 15. 95
Table 21 - Molar fractions for the multicomponent system [CO_2 (1) + CH_2Cl_2 (2) + H_2O (3) + ε-CL (4) + PCL (5)] for the mass ratio CO_2: CH_2Cl_2: (H_2O + ε-CL + PCL) of 1:1:1. In this case, PCL had number average molar mass (Mn) of 10,000 g·mol^{-1} and dispersion (D) of 1.40. Molar fractions related to the data presented in Table 16. 96
Table 22 - Molar fractions for the multicomponent system [CO_2 (1) + CH_2Cl_2 (2) + H_2O (3) + ε-CL (4) + PCL (5)] for the mass ratio CO_2: CH_2Cl_2: (H_2O + ε-CL + PCL) of 1:0.5:1. In this case, PCL had number average molar mass (Mn) of 80,000 g·mol^{-1} and dispersion (D) of 1.74. Molar fractions related to the data presented in Table 17. 96
Table 23 - Molar fractions for the multicomponent system [CO_2 (1) + CH_2Cl_2 (2) + H_2O (3) + ε-CL (4) + PCL (5)] for the mass ratio CO_2: CH_2Cl_2: (H_2O + ε-CL + PCL) of 1:1:1. In this case, PCL had number average molar mass (Mn) of 80,000 g·mol^{-1} and dispersion (D) of 1.74. Molar fractions related to the data presented in Table 18. 97
Table 24 - Phase equilibrium results for the quaternary system [CO_2 (1) + CH_2Cl_2 (2) + ε-CL (3) + PCL (4)] for the mass ratio CO_2: CH_2Cl_2: (H_2O + ε-CL + PCL) of 1:0.5:1.

In this case the H_2O content in the ε-CL was 0.184 + 0.030 % and PCL had number average molar mass (Mn) of 10000 g.mol^{-1} and dispersion (D) of 1.4.....102
Table 25 - Phase equilibrium results for the quaternary system [CO_2 (1) + CH_2Cl_2 (2) + ε-CL (3) + PCL (4)] for the mass ratio CO_2: CH_2Cl_2: (H_2O + ε-CL + PCL) of 1:1:1. In this case the H_2O content in the ε-CL was 0.184 + 0.030 % and PCL had number average molar mass (Mn) of 10000 g.mol^{-1} and dispersion (D) of 1.4.....103
Table 26 - Molar fractions for the multicomponent system [CO_2 (1) + CH_2Cl_2 (2) + H_2O (3) + ε-CL (4) + PCL (5)] for the mass ratio CO_2: CH_2Cl_2: (H_2O + ε-CL + PCL) of 1:0.5:1. In this case, PCL had number average molar mass (Mn) of 10,000 g·mol^{-1} and dispersion (D) of 1.40. . Molar fractions related to the data presented in Table 24. 108
Table 27 - Molar fractions for the multicomponent system [CO_2 (1) + CH_2Cl_2 (2) + H_2O (3) + ε-CL (4) + PCL (5)] for the mass ratio CO_2: CH_2Cl_2: (H_2O + ε-CL + PCL) of 1:1:1. In this case, PCL had number average molar mass (Mn) of 10,000 g·mol^{-1} and dispersion (D) of 1.40. . Molar fractions related to the data presented in Table 25. 109

LIST OF ABBREVIATONS AND ACRONYMS

CH_2CL_2	Dichloromethane
ε-CL	ε-Caprolactone
CASRN	CAS number
CO_2	Carbon dioxide
H_2O	Water
IUPAC	International Union of Pure and Applied Chemistry
LCEP	Lower critical end point
LCST	Lower critical solution temperature
LLE	Liquid-liquid equilibrium
PCL	Poly(ε-caprolactone)
PC-SAFT	Perturbed-Chain Statistical Associating Fluid Theory
PR-EoS	Peng-Robinson equation of state
PSO	Particle swarm optimization
ROP	Ring-opening polymerization
e-ROP	Enzymatic ring-opening polymerization
SAFT	Statistical Association Fluid Theory
$scCO_2$	Supercritical carbon dioxide
SCF	Supercritical fluids
UCEP	Upper critical end point
UCSP	Under critical solution pressure
UCST	Under critical solution temperature
VLE	Vapor-liquid equilibrium
VLE-BP	Vapor-liquid equilibrium – Bubble point
VLLE	Vapor-liquid-liquid equilibrium
VLSE	Vapor-liquid-solid equilibrium

LIST OF SYMBOLS

a	Constant dependent of the polymer, solvent and temperature (-)
AD	Absolute deviation (MPa)
A_1	Helmholtz free energy of first-order perturbation term (J)
A_2	Helmholtz free energy of second-order perturbation term (J)
a_i	Peng-Robison parameter of component i (L.mol^{-1})
a_{ij}	Peng-Robison parameter of mixture of components i and j (L.mol^{-1})
a_j	Peng-Robison parameter of component j (L.mol^{-1})
$a(T)$	Peng-Robison parameter (MPa.L^2.mol^{-2})
A^{res}	Helmholtz free energy (J)
$\tilde{a}^{assoc}$	Contribution due the associating interactions (J)
$\tilde{a}^{disp}$	Contribution due to dispersive attraction (J)
$\tilde{a}^{hc}$	Hard-chain reference contribution (J)
$\tilde{a}^{hs}$	Helmholtz free energy of the had-sphere (J)
$\tilde{a}^{res}$	Residual Helmholtz free energy (J)
b	Peng-Robison parameter (L.mol^{-1})
b_i	Peng-Robison parameter of component i (L.mol^{-1})
D	Dispersion (-)
$d_i(T)$	Temperature-dependent segment diameter (Å)
$f(\omega, Tr)$	Dimensionless function of reduced temperature and acentric factor (-)
g_{ii}^{hs}	Radial distribution function of the hard-sphere fluid of component i (-)
k	Boltzmann constant (J.K^{-1})
k_{ij}	Binary interaction parameter
M	Molar mass (g.mol^{-1})
$\bar{m}$	Mean segment number in the mixture (-)
m_i	number of segments in the mixture of component i
$\bar{M}_n$	Number average molar mass (g.mol^{-1})
$\bar{M}_v$	Viscosity average molar mass (g.mol^{-1})
M_x	Average molar mass of size range x (g.mol^{-1})
$\bar{M}_w$	Mass average molar mass (g.mol^{-1})
N	Total number of molecules
N_{AV}	Avogadro's Number (mol^{-1})

N_x	Number of chains with size x (-)
OF	Objective function (MPa^2)
P	Pressure (MPa)
P_c	Critical pressure (MPa)
P_i^{exp}	Experimental pressure (MPa)
P_i^{cal}	Calculated pressure (MPa)
R	Molar gas constant ($J.mol^{-1}.K^{-1}$)
r	Radial distance between two segments (Å)
$rmsd$	Root mean square deviation values (MPa^2)
sd	Standard deviation (MPa)
s_1	Constant defining the pair potential (Å)
T	Temperature (K)
T_c	Critical temperature (K)
T_r	Reduced temperature (-)
$u(r)$	Pair potential (J)
X_{A_i}	Sites fraction A of component i that are not linked to other active sites (-)
x_i	Molar fraction of component i (-)
x_j	Molar fraction of component j (-)
v	Molar volume ($L.mol^{-1}$)
w	Total mass of all molecules in a polymer sample (g)
w_x	Fraction mass x (-)
Z	Compressibility factor (-)
Z_c	Critical compressibility factor (-)
$\Delta^{A_iB_j}$	Association force (N)
ε	Depth of potential well (J)
$\varepsilon^{A_iB_j}$	energy of association between the site A of molecule i and the site B of molecule j (J)
ϵ_{ij}/k	Energy parameter of component i and j (J)
$\kappa^{A_iB_j}$	Volume of association between the site A of molecule i and the site B of molecule j (-)
λ	Reduced well width of square-well potential (-)
ρ	Total number density molecules ($Å^{-3}$)

σ	Segment diameter (Å)
σ_{ij}	Segment diameter of component i and j (Å)
ω	Acentric factor (-)

SUMARY

1 INTRODUCTION 17
1.1 OBJECTIVES 19
1.1.1 General Objective 19
1.1.2 Specific Objectives 20
1.2 WORK STRUCTURE 20
2 LITERATURE REVIEW 22
2.1 POLYMERS 22
2.1.1 Molar mass distribution 24
2.2 POLY(ε-CAPROLACTONE) 27
2.3 WATER EFFECT ON POLYMERIZATION REACTION 29
2.4 SUPERCRITICAL FLUIDS 30
2.5 PHASE BEHAVIOR AT HIGH PRESSURES 33
2.6 CLASSIFICATION OF BINARY SYSTEMS 35
2.6.1 Type I – Phase behavior 36
2.6.2 Type II – Phase behavior 37
2.6.3 Type III – Phase behavior 39
2.6.4 Type IV – Phase behavior 41
2.6.5 Type V – Phase behavior 41
2.6.6 Type VI – Phase behavior 42
2.7 EXPERIMENTAL METHODS FOR DETERMINING PHASE EQUILIBRIUM 43
2.8 THERMODYNAMIC MODELING OF PHASE EQUILIBRIUM 44
2.8.1 Thermodynamic models 44
2.8.1.1 Cubic equation of state 44
2.8.1.2 Perturbation models 46
2.9 CONSIDERATIONS ON THE STATE OF THE ART 48
3 . RESULTS AND DISCUSSION 49

3.1 HIGH PRESSURE PHASE EQUILIBRIUM DATA FOR THE TERNARY SYSTEM CONTAINNIG CARBON DIOXIDE, DICHLOROMETHANE, AND ε-CAPROLACTONE 49
3.1.1 Introduction 49
3.1.2 Experimental 51
3.1.2.1 Materials 51
3.1.3 Phase equilibrium apparatus and procedure 52
3.1.4 Thermodynamic modeling 55
3.1.5 Results and Discussion 58
3.1.6 Partial Conclusion 71
3.1.7 Supporting Information 72
3.2 EFFECT OF DIFFERENT POLYMER MOLAR MASS ON THE PHASE BEHAVIOR OF CARBON DIOXIDE + DICHLOROMETHANE + ε-CAPROLACTONE + POLY(ε-CAPROLACTONE) SYSTEM 74
3.2.1 Introduction 74
3.2.2 Experimental 76
3.2.2.1 Materials 76
3.2.3 Phase equilibrium apparatus and procedure 77
3.2.4 Thermodynamic modelling 78
3.2.5 Results and Discussion 84
3.2.6 Partial Conclusion 94
3.2.7 Supporting Information 95
3.3 EFFECT OF WATER CONTENT ON THE HIGH PRESSURE CARBON DIOXIDE + ε-CAPROLACTONE + DICHLOROMETHANE + ε-CAPROLACTONE + POLY(ε-CAPROLACTONE) SYSTEM 98
3.3.1 Introduction 99
3.3.2 Experimental 100
3.3.2.1 Materials 100

3.3.3 Phase equilibrium apparatus and procedure 100
3.3.4 Results and Discussion 101
3.3.5 Partial Conclusion 107
3.3.6 Supporting Information 108
4 CONCLUSIONS 110
4.1 SUGGESTIONS FOR FUTURE RESEARCH 111
REFERENCES 112

CONCEPTUAL DIAGRAM OF WORK

Phase equilibrium data and thermodynamic modeling of ε-caprolactone and poly(ε-caprolactone) systems at high pressures

Why?

- Necessity to understand the thermodynamic behavior of the ternary [carbon dioxide + dichloromethane + ε-caprolactone] and quaternary [carbon dioxide + dichloromethane + ε-caprolactone + poly(ε-caprolactone)] systems in order to understand the thermodynamic phenomena that occur in the polymerization of the ε-caprolactone in high pressure.

Who has done it?

- In the literature, there are a series of studies that evaluated the behavior of phases of binary systems [carbon dioxide + ε-caprolactone] and [carbon dioxide + poly(ε-caprolactone)] and, ternary systems [carbon dioxide + dichloromethane + poly(ε-caprolactone)], but there are not studies that evaluate the phases behavior of the ternary system [carbon dioxide + dichloromethane + ε-caprolactone] and quaternary system [carbon dioxide + dichloromethane + ε-caprolactone + poly(ε-caprolactone)].

Hypotheses

- Is it possible to investigate experimentally the use of dichloromethane as co-solvent on the system [carbon dioxide + ε-caprolactone]?
- Is it possible to thermodynamically model the effect of dichloromethane as co-solvent on the system [carbon dioxide + ε-caprolactone]?
- Is it possible to investigate experimentally the thermodynamic behavior of the quaternary system [carbon dioxide + dichloromethane + ε-caprolactone + poly(ε-caprolactone)]?

- Is it possible to thermodynamically model the quaternary system [carbon dioxide + dichloromethane + ε-caprolactone + poly(ε-caprolactone)]?
- Is it possible to investigate experimentally the influence of the molar mass of poly(ε-caprolactone) and water content in ε-caprolactone in the quaternary system [carbon dioxide + dichloromethane + ε-caprolactone + poly(ε-caprolactone)]?

How to make?

- Through high pressure phase equilibria experiments analyzing the use of dichloromethane as co-solvent on the system [carbon dioxide + ε-caprolactone];
- Through high pressure phase equilibrium experiments of quaternary system [carbon dioxide + dichloromethane + ε-caprolactone + poly(ε-caprolactone)], where:
  - different poly(ε-caprolactone) mass fractions (reaction conversion) will be evaluated;
  - different molar masses of poly(ε-caprolactone) will be evaluated;
  - different water contents in ε-caprolactone will be evaluated.
- Through the application of thermodynamic models as Peng-Robinson and PC-SAFT EoS to the experimental data that will be obtained in this work.

1 INTRODUCTION

The polymerization of lactones by ring-opening polymerization via enzyme-catalyzed reaction was studied for the first time in the beginning of the 1990s by Uyama and Kobayashi (1993). Since then, the number of researches about this technique has grown exponentially as the scientific community began to see the potentialities of this process.

The first works of polymerization of lactones by ring-opening that used lipases from *Pseudomonas fluorescences*, *Candida cylindracea*, *Aspergillus niger*, *Candida rugosa*, and porcine pancreatic lipase obtained low monomer conversion and low molar mass (UYAMA; KOBAYASHI, 1993; UYAMA et al., 1995; UYAMA; TAKEYA; KOBAYASHI, 1995; MACDONALD et al., 1995; HENDERSON et al., 1996). Only with the beginning of the use of Novozym 435, CALB lipase immobilized on an hydrophobic carrier (acrylic resin), it was observed a considerable evolution in monomer conversion rates and molar mass growth (BISHT et al., 1997a, 1997; BISHT et al., 1997b; KUMAR; GROSS, 2000; BANKOVA et al., 2002; MEI; KUMAR; GROSS, 2003).

The lactones are cyclic esters formed by condensation reaction between a functional alcohol group and a carboxylic acid group. The lactones can be classified in smaller sizes (4-carbons), medium sizes (6- and 7-carbons) and macrolides (12-, 13- to 16-carbons) (UYAMA; TAKEYA; KOBAYASHI, 1995).

The ε-caprolactone is a cyclic lactone with 6 carbons and from this lactone it is possible to synthesize the poly(ε-caprolactone). This polymer is a biodegradable, bioresorbable and biocompatible polymer used in a wide variety of high-value biomedical, pharmaceutical, and food applications and eliminated from the human body as low molar mass by-products, with no residual side effects (BENDER et al., 2010a; COMIM et al., 2015; BANG; LEE, 2019).

For poly(ε-caprolactone) to have a noblest application in biomedical, pharmaceutical, and food applications it is necessary to be free of toxic residues. The use of enzymes as catalysts already makes this technique cleaner; however, there may still be residues from organic solvents. One of the alternatives found was to replace the organic solvent by supercritical carbon dioxide (LOEKER et al., 2004;

THURECHT et al., 2006; COMIM et al., 2013; COMIM et al., 2015). The supercritical carbon dioxide can be easily separated at the end of the process from the reaction medium by a simply decompression of the system. This is interesting since both solvent and enzyme can be recovered and thus providing the enzyme and solvent reuse.

Though supercritical carbon dioxide may be a good solvent for ε-caprolactone, it is not a proper solvent for poly(ε-caprolactone), leading to the sedimentation of its organic solutions upon mixing (KALOGIANNIS; PANAYIOTOU; 2006; BENDER et al., 2010a). An alternative to overcome such drawback is to use a co-solvent together with supercritical carbon dioxide, as for example dichloromethane. Dichloromethane is a colorless and volatile liquid at ambient conditions, being widely used as a solvent because it is considered one of the least harmful organochloride compounds (ROSSBERG et al., 2012).

Literature data show that the enzymatic ring-opening polymerization of ε-caprolactone in supercritical carbon dioxide medium leads to yields and molar mass similar to those reactions in organic solvents and metallic catalysts (THURECHT et al., 2006; COMIM et al., 2015). However, it is still necessary to better understand the thermodynamic behavior of the chemical species during the process of polymerization as carbon dioxide, dichloromethane, ε-caprolactone and poly(ε-caprolactone).

In the literature, there are a series of studies that evaluate the behavior of phases of binary systems [carbon dioxide + ε-caprolactone] (XU; WAGNER; DAHMEN, 2003; BERGEOT et al., 2004; BENDER et al, 2010b) and [carbon dioxide + poly(ε-caprolactone)] (de PAZ et al., 2010; BANG; LEE, 2019) and, ternary system [carbon dioxide + dichloromethane + poly(ε-caprolactone)] (KALOGIANNIS; PANAYIOTOU, 2006; BENDER et al, 2010a)], but there are not studies that evaluate the phases behavior of the ternary systems [carbon dioxide + dichloromethane + ε-caprolactone] and quaternary system [carbon dioxide + dichloromethane + ε-caprolactone + poly(ε-caprolactone)].

Note that up to now phase equilibrium studies with carbon dioxide and ε-caprolactone are aimed at the initial stage of the polymerization reaction. Therefore, there is no information about the phase behavior during the stages of the polymerization reaction. In the literature, there is only one work that evaluated the phase behavior during the polymerization reaction that was the work performed by

Nascimento (2019). In this work it has been evaluated the phase equilibrium of quaternary system [carbon dioxide + chloroform + ω-pentadecalactone + poly(ω-pentadecalactone)], where solvents mass ratio was kept fixed and ω-pentadecalactone and poly(ω-pentadecalactone) mass ratio was varied (trying to imitate a polymerization reaction through the conversion of ω-pentadecalactone to poly(ω-pentadecalactone)).

The work of Nascimento (2019) is very important since it evaluates the stages of the polymerization reaction (monomer to polymer transformation). This transformation generates the system composition change and consequently affecting the phase equilibrium.

Therefore, the study of ternary system [carbon dioxide + dichloromethane + ε-caprolactone] and quaternary system [carbon dioxide + dichloromethane + ε-caprolactone + poly(ε-caprolactone)] is important for the development and understanding of the polymerization of the poly(ε-caprolactone) in high pressure. In addition to obtaining phase equilibrium data, thermodynamic modeling by the use of appropriate equations of state is also important, since it is possible to simulate experimental conditions not tested, and thus with a significant saving in time and operating costs.

1.1 OBJECTIVES

1.1.1 General Objective

The general objective of this work is to study the phase behavior of the ternary system [carbon dioxide + dichloromethane + ε-caprolactone] and the influence of the molar mass of poly(ε-caprolactone) and water content on ε-caprolactone in the quaternary system [carbon dioxide + dichloromethane + ε-caprolactone + poly(ε-caprolactone)] at high pressures through experimental data collection and thermodynamic modeling of the referred systems.

1.1.2 Specific Objectives

a) Determine experimentally phase equilibrium data for the ternary system [carbon dioxide + dichloromethane + ε-caprolactone] over the temperature range from 323.15 to 353.15 K and on different mass ratios of dichloromethane:ε-caprolactone (0.5:1, 1:1 and 2:1).
b) Model the phase equilibrium data for the ternary system [carbon dioxide + dichloromethane + ε-caprolactone] using the Peng-Robinson EoS with the van der Waals mixing rule.
c) Evaluate experimentally the influence of poly(ε-caprolactone) molar mass on the quaternary system [carbon dioxide + dichloromethane + ε-caprolactone + poly(ε-caprolactone)] over the temperature range from 323.15 to 353.15 K on different mass ratios of carbon dioxide:dichloromethane:[water + ε-caprolactone + poly(ε-caprolactone)] (1:0.5:1 and 1:1:1) and on different poly(ε-caprolactone) mass fractions (reaction conversion) from 0.0 up 15.0 wt%.
d) Model the influence of poly(ε-caprolactone) molar mass on the quaternary system [carbon dioxide + dichloromethane + ε-caprolactone + poly(ε-caprolactone)] using the PC-SAFT EoS.
e) Evaluate experimentally the influence of water content in ε-caprolactone on the quaternary system [carbon dioxide + dichloromethane + ε-caprolactone + poly(ε-caprolactone)] over the temperature range from 323.15 to 353.15 K on different mass ratios of carbon dioxide:dichloromethane:[water + ε-caprolactone + poly(ε-caprolactone)] (1:0.5:1 and 1:1:1) and on different poly(ε-caprolactone) mass fractions (reaction conversion) from 0.0 up 15.0 wt%.

1.2 WORK STRUCTURE

In order to provide a better understanding of the activities developed in this work, it is divided into 4 chapters. In Chapter 1, there are presented the motivation and the objectives for the realization of this work. In Chapter 2, it is presented a brief bibliographic review of the main concepts and publications concerning to phase equilibrium of the system involving ε-caprolactone and poly(ε-caprolactone). In

Chapter 3, it is presented the results and discussions obtained in this work in the form of three scientific articles. Finally, Chapter 4 presents the conclusions of this work and the suggestions for future work.

2 LITERATURE REVIEW

This chapter will present a brief review of the available literature on the subjects pertinent to this work. Firstly, an overview of polymers, mainly poly(ε-caprolactone) is presented. Then, some important thermodynamics concepts are described as supercritical fluids, high pressure phase behavior, experimental methods for determination of phase equilibrium, and thermodynamic models. Finally, it is presented the current state of the art of the importance of attainment of the phase equilibrium data and thermodynamic modeling of ε-caprolactone and poly(ε-caprolactone) systems at high pressures.

2.1 POLYMERS

Polymers are large, chain-like molecules composed of many (Greek: poly-) structural repeating units, or “mers” (Greek: meros meaning part) (PRAUSNITZ; LICHTENTHALER; AZEVEDO, 1999). Thus, a polymer is a macromolecule compost by many (tens of thousands) units of repetition joined by the covalent bonds. The raw material for the production of a polymer is the monomer, in other words, the monomer is a molecule with a unit of repetition (CANEVAROLO JÚNIOR, 2002).

The polymerization is a set of chemicals reactions in which monomers chemically combine (covalent bonds) to form long molecules, more or less branched with the same centesimal composition (CANEVAROLO JÚNIOR, 2002; AKCELRUD, 2007).

The polymeric chains can be classified according to:

- Structural formula: linear (where mers are with another one forming a continuous chain), branched (there are side chains), reticulated (there are cross-links between the adjacent chains) and networks (where their units are three-dimensionally connected forming networks);
- Tacticity: isotactic, syndiotactic and atactic;
- Solid state morphology: amorphous and semi-crystalline;
- Mechanical behavior: rubber or elastomer, flexible plastic, rigid plastic, fibers and resins;
- Fusibility: thermoplastics or thermoset;

- Type of application: high performance polymers, engineering polymers and general purpose polymers;
- Chemical composition: condensation and addition (proposed by Carothers (1929));
- Polymerization mechanism: step and chain (proposed by Flory (1953)).

There has been and still is considerable confusion in the classification of polymers. This is especially the case for the beginning student who must appreciate that there is no single generally accepted classification that is unambiguous. During the development of polymer science, two types of classifications have come into use. One classification is based on polymer structure and divides polymers into condensation and addition polymers. The other classification is based on polymerization mechanism and divides polymerizations into step and chain polymerizations. Confusion arises because the two classifications are often used interchangeably without careful thought. The terms condensation and step are often used synonymously, as are the terms addition and chain. Although these terms may often be used synonymously because most condensation polymers are produced by step polymerizations and most addition polymers are produced by chain polymerizations, this is not always the case. The condensation–addition classification is based on the composition or structure of polymers. The step–chain classification is based on the mechanisms of the polymerization processes (ODIAN, 2004).

There is in the market a large number of polymers, derived from different chemical compounds. Each polymer can be indicated for one or more applications, depending on their physical, mechanical, electrical, optical properties, according to Table 1.

The polymers types most consumed currently are polyethylene, polypropylene, polystyrene, polyester, and polyurethane, which due to their production and utilization are called commodity polymers. Several other polymers are produced to a lesser extent due to specific applications or high costs and therefore are called engineering plastics (FERNANDES; LONA, 2004).

Table 1 - Polymers types and applications.

Polymers Types	Applications
Acrylonitrile butadiene styrene (ABS)	Automotive parts
Nylon	Fibers, clothes and carpets
Polyvinyl acetate	Coatings
Polyacrylamide	Contact lenses
Polycarbonate	Ophthalmic lenses
Polyester	Packages, films and clothes
Polystyrene	Packages, household utensils and heat insulator
Polyethylene	Packages and films
Polymethyl methacrylate	Paints
Polypropylene	Packages
Polysoprene	Rubber
Polyurethane	Foams and insulating clothes
Polyvinyl chloride (PVC)	Pipes and fittings
Styrene butadiene rubber (SBR)	Tires, shoes, stickers
Polytetrafluoroethylene (Teflon)	Non-stick

Source: FERNANDES; LONA, 2004.

Currently, a new class of biological polymers (biopolymers) has attracted the attention of type researches because of its applications in medical, pharmaceutical and food areas, as polyester produced by enzymatic catalysis of cyclic lactones.

2.1.1 Molar mass distribution

The polymers are formed by repetition of a large number of chemicals units. The chemicals units are linked together by means of polymerization reactions. It is known that during the polymerization reactions polymers are formed with different sizes, in other words, a polydispersed mixture (COMIM, 2012). Thus, polymer molar mass should be expressed as average molar mass and its calculation must be statistical.

The molar mass most frequently used are the number average molar mass ($\bar{M}_n$) and the mass average molar mass ($\bar{M}_w$). According to Canevarolo Júnior (2002) the $\bar{M}_n$ is defined as the molar mass of all chains divided by total number of chains, in other words, the $\bar{M}_n$ is molar mass that takes into account more strongly the number of chains.

$$\overline{M}_n = \frac{w}{\sum_{x=1}^{\infty} N_x} = \frac{\sum_{x=1}^{\infty} N_x M_x}{\sum_{x=1}^{\infty} N_x} \tag{1}$$

where w is the total mass of all molecules in a polymer sample, N_x is the number of chains with size x and M_x average molar mass of size range x.

The $\bar{M}_w$ is another form to calculate average molar mass, where the polymeric chain mass is the most important (CANEVAROLO JÚNIOR, 2002). Thus, molar mass of each fraction contributes in a way weighted to the calculation of the average as show in Eq. (2):

$$\overline{M}_w = \frac{\sum_{x=1}^{\infty} w_x M_x}{\sum_{x=1}^{\infty} w_x} = \frac{\sum_{x=1}^{\infty} N_x M_x^2}{\sum_{x=1}^{\infty} N_x M_x} \tag{2}$$

where w_x is the fraction mass x.

According to Canevarolo Júnior (2002), there is also the viscosity average molar mass ($\bar{M}_v$). This average molar mass is determined from the viscosity of dilute solutions in function of the hydrodynamic volume of the solute in the solution (in other words, its molar mass). The viscosity average molar mass can be calculated by Eq. (3):

$$\overline{M}_v = \left[\frac{\sum_{x=1}^{\infty} N_x (M_x)^{1+a}}{\sum_{x=1}^{\infty} N_x M_x} \right]^{\frac{1}{a}} \quad (3)$$

where a is a constant dependent of the polymer, solvent and temperature.

The ponderable distribution of $\overline{M}_n$, $\overline{M}_w$, and $\overline{M}_v$ can be represented by a molar mass distribution curve. A schematic representation is shown in Figure 1.

Figure 1 - Molar mass distribution curve typical of a polymer showing the three main mean values ($\overline{M}_n$, $\overline{M}_w$, and $\overline{M}_v$).

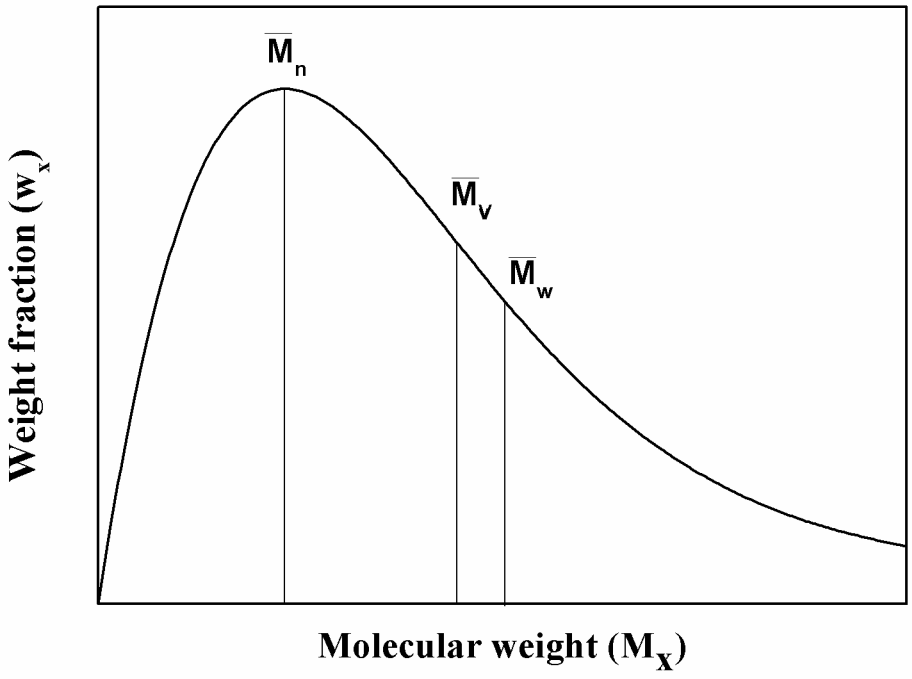

Source: Author himself.

From the definition of each average type it can be proved that this always has the same sequence $\overline{M}_n < \overline{M}_v < \overline{M}_w$. A simple form to know how wide or narrow is the molecular mass distribution curve is through of dispersion (D), that is defined by ratio between the $\overline{M}_w$ and $\overline{M}_w$, as show in Eq. (4):

$$D = \frac{\overline{M}_w}{\overline{M}_n} \quad (4)$$

When the difference between $\overline{M}_w$ and $\overline{M}_n$ is small, the mass molar dispersion is narrow and when not, it is wide.

2.2 POLY(ε-CAPROLACTONE)

The poly(ε-caprolactone) (PCL) is an aliphatic polyester with melting temperature between 329.15 - 338.15 K and glass transition temperature of 213.15 K. Its official nomenclature according to the International Union of Pure and Applied Chemistry (IUPAC) is (1,7)-polyoxepan-2-one. This polymer has been part of the group of polymers defined as absorbable and bioresorbable.

The absorbable and bioresorbable polymers are materials with characteristics to be degraded and eliminated from the human body as low molar mass by-products, with no residual side effects (COMIM et al., 2013; BENDER et al., 2010a).

Figure 2 shows the chemical structure of ε-caprolactone (ε-CL) in its cyclical form and the monomeric unit of the PCL with the ring open.

Figure 2 - (a) Chemical structure of ε-caprolactone; (b) Chemical structure of the repeating monomeric unit of poly(ε-caprolactone).

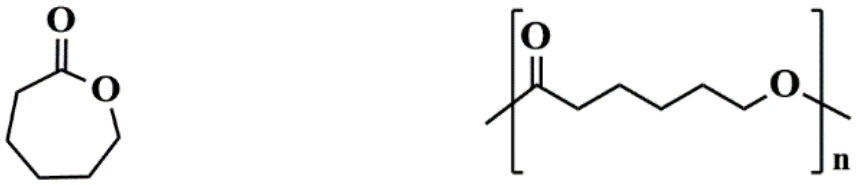

(a) **(b)**

Source: Author himself.

The physical, thermal and mechanical PCL properties depend on its molar mass and crystallinity degree. The PCL has a rare property to be miscible in others polymers, such as, poly(vinyl chloride), poly(styrene-acrylonitrile), poly(acrylonitrile

butadiene styrene), poly(bisphenol-A), polycarbonates, nitrocellulose and cellulose butyrate. The PCL also has the properties to be mechanically compatible with polyethylene, polypropylene, natural rubber, poly(vinyl acetate) and poly(ethylene-propylene) rubber (ALBUQUERQUE et al., 2014).

Due to the great versatility, degradability, miscibility, and compatibility with a large number of polymers the production of PCL was much studied in the 90's and 2000's (MACDONALD et al., 1995; HENDERSON et al., 1996; DENG; GROSS, 1999; KUMAR; GROSS, 2000; BANKOVA et al., 2002; MEI; KUMAR; GROSS, 2003; KUNDU et al., 2011; JOHNSON; KUNDU; BEERS, 2011).

It was described in literature two main pathways to produce PCL: polycondensation of a hydroxycarboxylic acid of 6-hydroxyhexanoic, and the ring-opening polymerization (ROP) of lactones (LABET; THIELEMANS, 2009). Synthesis of PCL by ROP can be performed by enzymatic, organic and metal catalysts. However, biomedical and food applications require highly pure polymers. Thus, in order to produce a polymer free of toxic residues, the ring-opening polymerization via enzyme-catalyzed reaction, also known as enzymatic ring-opening polymerization (e-ROP), stands out in relation to the other techniques.

Figure 3 shows the kinetic reactions mechanism of PCL synthesis by enzyme-mediated proposed by Johnson, Kundu and Beers (2011). This mechanism can be considered the more complete of literature and is based in a mechanism presented by Gross, Kumar and Gross (2003), however reorganized in four steps: (1) ring opening; (2) initiation; (3) propagation of linear polymers; (4) propagation of cyclic polymers.

Currently, the search a PCL production without toxic residues from metallic catalysts and organic solvents for direct application in the medical, pharmaceutical and food areas. An alternative found was to produce a catalyst PCL using enzymes in supercritical CO_2 (LOEKER et al., 2004; THURECHT et al., 2006; COMIM et al., 2013; COMIM et al., 2015). This technology is effective, because solvent and enzyme can be recovered at the end of the process, thus providing both enzyme and solvent reuse. There are works in the literature such as COMIM et al. (2015) that have been able to produce PCL with $\bar{M}_n$ of 35,800 g.mol^{-1}.

Figure 3 - Kinetic reactions mechanism of poly(ε-caprolactone) synthesis by enzyme-mediated.

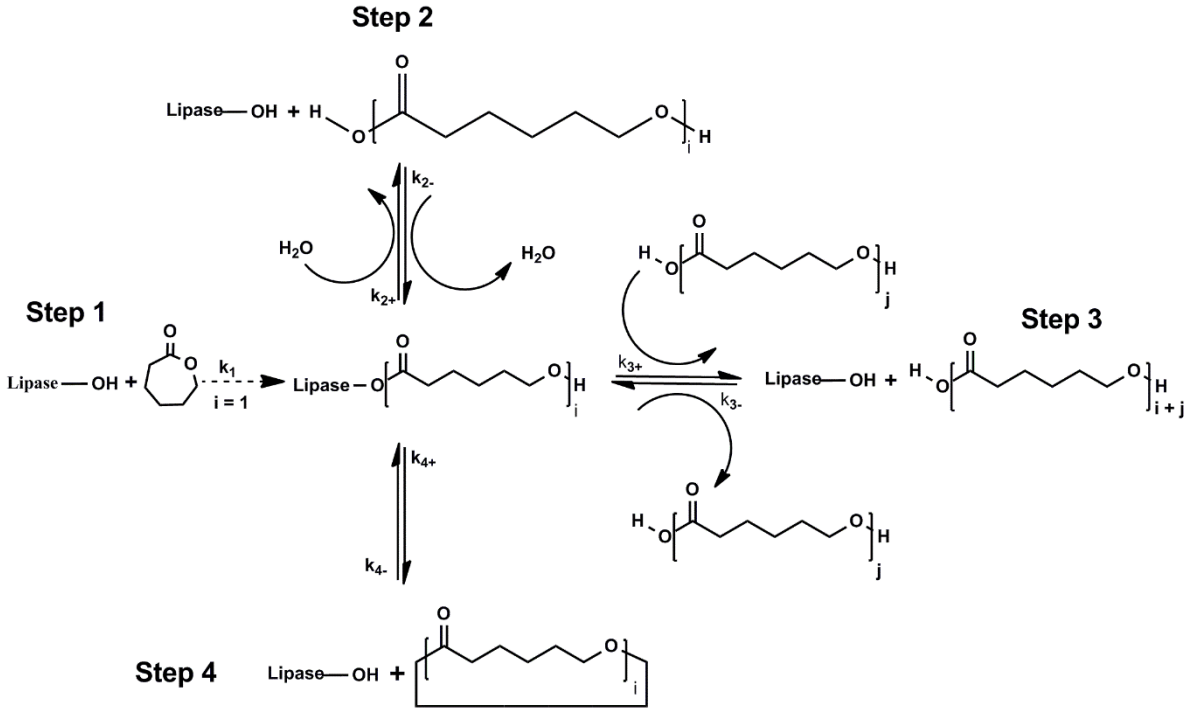

Source: JOHNSON; KUNDU; BEERS, 2011

2.3 WATER EFFECT ON POLYMERIZATION REACTION

The water (H_2O) has an important role in the polymerization process of lactones by e-ROP, because the H_2O content present in the reaction medium determines the molar mass of the polymer. Dong et al. (1999) and Mei, Kumar and Gross (2003) carried out a series of experiments with different H_2O content in ε-CL and verified that high H_2O content provides the formation of polymers with low molar mass, whereas the opposite is noted for low H_2O concentrations.

Water can act as an initiator in the e-ROP and H_2O has an important role in the conformation and flexibility of enzymes, which enables greater stability of enzymes.

According to Lee et al. (1998), the enzymes contain three H_2O levels, Eq. (5). The first level is the H_2O strongly linked to the enzyme (B_1), in other words, H_2O is not available for exchange, but this H_2O stabilizes the enzyme's active conformation by hydrating all polar and ionic groups. The second level is the H_2O poorly linked to the

enzyme (B_2). In this second level, the H_2O promotes the complete coverage of hydrogen bonding sites and form a monolayer on all non-polar surfaces. As the H_2O molecules in this level are poorly linked with the enzyme, this H_2O can be exchanged with the H_2O of level three (B_3), the free H_2O, in other words, the H_2O of level three don't have a specific function in the enzyme.

$$\left(H_2O\right)_{B_1} \leftarrow \times \rightarrow \left(H_2O\right)_{B_2} \leftrightarrow \left(H_2O\right)_{B3} \tag{5}$$

Eq. (5) presents a simple schematic form showing these three H_2O levels with possible variations of water molecules in which exchanges between layers B_2 and B_3 are freely released while for variations B_1 and B_2 not.

In this way, it is evident that to control the e-ROP it is necessary to know the ideal water content in the reactional medium.

2.4 SUPERCRITICAL FLUIDS

Supercritical fluids (SCF) are defined as any pure substance in which the temperature and pressure are above its critical conditions, in other words above of critical temperature (T_c) and critical pressure (P_c), as shown in Figure 4.

Close to the critical density, SCFs display properties that are to some extent intermediate between those of a liquid and a gas (COOPER, 2000). For example, a SCF may be relatively dense and dissolve certain solids while being miscible with permanent gases and exhibiting high diffusivity and low viscosity. In addition, supercritical fluids are highly compressible and the density (and therefore solvent properties) can be "tuned" over a wide range by varying pressure, as shown in Figure 5.

The supercritical carbon dioxide ($scCO_2$) has T_c of 304.19 K and T_c 7.38 MPa. These properties are obtained easily in the industrial process. Furthermore, the $scCO_2$ has good characteristics (low-cost solvent, inert, non-toxic and non-flammable) and favorable transport properties that can accelerate the mass transfer in chemical reactions (COMIM et al., 2013; REBELLATO et al., 2018a).

The $scCO_2$ is a commercially viable solvent for the synthesis of organic compounds in the industry, mainly because it can be removed from polymerization

products by simple depressurization. This promotes the obtaining of a clean and dry product, which can reduce the costs to the recuperation of the final product in industrial scale (LICENCE et al., 2003).

Figure 4 - Schematic P-T diagram for a pure component showing the liquid phase region, solid phase region, the vapor phase region, the supercritical fluid (SCF) region, the critical point and triple point.

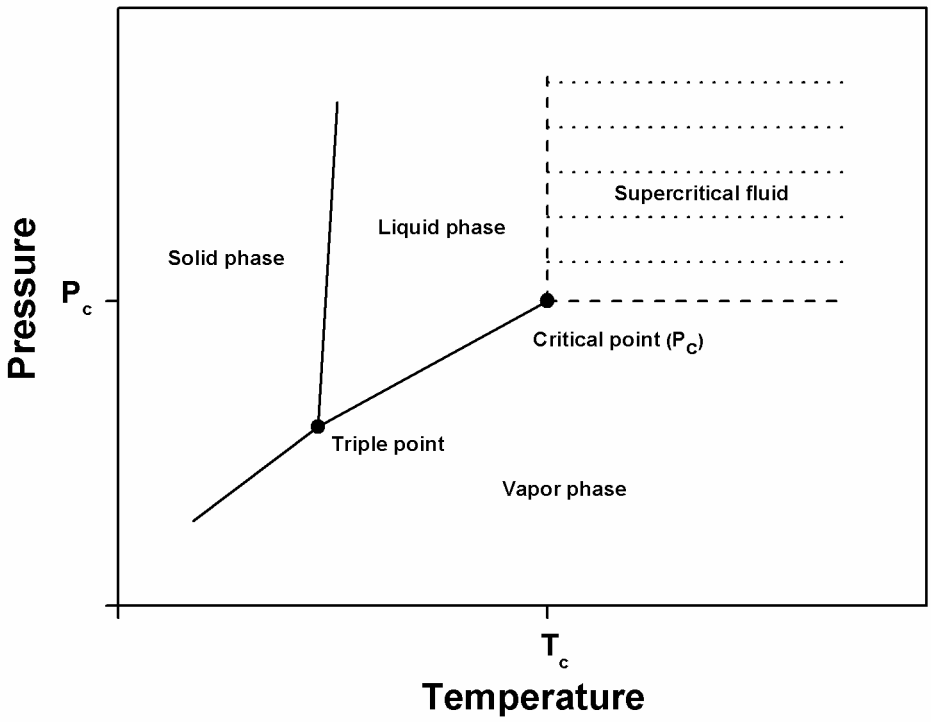

Source: Adapted from REBELATTO, 2018

One of the main advantages cited for the use of supercritical fluids as solvents in chemical reactions is the fact that the values of the physical properties of these fluids are favorable for the reaction kinetics when compared to the typical values for a liquid solvent. Lower viscosity and higher diffusivity are the most cited advantages, but others, like heat capacity, have also been mentioned. Bringing all reactants into the same phase eliminates the resistance of mass transport across the gas–liquid (or solid)

interface. All of this, of course, holds true only when the reaction medium is a single phase (NUNES DA PONTE, 2009).

Figure 5 - Variation in density for pure CO_2 at 308.15 K. At this temperature (i.e., close to T_c for CO_2) there is a rapid but continuous increase in density near the critical pressure (P_c).

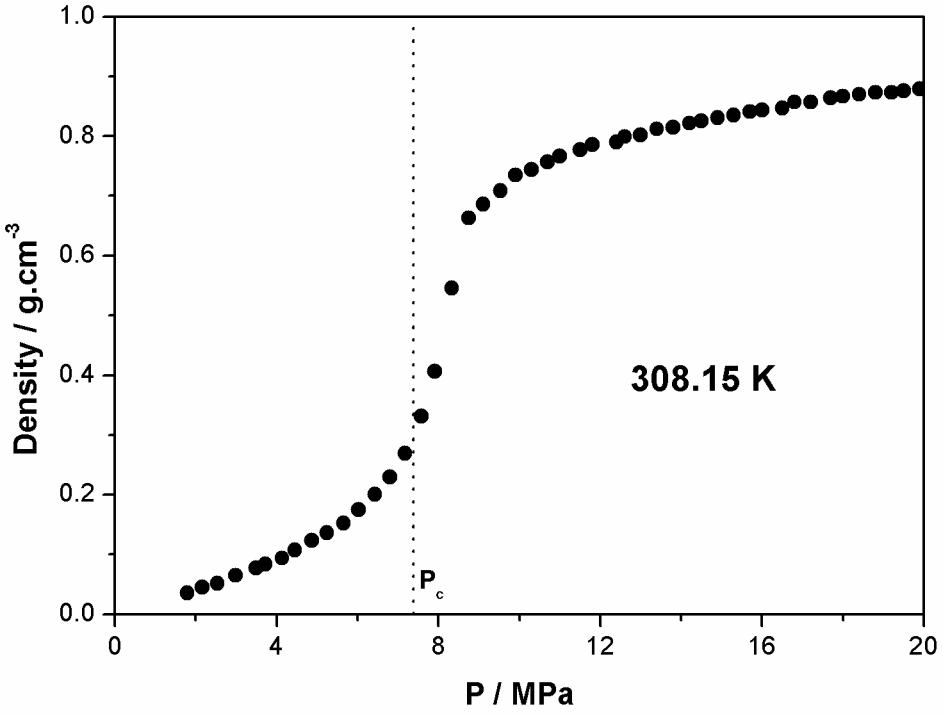

Source: Adapted from COOPER, 2000

Therefore, in order to understand the chemical reaction aspects, as the mass transfer, macromolecule size, dispersion, etc., it is necessary to determine the phase equilibrium between the reactants involved (SCF, monomer, co-solvent, polymer, among others). Through the temperature and pressure variation, in a given composition, it is possible to observe if the system is in a single-phase, two-phase or three-phase. For example, in heterogeneous catalysis (two-phase or three-phase and immobilized enzyme) possibly the chemical reaction will be smaller conversion or the chemical reaction time will present a low comparison with homogeneous catalysis (single-phase), invalidating the chemical reaction under these conditions of composition, temperature, and pressure. Thus, the viability of chemical reaction can only be confirmed by studying the phase behavior in question (BENDER, 2014).

2.5 PHASE BEHAVIOR AT HIGH PRESSURES

The study of phase behavior depends strongly of the energetic interactions and differences between chemical species involved in the systems. Both effects are always present and the results depend on temperature, pressure and system composition. The obtained phase equilibrium experimental data is very important, even when thermodynamic models are used. Although mathematical modeling can help reduce the number of experiments, it is necessary to adjust the interaction model (DOHRN, BRUNNER, 1995).

The high pressure polymerization process needs knowledge of its phase behavior. For example, solubility data, solid-phase formation, supersaturation of the system, etc., can be determined through phase equilibria experiments. The polymeric systems often exhibit the phase separation on liquid-liquid type, and depends of temperature, pressure, molar mass, and dispersion. Typically, when an increase in temperature occurs, particularly in regions close to the critical point of the solvent, polymeric solutions exhibit liquid-liquid immiscibility due to the “free volume” difference between the polymer and solvent molecules, this effect being caused by the greater expansiveness of the solvent relative to the polymer (CHEN; RADOSZ, 1992; KONTOGEORGIS; SARAIVA; FREDENSLUD, 1995).

In the phase transitions in which an increase in pressure transition occurs as a function of increased temperature gives the name Lower Critical Solution Temperature (LCST), i.e. $(\partial P/\partial T)_x > 0$. In this type of transition, it is assumed that the differences between solute and solvent free volume decrease with increasing pressure, making them more “compatible”. In the case of a decrease in temperature, this is the behavior called Upper Critical Solution Temperature (LCST), i.e. $(\partial P/\partial T)_x < 0$. In this case, the polymeric solutions exhibit a region with limited solubility due to differences between the energetic interactions between polymer and solvent. If temperatures are between UCST and LCST, the system will be miscible for all compositions (PRAUSNITZ; LICHTENTHALER; AZEVEDO, 1999).

To date, there are few studies in the literature involving the study of phase equilibrium of ε-CL and PCL. In Table 2, there is presented an overview of the existing

works in the literature about phase equilibrium data of ε-CL and PCL systems at high pressures.

Note in Table 2 that the studies evaluated only the behavior of phases of binary systems [CO_2 + ε-CL] and [CO_2 + PCL], ternary systems [CO_2 + CH_2Cl_2 + PCL] and [CO_2 + $CHCl_3$ + PCL], but there are no studies that evaluate the phases behavior of the ternary systems [CO_2 + CH_2Cl_2 + ε-CL] and quaternary system [CO_2 + CH_2Cl_2 + ε-CL + PCL].

Table 2 - An overview of the existing works in the literature about phase equilibrium data of ε-caprolactone and poly(ε-caprolactone) systems at high pressures.

System	*T*/K	*P*/MPa	Transition type	References
Binary system				
CO_2 + ε-CL	303.15 - 343.15	3.46 - 20.83	VLE - LLE - VLLE	Bender et al., 2010b
	323.15 - 383.15	7.48 - 33.90	VLE	Bergeout et al., 2004
	313.15 - 363.15	8.30 - 19.60	VLE	Xu et al., 2003
CO_2 + PCL	393.15 - 503.15	203 – 284	VLE	Bang; Lee, 2019
	314.15 - 335.15	6.10 - 27.10	VLSE	de Paz et al., 2010
Ternary system				
CO_2 + CH_2Cl_2 + PCL	303.15 - 343.15	2.86 - 20.89	VLE - LLE - VLLE	Bender et al., 2010a
	308.15 - 373.15	3.46 - 19.25	VLE - LLE	Kalogiannis; Panayiotou, 2006
CO_2 + $CHCl_3$ + PCL	308.15 - 373.15	4.11 - 20.13	VLE - LLE	Kalogiannis; Panayiotou, 2006

That is, there is a lack in the literature concerning studies evaluating the interaction between the ε-CL and PCL. The knowledge of this interaction is important for the application of the mathematical model developed by Johnson, Kundu and Beers (2011) in the polymerization system of PCL in high pressure. In other words, it is necessary to know the thermodynamic behavior of all chemical species present in the polymerization reaction as CO_2, ε-CL, and PCL. In addition, also it is necessary to

know the behavior of the H_2O, which is the initiator of the reaction of polymerization, and the CH_2Cl_2, which can be added as co-solvent to improve the solubility of PCL in the reaction medium.

2.6 CLASSIFICATION OF BINARY SYSTEMS

Scott and van Konynenburg (1970) showed that it is possibly to classify the phase diagrams in five basic types. These phase diagrams can be described by van der Waals equation (1873). The objective is to determine the critical lines of the system in pressure, temperature, and composition coordinates. Differences that occur in the phase behavior in binary mixtures can be qualitatively related in terms of changes in thermodynamic properties near the critical points. These phase diagrams can be grouped or not by presence of three phase lines, for the liquid-vapor-liquid equilibrium and the way in which these critical lines are connected (VAN KONYNENBURG; SCOTT, 1980).

Rowlinson and Swinton (1982) introduced a phase diagram of the sixth type. This phase diagram is found in the system containing water and it can be described though potential functions.

Figure 6 shows the six types of phase diagrams. These phase diagrams exhibit liquid-liquid immiscibility, except for Type I, and can occur due the molecular asymmetry (size difference, polarity, and molecular functionality) between components.

In Figure 6, the liquid phases that presented different compositions are identified as l_1 or l_2. The three-phase equilibrium is indicated as $l_1 l_2 g$ (liquid-liquid-vapor). The critical points of the mixture ($l_1 = g$) represented the curve formed by all points where a liquid and a vapor phase coexist with the same composition. The curve formed by two liquid phases is indicated by $l_1 = l_2$. The points where two critical liquid phases (with the same composition) are in equilibrium with a vapor phase are identified by $l_1 = l_2 + g$. When there is a coexistence of a liquid phase with a gas phase (same composition) in equilibrium with other liquid phase, so $l_1 = g + l_2$. In these last two cases ($l_1 = l_2 + g$ and $l_1 = g + l_2$), at the pressure and temperature that represent

these points, it occurs the disappearance of a liquid phase. If this occurs with increasing temperature, it happens a point known as Upper Critical End Point (UCEP). If this occurs with temperature decrease, the point is known as Lower Critical End Point (LCEP). The UCEP and LCEP points are related to the disappearance of a liquid phase in the vapor-liquid-liquid equilibrium because the temperature variation.

Figure 6 - Classification of *P-T* diagrams of binary systems (Classification of van Konynenburg and Scott (1980)).

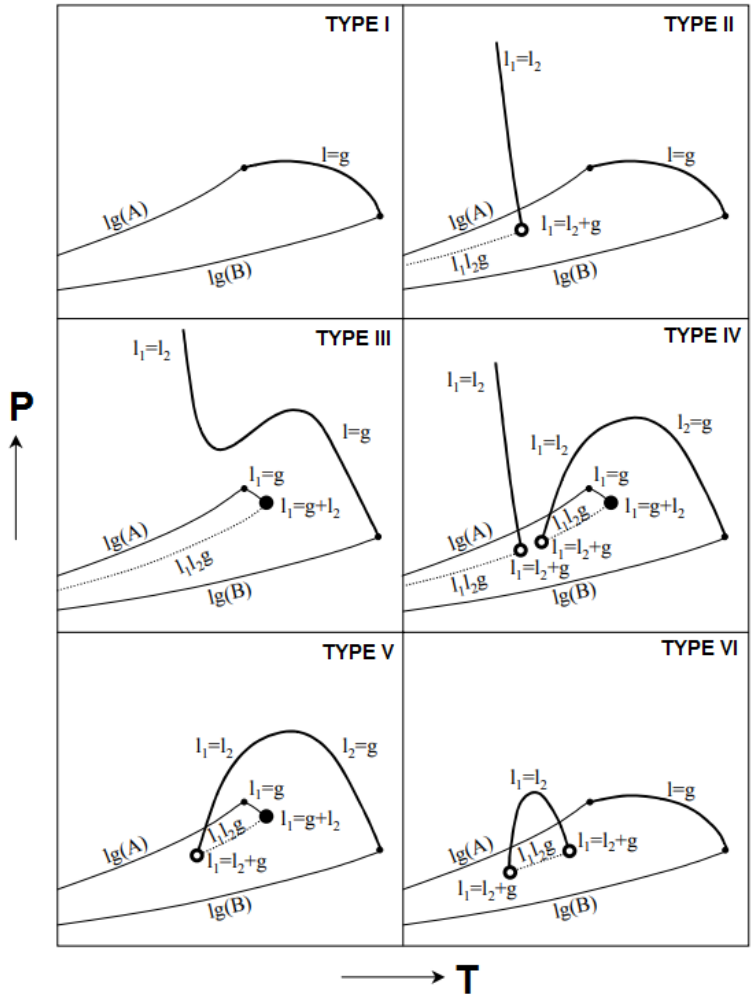

Source: ESPINOSA, 2001

2.6.1 Type I – Phase behavior

In Figure 7, it is shown a simple case of the diagram of Type I, the line ending at C_1 is the vapor-liquid coexistence curve for pure 1 while the line ending at C_2 is the vapor-liquid coexistence curve for pure 2. C_1 and C_2 are the critical points. The dashed

line joining these points is the critical locus; each point on that line is the critical point for a mixture of fixed composition. The continuous vapor-liquid critical line and the absence of liquid-liquid immiscibility is often observed for mixtures where the two components are chemically similar and/or their critical properties are comparable. Typical examples are methane/ethane, carbon dioxide/*n*-butane, and benzene/toluene (PRAUSNITZ; LICHTENTHALER; AZEVEDO, 1999).

Figure 7 - Phase diagram (Type I): (a) *P-T-*x surface; (b) *P-T* projection showing vapor-liquid equilibria for a simple binary mixture.

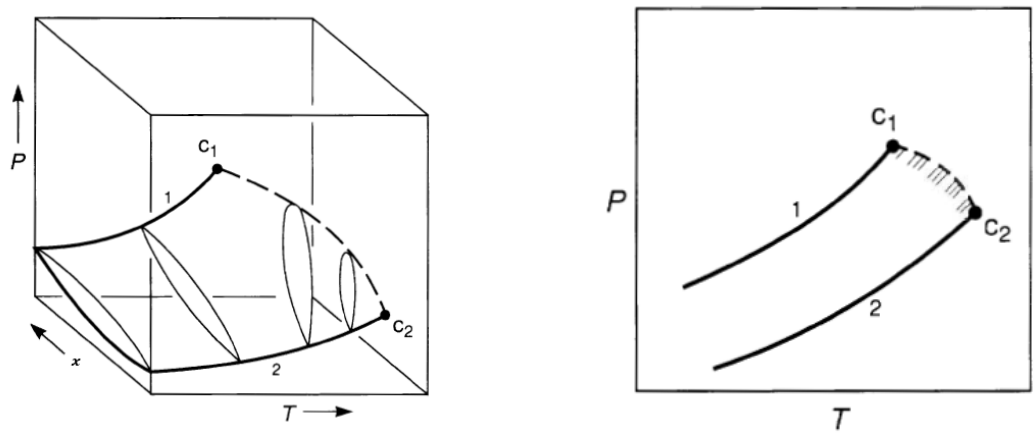

(a) **(b)**

Source: Adapted from PRAUSNITZ; LICHTENTHALER; AZEVEDO, 1999.

2.6.2 Type II – Phase behavior

This type of phase behavior is similar to Type I, however in temperatures below the critical temperature of the most volatile compound, a liquid-liquid immiscibility occurs.

In Figure 8, it is observed the *P-*x, *T-*x and *P-T* projection of phase behavior of Type II. These diagrams are related to each other through dotted lines. The *P-*x diagram shows the behavior of seven isotherms (increasing of T_1 to T_7), where T_1, T_2 and T_3 exhibit beyond of vapor-liquid-liquid (VLLE) and liquid-liquid (LLE) equilibrium, while T_4 to T_7 only exhibit vapor-liquid (VLE) equilibrium.

Isotherms that are under the critical temperatures of compounds A and B intersect the vertical axes at vapor pressures on pure components. In relation to the isotherms that are over the critical temperature of compound A, has a critical point of the mixture more near B as the temperature increase. The discontinuous line $l = g$ (shown in the three diagrams) that goes de C_A to C_B unites all the critical points of binary mixture. For the isotherm T_3, the low pressures, the vapor phase is on the equilibrium with a liquid phase.

Figure 8 - Phase diagram (Type II): (a) *P-x*, *P-T* and *T-x* projections.

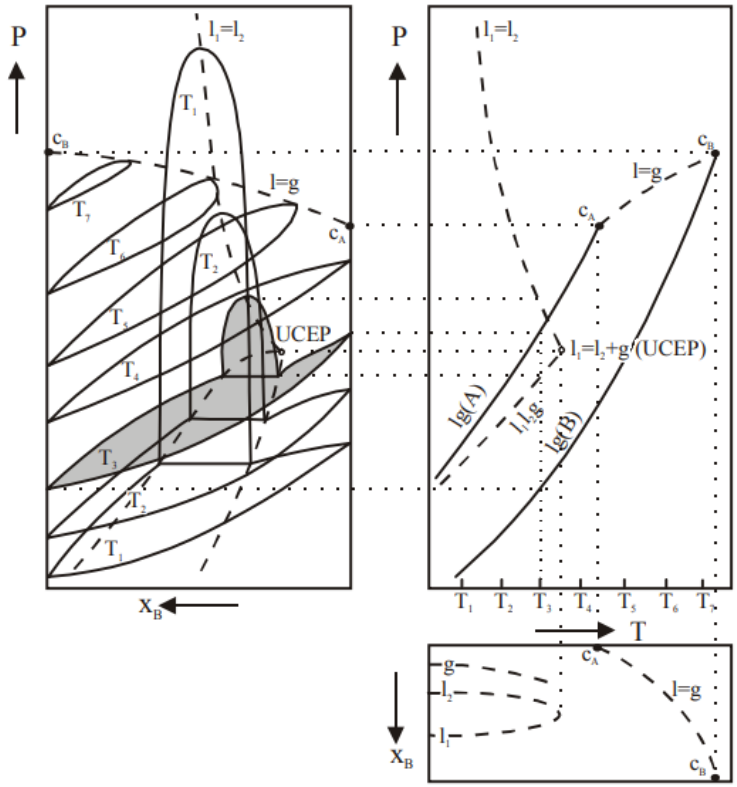

Source: ESPINOSA, 2001

With the increase of pressure, the liquid phase is divided into two liquids phases (l_1 and l_2), of different compositions. Thus, for each temperature will be a pressure in which there are three phases in equilibrium. Uniting all three-phase equilibrium points and projecting over the *P-T* plan, it is obtained the llg line. The characteristic domain of the liquid-liquid equilibrium decreases as the temperature increase, to the point $l_1 = l_2 + g$ where the second phase disappears, corresponding to the UCEP (PRAUSNITZ; LICHTENTHALER; AZEVEDO, 1999; NDIAYE, 2004).

The maximums of the liquid-liquid immiscibility zone are united by the discontinuous line $l_1 = l_2$. The line $l_1 = l_2$ correspond the critical points of solution (CST and CSP). The region size of liquid-liquid immiscibility decrease with the temperature increase to the pressure constant (UCST) or with the increase of pressure maintain the temperature constant (UCSP) (NDIAYE, 2004).

2.6.3 Type III – Phase behavior

In cases where the mixture liquid-liquid immiscibility is sufficiently large, three-phase region presented in conditions very close to critical point of more volatile component. In this case, the axes of liquid-liquid equilibrium critical line are displaced for temperature more elevates, can intercept the vapor-liquid equilibrium critical line, dividing into two branches. The first one started in the critical point of the component more volatile and join the $l_1 = l_2$ line in high pressures. Already the second branch start at the critical point of compost more volatile and intercept the three-phase line in the point $l_1 = g + l_2$, which by definition corresponds to a terminal upper critical point.

The Type III diagrams characterized by the intersection of regions with phase coexistence, besides presenting a divergent line of critical points. The Figure 9 shows the evolution of liquid-liquid immiscibility in different temperatures. It is observed from the *P-x* diagram that an increase of temperature from C_B modifies the three-phase region form, with a type of gradual transition from typical equilibrium $l = g$ forms for those with a characteristic domain of liquid-liquid equilibrium. In all cases, the critical locus extends from the critical point of less component volatile (B) to the high pressure zone (PRAUSNITZ; LICHTENTHALER; AZEVEDO, 1999).

In Figure 10, it is observed as the critical locus can vary greatly, as the differences between the components increases. These diagrams are typical of binary mixture involving CO_2 with hexadecane, 2-5-hexanediol and water.

Figure 9 - Phase diagram (Type III): (a) *P-x*, *P-T* and *T-x* projections.

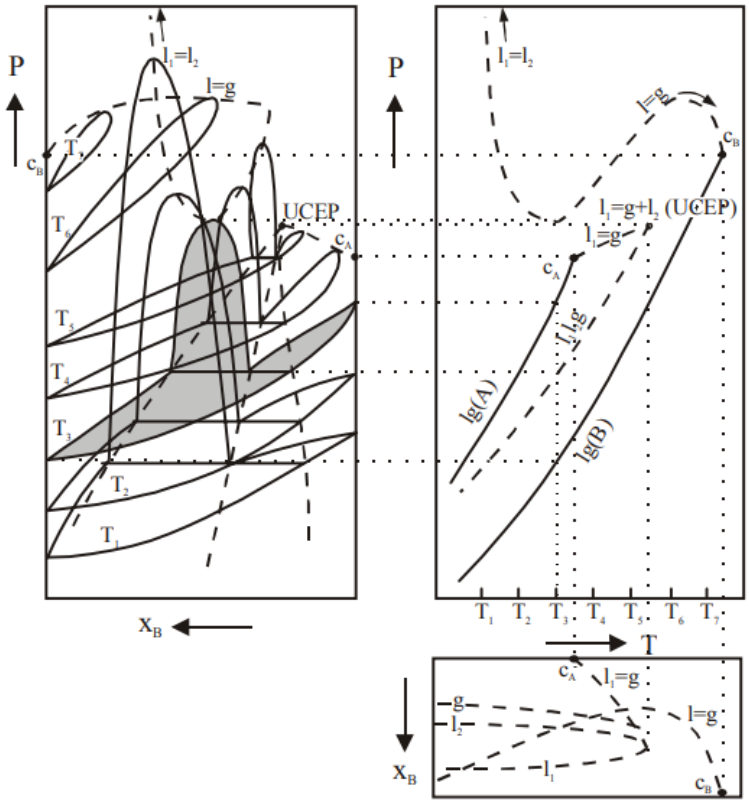

Source: ESPINOSA, 2001

Figure 10 - Phase diagram (Type III): Possible forms of critical lines $l = g$ and $l = l$.

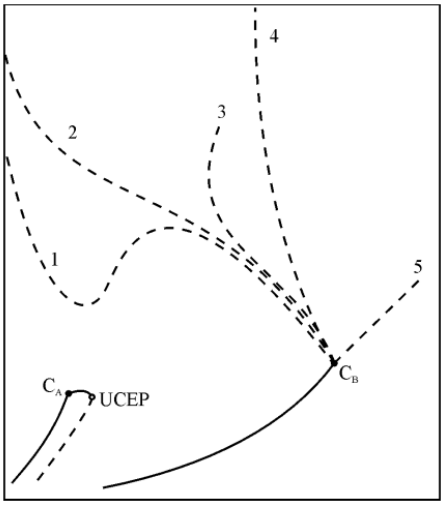

Source: ESPINOSA, 2001

2.6.4 Type IV – Phase behavior

The Type IV diagrams are obtained when the critical points line of the Type III diagrams bend to intercept the three-phase equilibrium curve $l_1 l_2 g$, obtaining the Type IV diagram with three critical curves: $l_1 = g$, $l_2 = g$ and $l_1 = l_2$. This diagram is similar to the Type V and it result to show a critical line from the critical point of the least volatile compound and converges to the phase equilibrium line with a transition continues of $l = g$ and $l = l$. At low temperatures, presents liquid-liquid equilibrium, which disappears at the point $l_1 = l_2 + g$, corresponding to the UCEP (BENDER, 2008; NDIAYE, 2004).

In Figure 9, it can be observed that, at high temperatures, occurs other point $l_1 = l_2 + g$, where a second liquid phase appears, corresponding to the LCEP, the three-phase equilibrium extends to a third point $l_1 = l_2 + g$ where occurs the disappearance of one of liquid phases, corresponding to the UCEP. The part of the three-phase curve observed at low temperature is similar to the behavior of Type II diagrams (Figure 8), with the critical line $l_1 = l_2$ ending in a UCEP, so that the behavior of the liquid-liquid immiscibility region can be analyzed from the *P*-x diagram in Figure 8. The CO_2/n-tridecane system exhibits this type of behavior (BENDER, 2008; NDIAYE, 2004).

2.6.5 Type V – Phase behavior

The Type V diagrams are in fact Type IV diagrams with LCEP hidden due to the presence of the solid phase. Diagrams of these types are hard to get experimentally, knowing that the solidification occurs beneath of LCEP or in some cases even above this. Figure 11 shows the *P*-x, *T*-x and *P*-*T* projection of the binary system with this behavior. As in the latter case, the critical line that is born on critical point C_B changes continuously of $l - g$ to $l - l$, as can be observed in the *P*-x projection.

Binary mixtures of alkanes exhibit this behavior type from a certain number of carbons. For example, mixtures with methane, the first hydrocarbon with liquid-liquid

immiscibility is the n-hexane, while for mixtures with ethane, the liquid-liquid immiscibility is the n-nonadecane.

This behavior type was also observed by Bender (2008) in the phase equilibrium between CO_2 and ε-CL. Near the CO_2 critical temperature (T_c = 304.21 K), there were found liquid-liquid transitions, and with the increase of temperature, the immiscibility region disappear.

Figure 11 - Phase diagram (type V): (a) *P-x*, *P-T* and *T-x* projections.

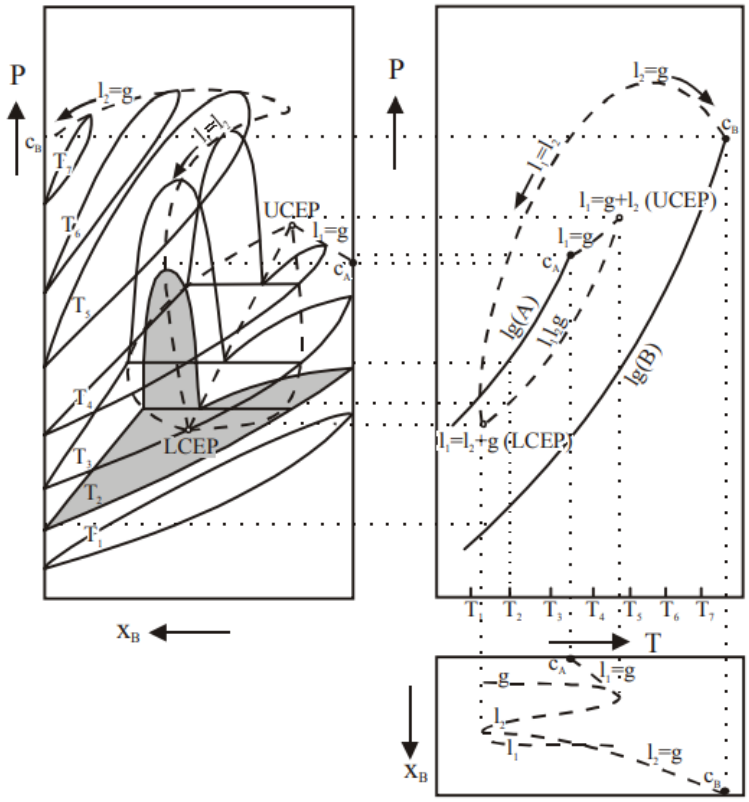

Source: ESPINOSA, 2001

2.6.6 Type VI – Phase behavior

This behavior is in binary systems where the compounds have any association degree. There is in this case, a liquid-liquid immiscibility region with a critical line that starts at one LCEP and converges to one UCEP. The critical line $l - g$ is similar to that shown in the Type I diagram.

Examples of this complex type of behavior are found in mixtures where one (or both) component is auto-associated by hydrogen bonds. An example of this type is

the H_2O/ethanol. In this diagram type, the solid phase occurs at low temperatures, not affecting phase behavior.

2.7 EXPERIMENTAL METHODS FOR DETERMINING PHASE EQUILIBRIUM

In literature it is presented and discussed different experimental methods for investigation of high pressure phase equilibria (FOENARI; ALESSI; KIKIC, 1990; DOHRN; BRUNNER 1995; BENDER, 2008). In general, it can be divided into two classes, depending on how the composition is determined: analytical methods (or direct sampling methods) and synthetic methods (or indirect methods). The experimental. The experimental methods can be divided into three categories, confirming the classification presented by Vieira de Melo (1997):

- Dynamic methods
  - Extractives (saturation)
  - Continuous
- Static methods
  - Synthetic
  - Analytical
- Recirculating Methods

The dynamic methods are those in which at least one of the phases of the system is subject to displacement relative to another. The two types of dynamic methods differ in the way in which the contact between the phases involved in equilibrium is established. Static methods present as a fundamental feature the fact that the system is closed. In this case, the coexisting phase compositions may be determined indirectly (synthetic) or directly, with taking samples from equilibrium phases for further analysis (analytical). Already the method with recirculation can be considered as dynamic, since there is a flow of one phase over another, or as static, due to the similarities in the sampling phase of the equilibrium phases.

2.8 THERMODYNAMIC MODELING OF PHASE EQUILIBRIUM

The calculus for the phase equilibria consists in the determination of the conditions of temperature, pressure, and composition in which occurs the equilibrium. In the multiphase system and multicomponent, where are a mechanic and thermic equilibria, it is necessary the thermodynamic equilibrium, in other words, it is necessary to calculate the fugacity in all phase.

The fugacity calculus can be made by thermodynamic models. These models can be totally empiric or based on simplified molecular models (the family of van de Waals equations and activity coefficients models), or by equations originating from statistical thermodynamics as the virial equations of state and the perturbation theory (PRAUSNITZ; LICHTENTHALER; AZEVEDO, 1999).

The development of equations to describe the phase behavior in systems that contain macromolecules is hard. The key issue is that the molecular architecture is not spherical and it has a strong influence in macroscopic thermodynamic behavior of the solutions, therefore the phase equilibrium of polymeric solutions depends strongly of the energetic interactions and size difference between the polymer molecules and of the solvent (KIAO; CARUTHERS; CHAO, 1996).

The thermodynamic models utilized for the study of the phase behavior of a high pressure system can be divided into two groups: cubic equation of state and perturbation models.

2.8.1 Thermodynamic models

2.8.1.1 Cubic equation of state

The first cubic equation was proposed by van der Waals (vdW-EoS) (1873), as shown:

$$P = \frac{RT}{v-b} - \frac{a}{v^2} \tag{6}$$

where P is the absolute pressure (MPa), T is the absolute temperature (K), a and b are called van der Walls constants, whose values depend upon the particular gas and

independent of temperature. Where a reflects how strongly the molecules of a gas attract each other and b reflects the size of the molecules (ATKINS; DE PAULA, 2008).

From the van der Waals equation many others cubic equation of state were proposed, for example Soave-Redlich (SR-EoS) (1949), Soave-Redlich-Kwong (SRK-EoS) (1972) and, Peng-Robison (PR-EoS) (1976).

The van der Waals cubic equations of state are usually presented through the following generic cubic state equation proposed by Smith, van Ness and Abbott, (2007):

$$P = \frac{RT}{v-b} - \frac{a(T)}{(v+\varepsilon b)(v+\sigma b)} \tag{7}$$

From Eq. (7), through the appropriate choices of $a(T)$, ε and σ the vdW-EoS, SR-EoS, SRK-EoS and PR-EoS are obtained. For example, when fixed $a(T) = a$, ε = 0 and σ = 0 vdW-EoS is obtained. In Table 3, it is shown the other numeric value of $a(T)$ ε and σ for other cubic state equations.

Table 3 - Parameters of state equations for use in the generalized equation, Eq. (7).

EoS	$a(T)$	σ	ε
vdW (1873)	1	0	0
RK (1949)	$T_r^{-1/2}$	1	0
SRK (1972)	$\alpha_{SRK}(T_r;\omega)$ *	1	0
PR (1976)	$\alpha_{PR}(T_r;\omega)$ **	1+$\sqrt{2}$	1-$\sqrt{2}$

* $\alpha_{\mathrm{SRK}}(T_r;\omega) = \left[1+\left(0.480+1.574\omega-0.176\omega^2\right)\left(1-T_r^{1/2}\right)\right]^2$

** $\alpha_{\mathrm{PR}}(T_r;\omega) = \left[1+\left(0.37464+1.54226\omega-0.26992\omega^2\right)\left(1-T_r^{1/2}\right)\right]^2$

Source: Adapted from SMITH; VAN NESS; ABBOTT, 2007

To calculate the coefficients a and b, Eq. (7), can be used the rules of quadratic mixture from van der Waals:

$$a = \sum_{i=1}^{n}\sum_{j=1}^{n} x_i x_j a_{ij} \tag{8}$$

$$b = \sum_{i=1}^{n}\sum_{j=1}^{n} x_i x_j b_{ij} \tag{9}$$

where a_{ij} is an attractive parameter present in the equation of state in relation to the molecules of components i and j and b_{ij} represents the repulsion between the molecules of the system components. For the calculus of a_{ij} and b_{ij} the following combination rules are used:

$$a_{ij} = \left(a_i a_j\right)^{0.5}\left(1 - k_{ij}\right) \tag{10}$$

$$b_{ij} = \frac{1}{2}\left(b_i + b_j\right)\left(1 - l_{ij}\right) \tag{11}$$

where k_{ij} and l_{ij} are adjustable parameters of binary interaction. The parameter k_{ij} is associated with the attraction energy between the molecules of the mixture (a_{ij}) and the parameter l_{ij} is associated with the repulsion energy between the molecules.

2.8.1.2 Perturbation models

In recent decades, it has been observed great interest in developing equations of state for pure fluids and for mixtures containing macromolecules. The essence of this progress is to use methods of statistical mechanics, as the perturbation theories, to relate the molecular properties with the macroscopic properties of the system of interest. In the perturbation models, a simple system is utilized as a reference. These reference systems incorporate basic aspects of a real system and is characterized by well-defined hypotheses. The difference between the real system and the reference system is computed by some correction terms. These correction terms are called perturbation terms and they are often based on semi-empirical models. The complexity and magnitude of the perturbations depend of precision degree with which the reference term can be specified (BENDER, 2008).

At the end of the 1980s and the start of the 1990s, Chapman et al. (1888, 1889, and 1990) presented a new model of the perturbation model family. This model is known as Statistical Associating Fluid Theory (SAFT) and it is based the Wertheim´s first order thermodynamic perturbation theory (TPT1) of Wertheim (1987). The essence of this theory is that the residual Helmholtz free energy is given from expressions that do not consider only the effects of repulsion and dispersion forces, but also takes into account two other effects: aggregation by chemical bonds (formation of stable chains) and the association and/or solvation (hydrogen bonds) between different molecules.

The main idea of the SAFT is the utilization of a reference system, which takes into consideration the length of the chain and molecular association in the place of the simpler hard sphere reference fluid. Thus, it is expected that the effects due to other intermolecular forces types (dispersion, induction, etc.) are weaker, thus being counted from a perturbation term. Therefore, it is expected that this theory will be capable to describe the major real fluids, like polymers and polar fluids.

From the SAFT theory publication, many other models were development from the modification of the equation of state terms. While the SAFT imposed the existence of a chain formatted by covalent bonded between spheres, the perturbation theory had used to represent the attraction forces only the force of the spheres, without considering the structure of the molecule formed, the responsibility of this interactions.

Since the dispersive forces appeared by potential induction in the molecules, the idea is that the behavior of these molecules can be represented if the attraction interactions were modeled considering the molecule structure. Using the perturbation development by Barker and Henderson (1967a). Gross and Sadowski (2001) developed an equation of state to model the dispersive interactions generated by long molecular chains. Gross and Sadowski (2001) introduced a term previously developed in the SAFT equation of state aiming at the better modeling of substances that are not associated, but which present a relevant molecule with regard to attraction interactions, as is the case of polymers.

Gross and Sadowski (2001) did not changed of the hard-sphere and hard-chain terms in the SAFT, omitted the association term and used a new term to

represent the dispersive forces, thus they proposed thus a new equation of state, the Perturbed Chain-Statistical Associating Fluid Theory (PC-SAFT). This equation of state was called as state-of-the-art model for polymer by Lindving, Michelsen and Konto (2004).

2.9 CONSIDERATIONS ON THE STATE OF THE ART

Based on the literature review exposed in this chapter, it is possible to see that there is no study about the phase equilibrium of the ternary system [CO_2 + CH_2Cl_2 + ε-CL] and quaternary system [CO_2 + CH_2Cl_2 + ε-CL + PCL] in high pressure. The study of these systems is important for the development and understand of the polymerization of the PCL in high pressure. In addition to obtain phase equilibrium data, thermodynamic modeling is also important, since through it is possible to simulate experimental conditions not tested, and thus a significant saving in time and operating cost. In this way, an investigation is necessary to determine phase equilibrium data of the ternary system [CO_2 + CH_2Cl_2 + ε-CL] and quaternary system [CO_2 + CH_2Cl_2 + ε-CL + PCL] in high pressure and the development of the thermodynamic modeling with the equation of states appropriate for these systems.

3. RESULTS AND DISCUSSION

3.1 HIGH PRESSURE PHASE EQUILIBRIUM DATA FOR THE TERNARY SYSTEM CONTAINNIG CARBON DIOXIDE, DICHLOROMETHANE, AND ε-CAPROLACTONE

The results presented in this chapter were published in **Journal of Chemical & Engineering Data**, v. 64, p. 2036-2044, 2019**. DOI:** https://doi.org/10.1021/acs.jced.8b01017**.**

Abstract

This work reports experimental phase equilibrium data for the ternary system involving carbon dioxide, dichloromethane and ε-caprolactone. Such data provide fundamental information to conduct polymerization reactions in supercritical carbon dioxide medium. The experiments were performed using a variable-volume view cell over the temperature range from 323.15 to 353.15 K and different mass ratios of dichloromethane to ε-caprolactone (0.5:1, 1:1 and 2:1). Phase transitions of vapor-liquid at the bubble point (VLE-PB), liquid-liquid (LLE) and vapor-liquid-liquid (VLLE) types were observed. The experimental results were modelled using the Peng-Robinson EoS with the van der Waals mixing rule, resulting in a good representation of experimental phase equilibrium data.

Keywords: High pressure phase equilibrium; supercritical carbon dioxide; dichloromethane, ε-caprolactone

3.1.1 Introduction

Recently, considerable attention has been given to the production of biocompatible, biodegradable and non-toxic aliphatic polyesters. These compounds play an important role in biomedical, pharmaceutical and food applications (DOBRZYNSKI, 2007; KULPREECHANAN, et. al., 2013; COMIM et al., 2013). One polyester that has received growing interest is poly(ε-caprolactone) (PCL) because besides being compatible it can be also degraded and eliminated from the human body

as low molar mass by-products, with no residual side effects (COMIM et al., 2013; BENDER et al., 2010a; BENDER et al, 2010b).

PCL is a semicrystalline polymer with melting temperature between 329.15 - 338.15 K (LABET; THIELEMANS, 2009). There are in the literature described two techniques for produce PCL: polycondensation of a hydroxycarboxylic acid of 6-hydroxyhexanoic, and the ring-opening polymerization (ROP) of ε-caprolactone (ε-CL) (LABET; THIELEMANS, 2009). Synthesis of PCL by ROP can be performed by enzymatic, organic and metal catalysts. However, biomedical and food applications require highly pure polymers. Thus, in order to produce a polymer- free of toxic residues, the ring-opening polymerization via enzyme-catalyzed reaction, also known as enzymatic ring-opening polymerization (e-ROP), stands out in relation to the other techniques (COMIM et al., 2013; THURECHT et al., 2006).

Literature reveals several studies on ε-CL polymerization in organic solvents, like toluene, benzene and cyclohexane (MEI et al., 2003; JOHNSON; KUNDU; BEERS, 2011; DONG et al., 1999). Nevertheless, these solvents are toxic and hence supercritical carbon dioxide ($scCO_2$) appears as a good candidate for replacing such solvents due to its well-known characteristics (low-cost solvent, non-toxic and non-flammable) and favorable transport properties that can accelerate the mass transfer in enzymatic reactions (COMIM et al., 2013; REBELLATO et al., 2018a).

Though $scCO_2$ may be a good solvent for ε-CL, it is not a proper solvent for PCL, leading to the sedimentation of its organic solutions upon mixing (BENDER et al., 2010b; KALOGIANNIS; PANAYIOTOU, 2006). An alternative to overcome such drawback is to use a co-solvent together with $scCO_2$, e.g., dichloromethane (CH_2Cl_2). CH_2Cl_2 is a colorless and volatile liquid at ambient conditions, being widely used as a solvent because it is considered one of the least harmful organochloride compounds (ROSSBERG et al., 2012).

The literature presents some experimental data for the binary system [CO_2 + CH_2Cl_2] at different temperatures (VONDERHEIDEM et al., 1963; GONZALEZ et al., 2002; CORAZZA et al., 2003; TSIVINTZELIS et al., 2004; LAZZARONI et al., 2005; SHIRONO et al., 2008; SHIN et al., 2008). Gonzalez et al. (2002) investigated the high pressure vapor-liquid equilibrium for binary systems [CO_2 + CH_2Cl_2] at 311.41 and 326.95 K and Corazza et al. (2003) investigated the behavior of phase equilibrium between the CO_2 and CH_2Cl_2 in the temperature range from 313.15 at 343 K.

About the binary system [CO_2 + ε-CL], there are also in the literature some experimental data of phase equilibrium at different temperatures (BENDER et al., 2010b; BERGEOUT et al., 2004; XU et al., 2003). Bergeot et al. (2004) presented high pressure *P-x* data for the system [CO_2 + ε-CL], while Xu et al. (2003) investigated the vapor-liquid equilibrium of different lactones in scCO_2. Bender et al. (2010b) reported a study on the high pressure phase equilibria of scCO_2 and different lactones, among them, the ε-CL.

It is worth noting that there are no experimental data of phase equilibrium for the ternary system [CO_2 + CH_2Cl_2 + ε-CL] at different temperatures. This type of experimental data are important in the kinetics of polymerization. Veneral et al. (2013) investigated the kinetics of e-ROP of ε-CL by Novozym 435 using scCO_2 as solvent and CH_2Cl_2 as co-solvent in a packed-bed reactor (PBR) system. In that work, the authors observed that the use of CH_2Cl_2 as co-solvent resulted in an impressive improvement in the solubility and mass transfer of the studied system, which prevented accumulation or precipitation of polymer on the enzymatic porous beads surface.

In this context, the knowledge of phase behavior involving CO_2, CH_2Cl_2 and ε-CL is very important to better understand the several aspects in the polymerization reaction, mainly the mass transfer between chemical species involved in the polymerization reactions. The main objective of this work was to investigate experimentally the use of CH_2Cl_2 as co-solvent to the system [CO_2 + ε-CL] at different CH_2Cl_2 to ε-CL mass ratios (0.5:1; 1:1 and 2:1). In addition, the Peng-Robinson EoS (PENG; ROBINSON, 1976) with the van der Waals (vdW) mixing rule was employed to represent the experimental phase equilibrium data.

3.1.2 Experimental

3.1.2.1 Materials

The solvent CO_2 was bought from White Martins S.A. (Brazil), CH_2Cl_2 was used as a co-solvent and bought from Sigma-Aldrich (United States of America) and ε-CL (6-hexanolactone, CAS number 502-44-3) was bought from Sigma-Aldrich (United States

of America). The ε-CL was dried in a vacuum oven at 333.15 K and 0.01 MPa for 72 h, resulting in a water content of 0.184% with standard uncertainty of 0.030%, measured by the Karl Fischer Coulometric Titrator for moisture determination (HI-904 - HANNA® instruments). In Table 4, there are presented the molecular formula, supplier, purification method and minimum mass fraction purity of all components used in this work. The minimum mass fraction purity of all components was reported by the supplier.

Table 4 - Chemical name, molecular formula, provenance, purification method and purity of the materials used (purity provided by suppliers).

Chemical Name	Molecular formula	CAS Number	Supplier	Purification method	Minimum mass fraction purity
ε-Caprolactone	$C_6H_{10}O_2$	502-44-3	Sigma-Aldrich	Dried [a]	0.970
Dichloromethane	CH_2Cl_2	75-09-2	Sigma-Aldrich	None	0.998
Carbon dioxide	CO_2	124-38-9	White Martins S.A.	None	0.999

[a] The ε-caprolactone was dried at 333.15 K in a vacuum oven (0.01 MPa) for 72 h

3.1.3 Phase equilibrium apparatus and procedure

To obtain the experimental data of phase equilibrium at high pressures the synthetic static method was used. In this method, the composition of the equilibrium phases is determined indirectly, without the need for removal of the respective samples. Initially, precise quantities of the pure substances (ε-CL, CH_2Cl_2 and CO_2) were introduced into the equilibrium cell, such that the overall composition of the mixture, at the beginning of the experiment, was known. The pressure and temperature conditions were adjusted, promoting the formation of a homogeneous solution. Figures 12 and 13 show the equilibrium cell and the schematic diagram of the experimental apparatus used in this work, respectively. This is described in detail in a variety of

previous studies (OLIVEIRA et al., 2000; NDIAYE et al., 2001; DARIVA et al., 2001). This apparatus can be safely operated up to 27.50 MPa with pressure expanded uncertainty of 0.1 MPa, provided by the indicator systems.

Figure 12 - Equilibrium cell. (MB) magnetic bar; (SW) sapphire windows; (TC) thermocouple.

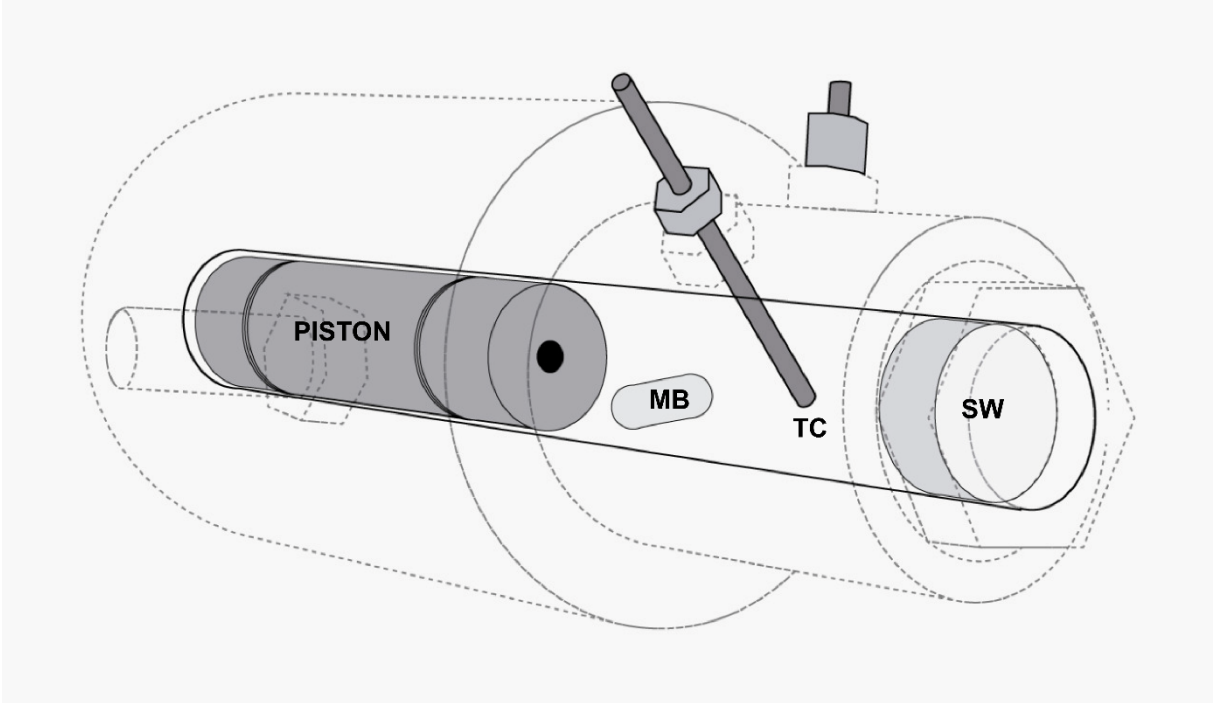

Source: GIRARDI, 2019 – Unpublished work.

For the phase equilibrium experiments, precise amounts of ε-caprolactone and dichloromethane were weighed on a precision balance scale (Shimadzu, Model AY220 with 0.0001 g accuracy) and placed quickly inside the equilibrium cell, which was quickly closed and connected to the pressure source. A known volume of CO_2 was added to the equilibrium cell using the syringe pump, which was maintained at 10.0 MPa and 280.15K. The system was continuously stirred with the help of a Teflon-Coated magnetic stir bar and the internal pressure of the cell was gradually increased until reaching a single-phase system. Finally, the heating system was started using the circulation bath (RB2). After stabilization of the temperature, measurements of the phase equilibria (bubble point) were initiated by reducing the pump pressure, by programming, until the appearance of a second phase that was detected through the

visualization through the sapphire window. Each measurement was repeated at least three times.

Figure 13 - High pressure phase equilibria apparatus. (SR_1) solvent reservoir (CO_2); (RB_1) cold recirculation bath; (RB_2) hot recirculation bath; (SP) syringe pump; (EC) equilibrium cell; (MS) magnetic stirrer; (LS) light source; (SW) sapphire windows; (TI) temperature indicator; (TC) thermocouple; (PI) pressure indicator; (PT) pressure transducer; (V_1, V_3, V_4, V_5, and V_6) ball valve; (V_2) check valve; (V_7 and V_8) micrometric valve.

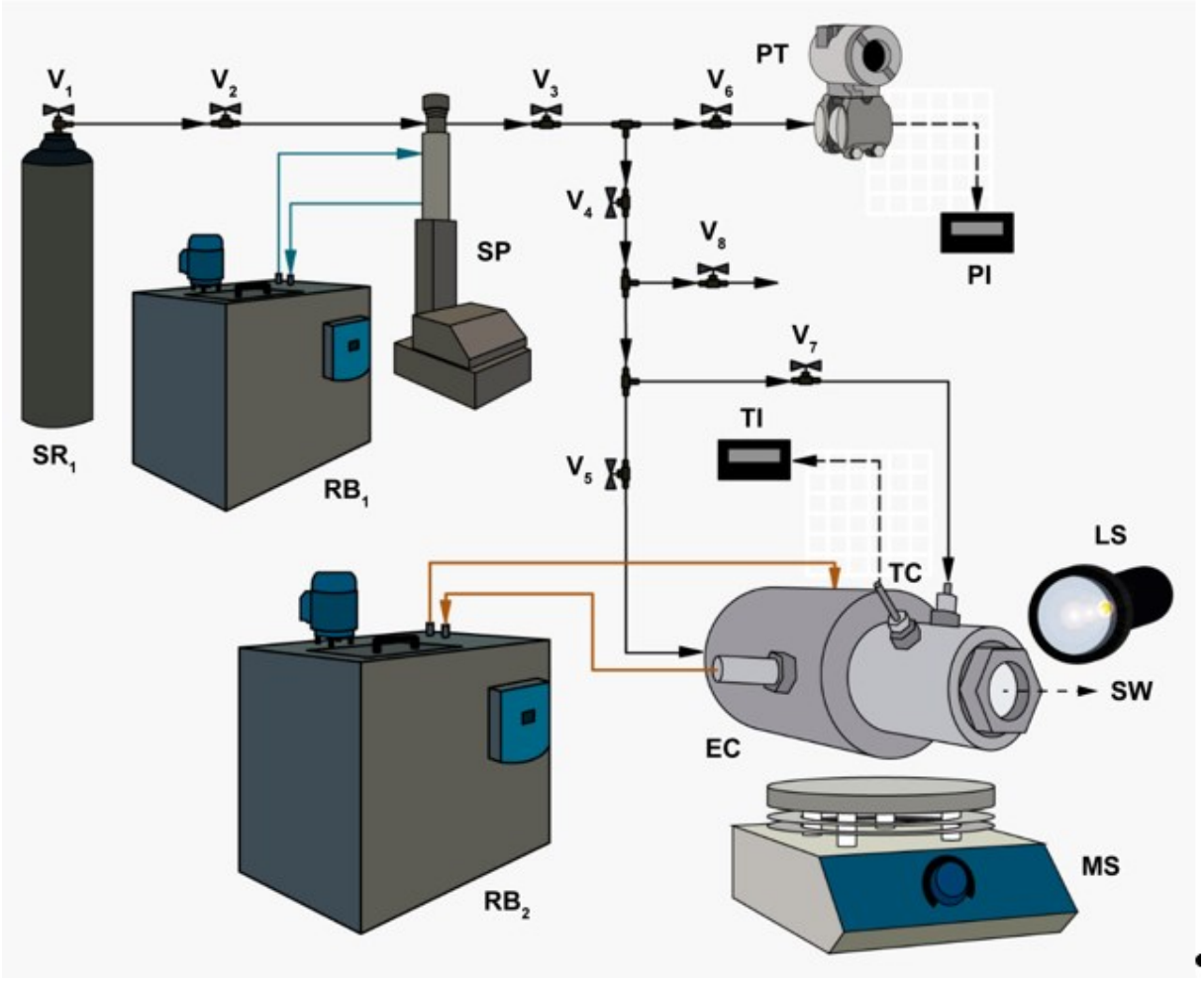

Source: GIRARDI, 2019 – Unpublished work.

For the system [CO_2 + CH_2Cl_2 + ε-CL] was investigated the vapor-liquid equilibrium at the bubble point (VLE-BP), liquid-liquid equilibrium (LLE) and vapor-liquid-liquid equilibrium (VLLE), changing the system pressure at constant temperature. According to Santos et al. (2019), the VLE-BP transition is characterized by the formation of a bubble at the top of the cell during system depressurization. When

the liquid-liquid equilibrium (LLE) appeared, the transition point was identified by the appearance of a new phase, which stretched across the top of the cell, followed by the complete system clouding. The depressurization was followed by the appearance of a third vapor phase at the top of the cell characterizing the vapor-liquid-liquid equilibrium (VLLE).

To facilitate the understanding of the effect of CH_2Cl_2 on system investigated, the ternary system [CO_2 (1) + CH_2Cl_2 (2) + ε-CL (3)] was treated as a pseudobinary system [CO_2 (1) + ε-CL (2)] in CH_2Cl_2 free-basis, at three different mass ratios of CH_2Cl_2 to ε-CL. The experimental phase equilibrium data were obtained in the temperature range from 323.15 to 353.15 K and pressures up to 25.8 MPa; the investigated mass ratio of CH_2Cl_2 to ε-CL was kept constant at 0.5:1, 1:1 and 2:1, corresponding to the following molar ratio: 0.67:1, 1.35:1 and 2.69:1, respectively. The overall mass fraction (w_1') of the system [CO_2 (1) + CH_2Cl_2 (2) + ε-CL (3)], in CH_2Cl_2 free-basis, was varied from 0.3671 to 0.6867; 0.3681 to 0.8010 and 0.6895 to 0.9376 for the mass ratio of CH_2Cl_2 to ε-CL of 0.5:1, 1:1, 2:1, respectively.

3.1.4 Thermodynamic modeling

In this work, the Peng-Robinson (PR) EoS (PENG; ROBINSON, 1976) was employed for representing the experimental phase equilibrium data. For PVT data correlations, the PR EoS represents a significant improvement when compared to the Soave-Redlich-Kwong (SRK) EoS (PENG; ROBINSON, 1976; ARAÚJO et al., 2016). While the SRK EoS predicts that the critical compressibility factor Z_c is 0.333 and, consequently, poor liquid density predictions are obtained; the value of Z_c predicted by the PR EoS is 0.307 (ARAÚJO et al., 2016).

$$P = \frac{RT}{v-b} - \frac{a(T)}{\left[v(v+b)+b(v-b)\right]} \tag{12}$$

where

$$b = 0.0778\,\frac{RT_c}{P_c} \tag{13}$$

$$a(T) = \frac{0.45724\,R^2 T_c^2}{P_c}\left[1 + f\left(\omega, T_r\right)\right]^2 \tag{14}$$

$$f\left(\omega, T_r\right) = \left(0.3764 + 1.5422\,\omega - 0.2699\,\omega^2\right)\left(1 - T_r^{0.5}\right) \tag{15}$$

For components with large acentric factor values $(\omega > 0.49)$, the following function is used:

$$f\left(\omega, T_r\right) = \left(0.379642 + 1.48503\,\omega - 0.164423\,\omega^2 - 0.016666\,\omega^3\right)\left(1 - T_r^{0.5}\right) \tag{16}$$

Application of the PR EoS to fluid mixtures requires a mixing rule in order to describe the mixture from the pure-component properties of the system, as:

$$a(T) = \sum_{i=1}^{n}\sum_{j=1}^{n} x_i x_j a_{ij} \tag{17}$$

$$b = \sum_{i=1}^{n} x_i b_i \tag{18}$$

with,

$$a_{ij} = \left[\left(a_i a_j\right)^{0.5}\right]\left(1 - k_{ij}\right) \tag{19}$$

where k_{ij} is the binary interaction parameter, usually estimated from fitting experimental data to the EoS. The pure component properties for CO_2, CH_2Cl_2 and ε-CL are presented in Table 5.

Table 5 - Characteristic parameters of pure compounds used in the work.

Compound	T_c/K	P_c/MPa	ω	M/g.mol^{-1}
CO_2	304.21 [b]	7.38 [b]	0.2236 [b]	44.01 [c]
CH_2Cl_2	51.0 [b]	6.08 [b]	0.1990 [b]	84.93 [c]
ε-CL	549.16 [a]	3.68 [a]	2.0567 [a]	114.15 [c]

T_c, critical temperature; P_c, critical pressure; ω, acentric factor; M, molar mass.

[a] Reference: BENDER et al., (2010b).

[b] Reference: REID, (1977)

[c] Reference: NIST (accessed 13.12.18)

A point of fundamental importance in the parameter estimation step is the definition of the objective function. In this work, for the estimation of the binary interaction parameters (k_{12}, k_{13} and k_{23}) the following objective function was defined:

$$OF = \sum_{i=1}^{nobs} (P_i^{cal} - P_i^{\exp})^2 \quad (20)$$

where OF denotes the objective function, P_i^{exp} represents the arithmetic mean of three experimental measurements of phase transition pressures, P_i^{cal} represents the calculated pressure by the mathematical model and $nobs$ denotes the number of observations. In this work, the OF was minimized and the results of the generated residues were presented by Absolute Deviation (AD), Eq. (21), and root mean square deviation values ($rmsd$), Eq. (22):

$$AD = \sum_{i=1}^{nobs} \frac{(P_i^{cal} - P_i^{\exp})}{nobs} \quad (21)$$

$$rmsd = \sum_{i=1}^{nobs} \frac{(P_i^{cal} - P_i^{\exp})^2}{nobs} \quad (22)$$

The estimation of the binary interaction parameters was performed by minimizing Eq. 20 using the Particle Swarm Optimization (PSO), a stochastic method while the optimization procedure was refined using the Simplex method. The Particle Swarm Optimization (PSO has been used in the last years in for parameter estimation

in phase equilibria processes, where the traditional newton methods face convergence problems (LAZZÚS, 2010; KHANSARY; SANI, 2014). The main characteristic of the stochastic PSO method is the independence of initial estimates, Stochastic methods are characterized by performing a large number of evaluations of the objective function throughout the search region, in order to increase the probability of finding the global optimum of the objective function. In addition, the randomness of the search procedure is high, to prevent local minima. Furthermore, these techniques do not need a very precise initial estimate of the solution and do not use the derivatives to reach the optimal point, thus, overcome the difficulties associated to the uses of Jacobian methods.

The deterministic simplex methods have as their main characteristic the use of derivatives function and are highly dependent on the initial guess. In this way, these methods can converge to local minimums. The main advantages are the rapid convergence at values close to the solution.

3.1.5 Results and Discussion

Tables 6 to 8 show the experimental phase transition data measured for the ternary system [CO_2 (1) + CH_2Cl_2 (2) + ε-CL (3)] in CH_2Cl_2 free-basis, at three different CH_2Cl_2 to ε-CL mass ratio, 0.5:1, 1:1, 2:1, respectively. These tables show the equilibrium results in terms of pressure, experimental error for each composition represented by the standard deviation of triplicate measurements of transition pressure values ($\boldsymbol{sd}$), and the phase transition type of phase equilibrium: the vapor-liquid equilibrium with bubble point transition (VLE-BP), liquid-liquid equilibrium (LLE) and vapor-liquid-liquid equilibrium (VLLE). The molar fractions tables for the ternary system are shown in the 3.1.7 Supporting Information.

Table 6 - Phase equilibrium results for the ternary system [CO_2 (1) + CH_2Cl_2 (2) + ε-CL (3)], in CH_2Cl_2 free-basis, at CH_2Cl_2 to ε-CL mass ratio of 0.5:1.

T/K	*P*/MPa	*sd*/MPa	Transition type
w_1'= 0.3671 (w_2'= 0.6329)			
323.15	6.83	0.02	VLE-BP
333.15	8.02	0.02	VLE-BP
343.15	9.42	0.02	VLE-BP
353.15	10.87	0.01	VLE-BP
w_1'= 0.4221 (w_2'= 0.5779)			
323.15	7.76	0.02	VLE-BP
333.15	9.24	0.02	VLE-BP
343.15	10.97	0.03	VLE-BP
353.15	12.83	0.02	VLE-BP
w_1'= 0.5006 (w_2'= 0.4994)			
323.15	8.53	0.03	VLE-BP
333.15	10.64	0.03	VLE-BP
343.15	13.19	0.02	VLE-BP
353.15	15.40	0.01	VLE-BP
w_1'= 0.5360 (w_2'= 0.4640))			
323.15	9.00	0.01	VLE-BP
333.15	11.09	0.01	VLE-BP
343.15	13.82	0.02	VLE-BP
353.15	16.42	0.01	VLE-BP
w_1'= 0. 5715 (w_2'= 0.4285)			
323.15	9.66	0.02	VLE-BP
333.15	12.52	0.02	VLE-BP
343.15	15.02	0.03	VLE-BP
353.15	17.60	0.01	VLE-BP
w_1'= 0.6070 (w_2'= 0.3930)			
323.15	10.53	0.06	LLE
323.15	10.40	0.01	VLLE
333.15	13.77	0.05	LLE
333.15	13.30	0.01	VLLE
343.15	16.93	0.02	LLE
343.15	16.50	0.01	VLLE
353.15	19.85	0.04	LLE
353.15	19.60	0.01	VLLE
w_1'= 0.6454 (w_2'= 0.3546)			
323.15	12.75	0.04	LLE
323.15	10.45	0.01	LLE
333.15	16.62	0.04	VLLE
333.15	13.40	0.01	LLE
343.15	19.77	0.05	VLLE
343.15	16.50	0.01	LLE
353.15	22.83	0.03	VLLE
353.15	19.70	0.01	LLE
w_1'= 0.6867 (w_2'= 0.3133)			
323.15	16.35	0.03	LLE
323.15	10.50	0.01	VLLE
333.15	19.78	0.03	LLE
333.15	13.50	0.01	VLLE
343.15	23.89	0.05	LLE
343.15	16.60	0.01	VLLE
353.15	19.70	0.01	LLE

VLE-BP denotes vapor-liquid-equilibrium, type bubble point or dew point (DP); LLE denotes liquid-liquid-equilibrium; VLLE denotes vapor-liquid-liquid equilibrium, *T*, system temperature, *P*, system pressure, sd is the standard deviation of the of triplicate measurements of phase transition pressure values in an individual experiment (i.e., divided by sqrt(n-1)) and w_1', denotes the mass fraction of CO_2 on an CH_2Cl_2 free-basis and w_2' denotes mass fraction of ε-CL (with 0.1843 ± 0.0447 wt% of water) on an CH_2Cl_2 free-basis. Variable expanded uncertainties with 95% of confidence level *T*: ± 0.50 K; *P*: ± 0.10 MPa; w_1' and w_2': ± 0.0010; CH_2Cl_2 to ε-CL mass ratio: ± 0.0019.

Table 7 - Phase equilibrium results for the ternary system [CO_2 (1) + CH_2Cl_2 (2) + ε-CL (3)], in CH_2Cl_2 free-basis, at CH_2Cl_2 to ε-CL mass ratio of 1:1.

T/K	*P*/MPa	*sd*/MPa	Transition type
w_1' = 0.3681 (w_2'= 0.6319)			
323.15	5.54	0.02	VLE-BP
333.15	6.35	0.04	VLE-BP
343.15	7.24	0.03	VLE-BP
353.15	8.17	0.03	VLE-BP
w_1' = 0.5022 (w_2'= 0.4978)			
323.15	7.02	0.03	VLE-BP
333.15	8.09	0.01	VLE-BP
343.15	9.50	0.01	VLE-BP
353.15	10.93	0.02	VLE-BP
w_1' = 0.6066 (w_2'= 0.3934)			
323.15	7.96	0.02	VLE-BP
333.15	9.54	0.01	VLE-BP
343.15	11.60	0.01	VLE-BP
353.15	13.96	0.01	VLE-BP
w_1' = 0.6453 (w_2'= 0.3547)			
323.15	8.36	0.01	VLE-BP
333.15	10.06	0.01	VLE-BP
343.15	12.49	0.04	VLE-BP
353.15	15.26	0.02	VLE-BP
w_1' = 0.6638 (w_2'= 0.3362)			
323.15	8.70	0.01	VLE-BP
333.15	10.30	0.02	VLE-BP
343.15	13.00	0.01	VLE-BP
353.15	16.16	0.02	VLE-BP
w_1' = 0.6872 (w_2'= 0.3128)			
323.15	9.65	0.03	LLE
323.15	8.40	0.01	VLLE
333.15	12.68	0.03	LLE
333.15	10.63	0.06	VLLE
343.15	16.11	0.05	LLE
343.15	13.07	0.06	VLLE
353.15	19.47	0.03	LLE
353.15	15.10	0.01	VLLE
w_1' = 0.7312 (w_2'= 0.2688)			
323.15	11.76	0.04	LLE
323.15	8.66	0.01	VLLE
333.15	14.87	0.06	LLE
333.15	10.83	0.01	VLLE
343.15	18.50	0.05	LLE
343.15	13.07	0.01	VLLE
353.15	21.53	0.05	LLE
353.15	16.30	0.01	VLLE
w_1' = 0.7728 (w_2'= 0.2272)			
323.15	19.07	0.02	LLE
323.15	8.90	0.01	VLLE
333.15	22.02	0.04	LLE
333.15	11.00	0.01	VLLE
343.15	25.47	0.05	LLE
343.15	13.20	0.01	VLLE
w_1' = 0.8010 (w_2'= 0.1990)			
323.15	25.75	0.04	LLE
323.15	8.81	0.01	VLLE

VLE-BP denotes vapor-liquid-equilibrium, type bubble point or dew point (DP); LLE denotes liquid-liquid-equilibrium; VLLE denotes vapor-liquid-liquid equilibrium, *T*, system temperature, *P*, system pressure, sd is the standard deviation of the of triplicate measurements of phase transition pressure values in an individual experiment (i.e., divided by sqrt(n-1)) and w_1', denotes the mass fraction of CO_2 on an CH_2Cl_2 free-basis and w_2' denotes mass fraction of ε-CL (with 0.1843 ± 0.0447 wt% of water) on an CH_2Cl_2 free-basis. Variable expanded uncertainties with 95% of confidence level *T*: ± 0.50 K; *P*: ± 0.10 MPa; w_1' and w_2': ± 0.0010; CH_2Cl_2 to ε-CL mass ratio: ± 0.0070.

Table 8 - Phase equilibrium results for the ternary system [CO_2 (1) + CH_2Cl_2 (2) + ε-CL (3)], in CH_2Cl_2 free-basis, at CH_2Cl_2 to ε-CL mass ratio of 2:1.

T/K	*P*/MPa	*sd*/MPa	Transition type
w_1'= 0.5012 (w_2'= 0.4988)			
323.15	5.05	0.04	VLE-BP
333.15	5.77	0.01	VLE-BP
343.15	6.57	0.01	VLE-BP
353.15	7.50	0.01	VLE-BP
w_1' = 0.6342 (w_2'= 0.3658)			
323.15	6.28	0.07	VLE-BP
333.15	7.49	0.01	VLE-BP
343.15	8.78	0.04	VLE-BP
353.15	10.20	0.01	VLE-BP
w_1' = 0.6857 (w_2'= 0.3143)			
323.15	6.97	0.02	VLE-BP
333.15	8.18	0.02	VLE-BP
343.15	9.64	0.03	VLE-BP
353.15	11.20	0.03	VLE-BP
w_1' = 0.7296 (w_2'= 0.2704)			
323.15	7.54	0.01	VLE-BP
333.15	8.95	0.01	VLE-BP
343.15	10.48	0.02	VLE-BP
353.15	12.15	0.03	VLE-BP
w_1' = 0.7528 (w_2'= 0.2472)			
323.15	7.76	0.01	VLE-BP
333.15	9.11	0.01	VLE-BP
343.15	10.75	0.01	VLE-BP
353.15	12.53	0.01	VLE-BP
w_1' = 0.7783 (w_2'= 0.2211)			
323.15	7.98	0.01	VLE-BP
333.15	9.57	0.01	VLE-BP
343.15	11.38	0.01	VLE-BP
353.15	13.16	0.01	VLE-BP
w_1'= 0.8011 (w_2'= 0.1989)			
323.15	10.99	0.05	LLE
323.15	8.00	0.01	VLLE
333.15	14.19	0.05	LLE
333.15	10.20	0.01	VLLE
343.15	17.18	0.04	LLE
343.15	12.00	0.01	VLLE
353.15	20.59	0.06	LLE
353.15	13.20	0.01	VLLE
w_1'= 0.8260 (w_2'= 0.1740)			
323.15	15.55	0.03	LLE
323.15	8.20	0.01	VLLE
333.15	18.83	0.03	LLE
333.15	10.30	0.01	VLLE
343.15	21.58	0.04	LLE
343.15	12.10	0.01	VLLE
353.15	24.53	0.03	LLE
353.15	13.50	0.01	VLLE
w_1' = 0.8799 (w_2'= 0.1201)			
323.15	8.30	0.01	VLLE
333.15	10.30	0.01	VLLE
343.15	12.20	0.01	VLLE
353.15	13.40	0.01	VLLE
w_1' = 0.9376 (w_2'= 0.0624)			
323.15	8.20	0.01	VLLE
333.15	10.40	0.01	VLLE
343.15	12.10	0.01	VLLE
353.15	13.60	0.01	VLLE

VLE-BP denotes vapor-liquid-equilibrium, type bubble point or dew point (DP); LLE denotes liquid-liquid-equilibrium; VLLE denotes vapor-liquid-liquid equilibrium, *T*, system temperature, *P*, system pressure, sd is the standard deviation of the of triplicate measurements of phase transition pressure values in an individual

experiment (i.e., divided by sqrt(n-1)) and w_1', denotes the mass fraction of CO_2 on an CH_2Cl_2 free-basis and w_2' denotes mass fraction of ε-CL (with 0.1843 ± 0.0447 wt% of water) on an CH_2Cl_2 free-basis. Variable expanded uncertainties with 95% of confidence level *T*: ± 0.50 K; *P*: ± 0.10 MPa; w_1' and w_2': ± 0.0010; CH_2Cl_2 to ε-CL mass ratio: ± 0.0126.

Figures 14 to 16 present the experimental and calculated phase equilibrium value in *P*-*w* diagrams forms at different mass rations of CH_2Cl_2 to ε-CL of 0.5:1, 1:1 and 2:1 and for the temperatures of 323.15, 333.15, 343.15 and 353.15 K. The upper limit of experimental pressure measurements was defined as 27.5 MPa, pressure at which the apparatus can be safely operated.

For the systems with mass ratio of 0.5:1, 1:1 and 2:1 of CH_2Cl_2 to ε-CL, for all isotherms of the 323.15, 333.15, 343.15 and 353.15 K, as shown in Tables 6 to 8 and Figures 14 to 16, it was observed phase transitions of VLE-BP type occurred until the mass fraction CO_2 of 0.5715, 0.6638 and 0.7783, respectively. The VLE-BP was characterized by the formation of a bubble at the top of the cell during the depressurization of the system. For mass fractions of CO_2 greater or equal to 0.6638, 0.6872 and 0.8011 it was observed the occurrence of phase transitions of LLE and VLLE types. The LLE was identified from the appearance of a new phase which stretched across the top of the cell, flowed by the complete system clouding and the VLLE was characterized by the appearance of a third vapor phase at the top of the cell during the depressurization of the system. It can also be noted that a decrease in CH_2Cl_2 mass ratio require higher pressures to solubilize all components, i.e., in other words, to reach the one-phase region. In addition, it has been observed that the higher the mass ratio of CH_2Cl_2 to ε-CL the VLE-BP predominated to higher mass fractions of CO_2.

With the increase of CO_2 mass fraction, a great increase in system pressure is required for the solubilization of the system occurred (mainly in the liquid-liquid region), which made difficult to measure data (liquid-liquid equilibrium) for the mass fractions higher than 0.6867, 0.8100 and 0.8260 for the respective CH_2Cl_2 to ε-CL mass ratio of 0.5:1, 1:1 and 2:1. This type of behavior was also observed in the work of Santos et al. (2019), who reported data for the system [CO_2 (1) + methyl methacrylate (2) + poly (dimethylsiloxane) (3)]. In both systems, the increase in the mass fraction of CO_2 perturbed the interactions between solute and co-solvent, due to the strong interactions that CO_2 has with CH_2Cl_2 in this work, and with methyl

methacrylate in the other case. Thus CO_2 acts in this case as antisolvent, due to the partition of the co-solvent (CH_2Cl_2) to the lightest phase CO_2- richest component, leading to higher pressure values to solubilize the system, i.e., to reach the one-phase region.

Figure 14 - Pressure−overall composition diagram for the system [CO_2 (1) + CH_2Cl_2 (2) + ε-CL (3)], in CH_2Cl_2 free-basis, at CH_2Cl_2 to ε-CL mass ratio of 0.5:1. Experimental data: 323:15 K: ◨ (BP), ■ (LL) and □ (LLV); 333:15 K: ◑ (BP), ● (LL) and ○ (LLV); 343:15 K: ◭ (BP), ▲ (LL) and △ (LLV); 353:15 K: ▼ (BP), ▼ (LL) and ▽ (LLV). Continuous lines denote calculated values applying the PR EoS model with global temperature fitted parameters.

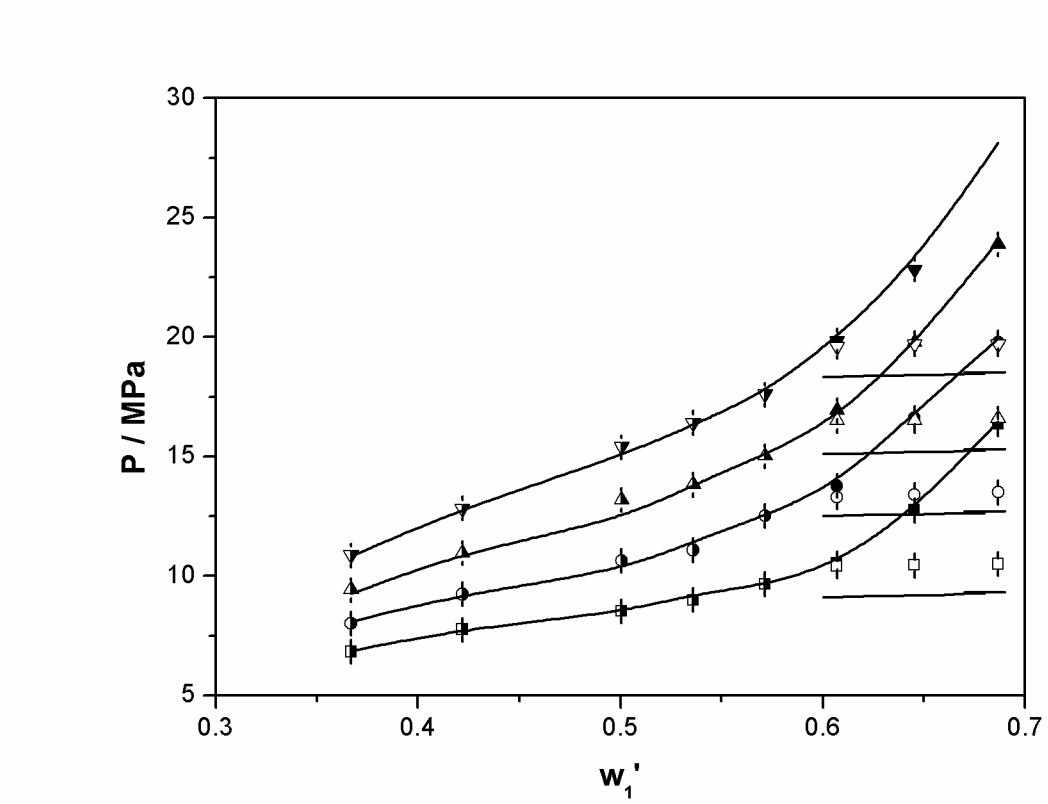

Source: Author himself.

Figure 15 - Pressure−overall composition diagram for the system [CO_2 (1) + CH_2Cl_2 (2) + ε-CL (3)], in CH_2Cl_2 free-basis, at CH_2Cl_2 to ε-CL mass ratio of 1:1. Experimental data: 323:15 K: ◨ (BP), ■ (LL) and □ (LLV); 333:15 K: ◑ (BP), ● (LL) and ○ (LLV); 343:15 K: ◭ (BP), ▲ (LL) and △ (LLV); 353:15 K: ▼ (BP), ▼ (LL) and ▽ (LLV). Continuous lines denote calculated values applying the PR EoS model with global temperature fitted parameters.

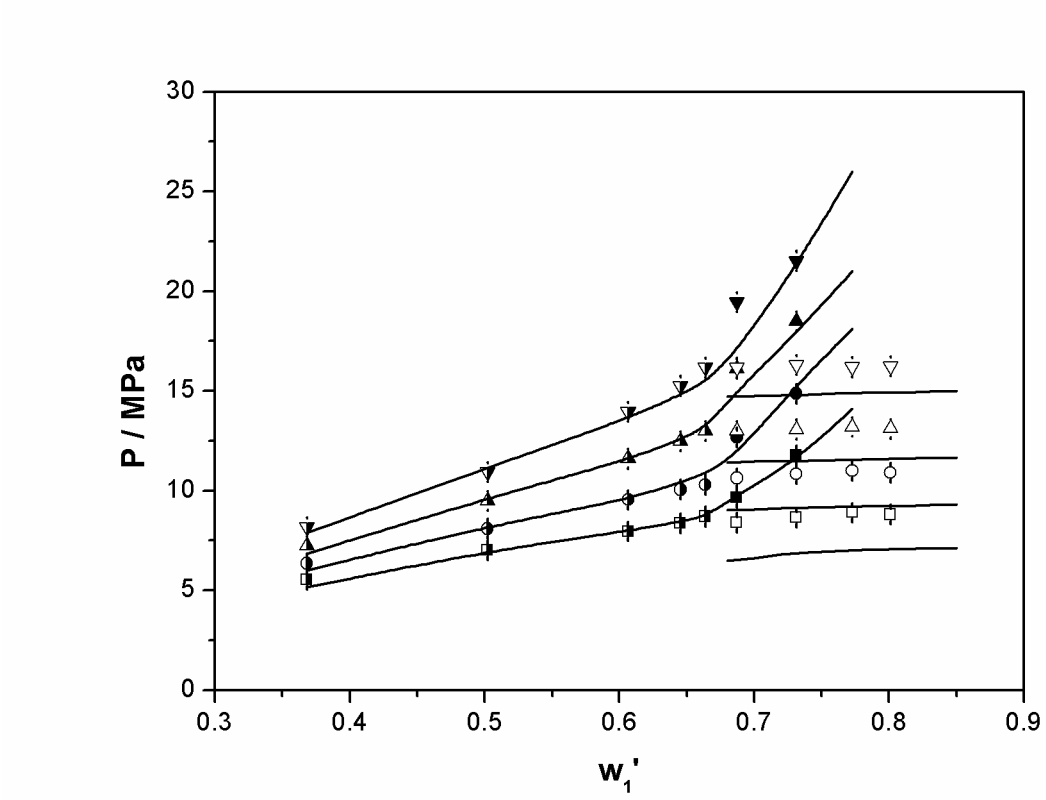

Source: Author himself.

Figure 16 - Pressure−overall composition diagram for the system [CO_2 (1) + CH_2Cl_2 (2) + ε-CL (3)], in CH_2Cl_2 free-basis, at CH_2Cl_2 to ε-CL mass ratio of 2:1. Experimental data: 323:15 K: ◨ (BP), ■ (LL) and □ (LLV); 333:15 K: ◑ (BP), ● (LL) and ○ (LLV); 343:15 K: ◭ (BP), ▲ (LL) and △ (LLV); 353:15 K: ▼ (BP), ▼ (LL) and ▽ (LLV). Continuous lines denote calculated values applying the PR EoS model with global temperature fitted parameters.

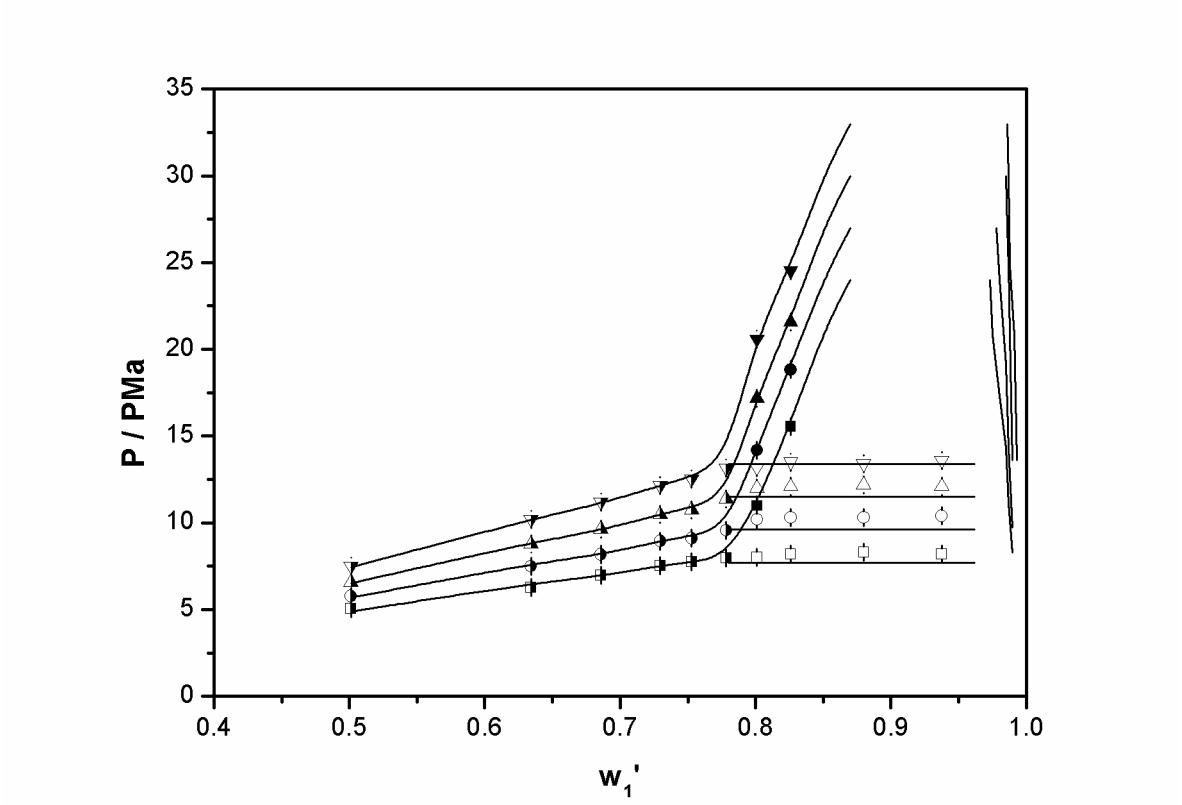

Source: Author himself.

Figures 17 to 19 illustrate the experimental and calculated phase equilibrium value in *P-T* diagrams forms at different mass rations of CH_2Cl_2 to ε-CL of 0.5:1, 1:1 and 2:1, respectively. In these figures, it is possible to observe that higher pressures are needed to solubilize all components in only one-phase with the increase of temperature. This is a behavior characteristic of a Lower Critical Solution Temperature (LCST), where below this temperature the components of a system are soluble in any proportion and above occurs the formation of two phases, vapor-liquid or liquid-liquid. This behavior is characteristic of the system involving lactones, solvents as chloroform

and CH_2Cl_2, and anti-solvent as CO_2 (REBELATTO et al., 2018a; REBELATTO et al., 2018b).

According to the classification of van Konynenburg and Scott (1980), the phase behavior of the ternary systems studied in this work may be classified as type V that was also found in the binary systems containing CO_2 and ε-CL.

Figure 17 - Pressure-temperature diagram for the system [CO_2 (1) + CH_2Cl_2 (2) + ε-CL (3)], in CH_2Cl_2 free-basis, at CH_2Cl_2 to ε-CL mass ratio of 0.5:1. Experimental data: ◨ (BP) – [w_1 = 0.2788; w_2 = 0.2405; w_3 = 0.4807]; ◑ (BP) – [w_1 = 0.4003; w_2 = 0.2004; w_3 = 0.3993]; ▶ (LL) – [w_1 = 0.5482; w_2 = 0.1506; w_3 = 0.3012]; ◀ (LL) – [w_1 = 0.5943; w_2 = 0.1347; w_3 = 0.2711]. Continuous lines denote calculated values applying the PR EoS model with global temperature fitted parameters.

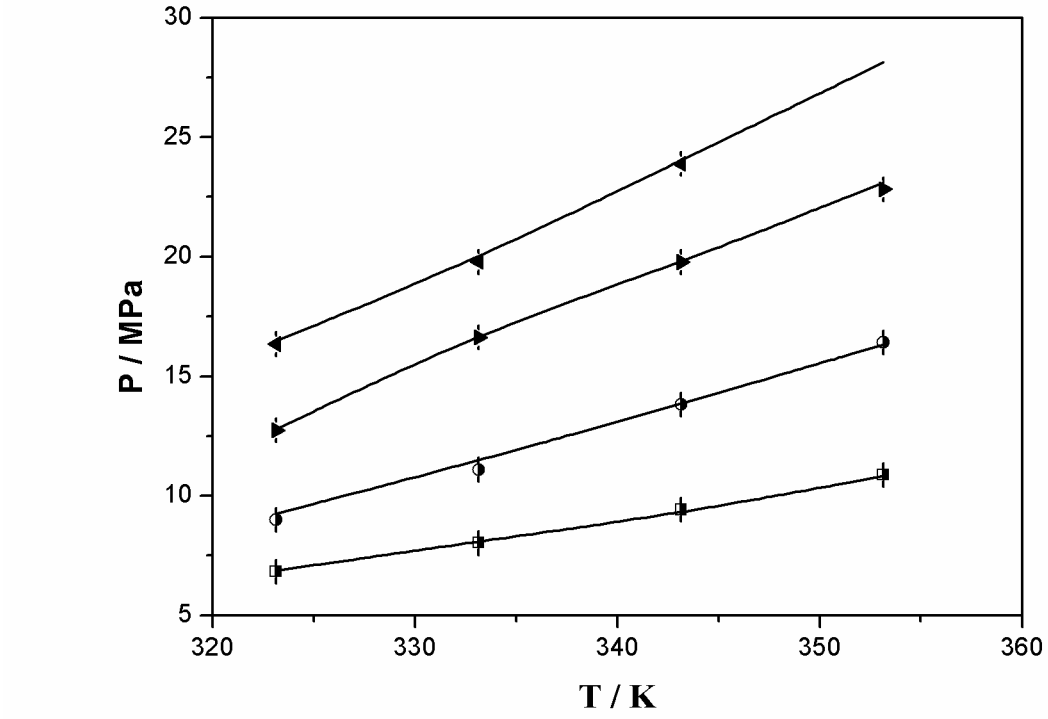

Source: Author himself.

Figure 18 - Pressure-temperature diagram for the system [CO_2 (1) + CH_2Cl_2 (2) + ε-CL (3)], in CH_2Cl_2 free-basis, at CH_2Cl_2 to ε-CL mass ratio of 1:1. Experimental data: ◨ (BP) – [w_1 = 0.2255; w_2 = 0.3875; w_3 = 0.3870]; ◑ (BP) – [w_1 = 0.4347; w_2 = 0.2834; w_3 = 0.2819]; ▶ (LL) – [w_1 = 0.5249; w_2 = 0.2362; w_3 = 0.2389]; ◀ (LL) – [w_1 = 0.5764; w_2 = 0.2117; w_3 = 0.2119]. Continuous lines denote calculated values applying the PR EoS model with global temperature fitted parameters.

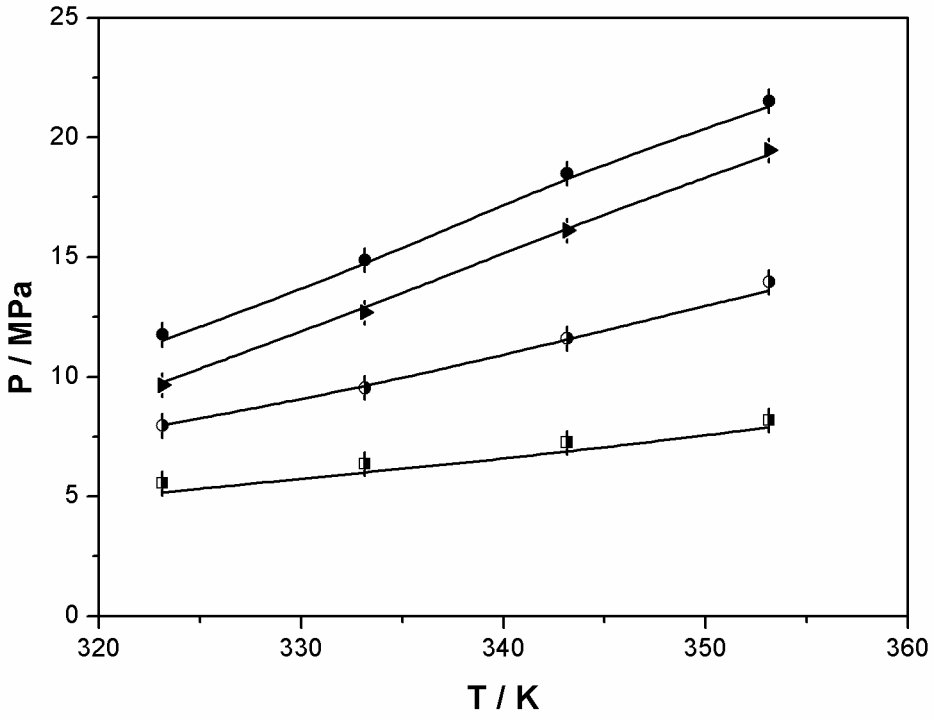

Source: Author himself.

Figure 19 - Pressure-temperature diagram for the system [CO_2 (1) + CH_2Cl_2 (2) + ε-CL (3)], in CH_2Cl_2 free-basis, at CH_2Cl_2 to ε-CL mass ratio of 2:1. Experimental data: ◨ (BP) – [w_1 = 0.2485; w_2 = 0.5042; w_3 = 0.2473]; ◑ (BP) – [w_1 = 0.3664; w_2 = 0.4223; w_3 = 0.2113]; ▶ (LL) – [w_1 = 0.5395; w_2 = 0.3069; w_3 = 0.1536]; ◀ (LL) – [w_1 = 0.5719; w_2 = 0.2861; w_3 = 0.1420]. Continuous lines denote calculated values applying the PR EoS model with global temperature fitted parameters.

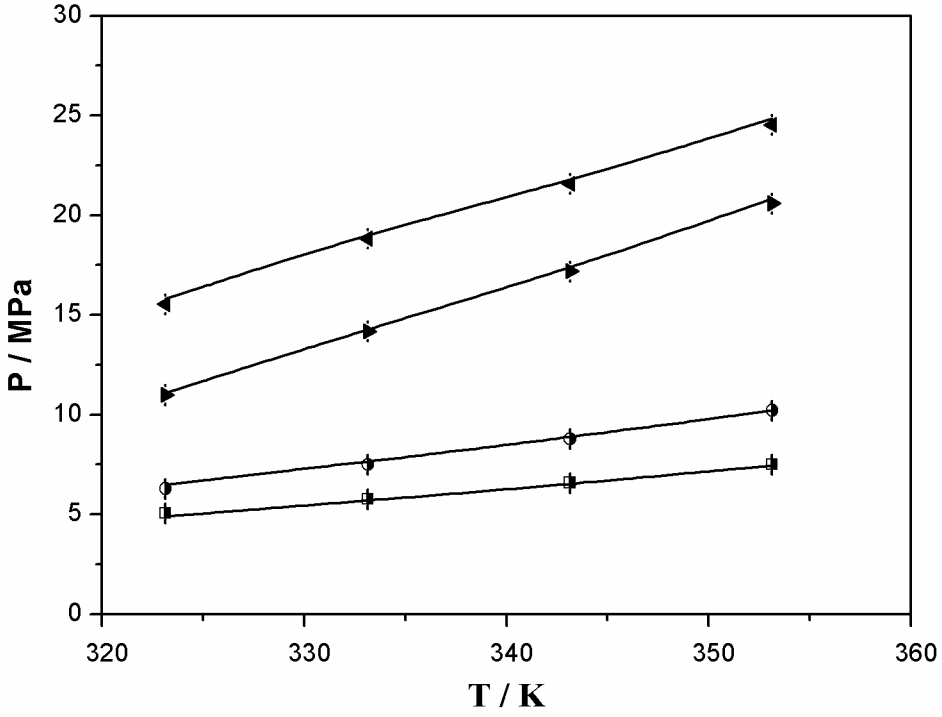

Source: Author himself.

The PR EoS model with the van der Waals quadratic mixing rule was employed to predict the phase equilibrium behavior for the ternary system [CO_2 (1) + CH_2Cl_2 (2) + ε-CL (3)]. The binary interaction parameters (k_{12}, k_{13} and k_{23}) were adjusted using the experimental phase equilibrium data obtained in this work. Several strategies were tested. First experimental data were fitted using all binary parameters independent of temperature. In a second step, the temperature dependence was included in all parameters. Results showed that k_{12} and k_{23} are not sensitive to temperature and thus, their values were kept constant and the temperature dependence of k_{13} was investigated. For this purpose, at each given temperature, the objective function was

minimized to find the corresponding k_{13} and then the obtained parameters were fitted as function of temperature to give the Eq. (23):

$$k_{13} = 0.001T[K] - 0.286 \quad (23)$$

The binary interaction parameters (k_{12}, k_{13} and k_{23}) together with the absolute deviation (AD) and mean square value ($rmsd$) are presented in Table 9, where it can be observed that the thermodynamic model was able to correlate properly phase equilibrium transition, with AD and $rmsd$ smaller and equal than 0.0101 MPa by isotherms.

Table 9 - Binary interaction parameters of PR EoS model fitted in this work for the ternary system [CO_2 (1) + CH_2Cl_2 (2) + ε-CL (3)].

T/K	k_{12}	k_{13}	k_{23}	AD/MPa	$rmsd$
323.15	0.0220	0.0343	- 0.0360	0.08	0.10
333.15	0.0220	0.0417	- 0.0360	0.08	0. 10
343.15	0.0220	0.0510	- 0.0360	0.07	0.10
353.15	0.0220	0.0642	- 0.0360	0.07	0.10
$k_{13} = 0.001 \times T\ [K] - 0.2865$					

The good performance of PR EoS model with the vdW mixing rule becomes more evident analyzing Figures 14 to 19, where the model was able to represent different types of phase equilibrium, vapor-liquid and liquid-liquid equilibrium, for different mass ratio of CH_2Cl_2 to ε-CL of 0.5:1,1:1 and 2:1, with a set of parameters (k_{12}, k_{13} and k_{23}), for all isotherms of the 323.15, 333.15, 343.15 and 353.15 K.

Figure 20 shows the experimental values obtained in this work at temperature of 333.15 K for the ternary system [CO_2 (1) + CH_2Cl_2 (2) + ε-CL (3)], on a CH_2Cl_2 free-basis, for the mass ratios of CH_2Cl_2 to ε-CL 0.5:1, 1:1 and 2:1. These values are compared with experimental results reported by Bender et al. (2010b) for the binary system of [CO_2 (1) + ε-CL (2)] at temperature of 333.15 K. It can be clearly seen from

this figure that an increase in CH_2Cl_2 concentration results in reduction of the phase transition pressures, when compared to the binary system. This fact elucidates the effect of CH_2Cl_2 on the system phase behavior, showing that it can be advantageously used as a co-solvent to solubilize the system investigated.

Figure 20 - Comparison between experimental values obtained in this work for the ternary system [CO_2 (1) + CH_2Cl_2 (2) + ε-CL (3)], on a CH_2Cl_2 free-basis with three different CH_2Cl_2 to ε-CL mass ratios, 0.5:1 [◨ (BP), ■ (LL) and □ (LLV)], 1:1 [◑ (BP), ● (LL) and ○ (LLV)] and 2:1 [◭ (BP), ▲ (LL) and △ (LLV)] with the literature (Bender et al., (2010a)) for the binary system [CO_2 (1) + ε-CL (2)] [+ (BP), ⁎ (DP)] at the temperature of 333.15 K.

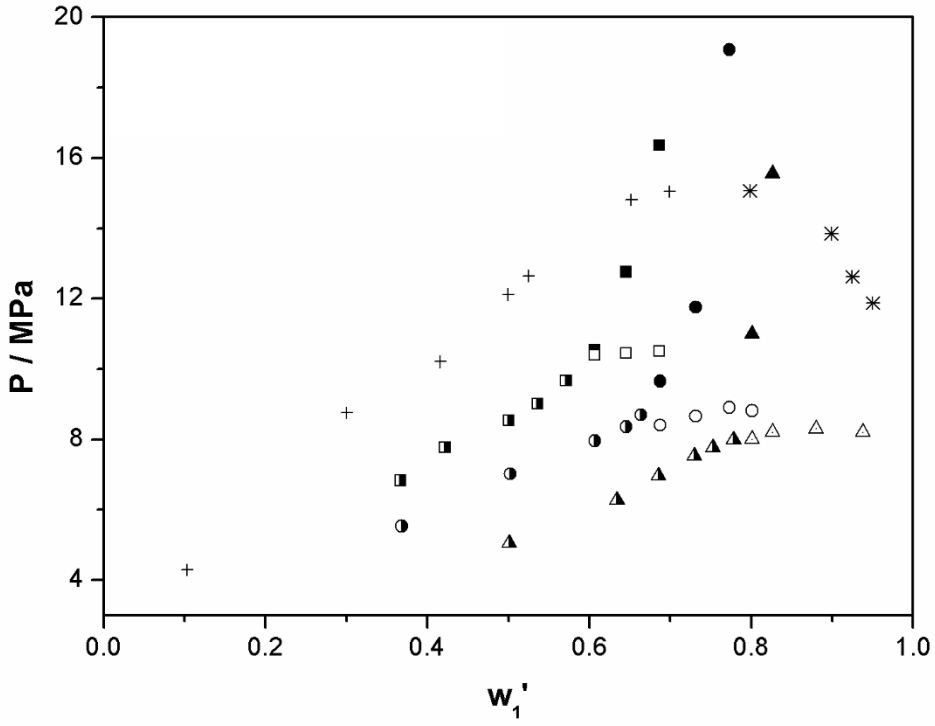

Source: Author himself.

The presence of CH_2Cl_2 can be highlighted in terms of its polar characteristic, different from CO_2, a non-polar solvent. As the monomer used in this work is also polar, a decrease in CH_2Cl_2 content caused a corresponding decrease in the system polarity, reducing the solvating power of the whole solvent medium [CO2 + CH_2Cl_2] in the mixture, hence requiring higher pressures to reach a homogeneous, one phase, system.

3.1.6 Partial Conclusion

Phase behavior of the ternary system [CO_2 (1) + CH_2Cl_2 (2) + ε-CL (3)] at different CH_2Cl_2 to ε-CL mass ratio (0.5:1, 1:1 and 2:1) was experimentally investigated in this work over the temperature range of 323.15 to 353.15 K in a wide overall composition range of CO_2, resulting in phase transition pressure up to 25.8 MPa. Experimental observations show that for all cases investigated an increase in CH_2Cl_2 to ε-CL mass ratio resulted in a decrease in pressure necessary to reach a single phase. Besides vapor-liquid equilibrium with bubble point transition presented for all systems, liquid-liquid, and vapor-liquid-liquid equilibrium transitions were observed for the system studied in this work. The PR EoS provided good performance of the experimental phase equilibrium results obtained when the global fitting was employed for data fitting. Experimental results obtained here are of value for conducting polymerization reactions with ε-CL in CO_2 as solvent and CH_2Cl_2 as co-solvent.

3.1.7 Supporting Information

Table 10 - Molar fractions for the multicomponent system [CO_2 (1) + CH_2Cl_2 (2) + ε-CL (3)] in CH_2Cl_2 free-basis, at CH_2Cl_2 to ε-CL mass ratio of 0.5:1. Molar fractions related to the data presented in Table 6.

w_1'	x_1	x_2	x_3
0.3671	0.4735	0.2117	0.3148
0.4221	0.5308	0.1889	0.2803
0.5006	0.6082	0.1578	0.2340
0.5360	0.6421	0.1435	0.2143
0.5715	0.6737	0.1316	0.1948
0.6070	0.7055	0.1184	0.1761
0.6454	0.7385	0.1052	0.1564
0.6867	0.7732	0.0908	0.1360

w_1', denotes the mass fraction of PCL on in CO_2 and CH_2Cl_2 free-basis; x_1, molar fraction for the CO_2; x_2, molar fraction for the CH_2Cl_2; x_3, molar fraction for the ε-CL.

Table 11 - Molar fractions for the multicomponent system [CO_2 (1) + CH_2Cl_2 (2) + ε-CL (3)] in CH_2Cl_2 free-basis, at CH_2Cl_2 to ε-CL mass ratio of 1:1. Molar fractions related to the data presented in Table 7.

w_1'	x_1	x_2	x_3
0.3681	0.3918	0.3490	0.2593
0.5022	0.5274	0.2711	0.2015
0.6066	0.6298	0.2128	0.1575
0.6453	0.6683	0.1900	0.1417
0.6638	0.6861	0.1799	0.1340
0.6872	0.7099	0.1655	0.1246
0.7312	0.7507	0.1429	0.1064
0.7728	0.7886	0.1220	0.0894

w_1', denotes the mass fraction of PCL on in CO_2 and CH_2Cl_2 free-basis; x_1, molar fraction for the CO_2; x_2, molar fraction for the CH_2Cl_2; x_3, molar fraction for the ε-CL.

Table 12 - Molar fractions for the multicomponent system [CO_2 (1) + CH_2Cl_2 (2) + ε-CL (3)] in CH_2Cl_2 free-basis, at CH_2Cl_2 to ε-CL mass ratio of 1:2. Molar fractions related to the data presented in Table 8.

w_1'	x_1	x_2	x_3
0.5012	0.4107	0.4318	0.1576
0.6342	0.5496	0.3282	0.1222
0.6857	0.6031	0.2903	0.1066
0.7296	0.6545	0.2520	0.0935
0.7528	0.6794	0.2346	0.0860
0.7783	0.7120	0.2098	0.0782
0.8011	0.7380	0.1913	0.0706
0.8260	0.7696	0.1679	0.0625

w_1', denotes the mass fraction of PCL on in CO_2 and CH_2Cl_2 free-basis; x_1, molar fraction for the CO_2; x_2, molar fraction for the CH_2Cl_2; x_3, molar fraction for the ε-CL.

3.2 EFFECT OF DIFFERENT POLYMER MOLAR MASS ON THE PHASE BEHAVIOR OF CARBON DIOXIDE + DICHLOROMETHANE + ε-CAPROLACTONE + POLY(ε-CAPROLACTONE) SYSTEM

The results presented in this chapter were submitted in **The Journal of Chemical Thermodynamics** on November 27, 2019.

Abstract

The phase behavior of [carbon dioxide + dichloromethane + ε-caprolactone + poly(ε-caprolactone)] system was investigated in order to provide fundamental information to understand the polymerization reaction in a high pressure system. The experiments were performed using a variable-volume view cell over the temperature range from 323.15 to 353.15 K, different mass ratios of carbon dioxide:dichloromethane:[water + ε-caprolactone + poly(ε-caprolactone)] (1:0.5:1 and 1:1:1), different number average molar mass of poly(ε-caprolactone) (10,000 and 80,000 $g \cdot mol^{-1}$), and different poly(ε-caprolactone) mass fractions (reaction conversion) from 0.0 up 15.0 wt%. Phase transitions of vapor-liquid bubble point type were verified and lower critical solution temperature (LCST) behavior phase in *P-T* diagrams was observed. The experimental results were modeled using the PC-SAFT EoS, providing a good representation of the experimental phase equilibrium data.

Keywords: Lactones; phase equilibria; supercritical fluids; PC-SAFT.

3.2.1 Introduction

Poly(ε-caprolactone) (PCL) is a biodegradable, bioresorbable and biocompatible polymer used in a wide variety of high-value biomedical applications (COMIM et al., 2015; BANG; LEE, 2019). It was described in literature two main pathways to produce this polyester: polycondensation of a hydroxycarboxylic acid of 6-hydroxyhexanoic, and the ring-opening polymerization (ROP) of ε-caprolactone (ε-CL) (MAYER et al., 2019). However, ROP using enzymatic catalysts and carbon dioxide (CO_2) as solvent has stood out in relation to the other methods.

Literature data showed that the ROP of ε-CL by enzymatic catalysis (e-ROP) in CO_2 has yield and molar mass similar those reactions in organic solvents and

metallic catalysts (COMIM et al., 2015; THURECHT et al., 2006). However, it is still necessary better understanding the kinetic reactions and thermodynamic behavior of the chemical species during the process of polymerization.

In this sense, mathematical modelling can be a good tool to improve these results, through a mathematical model is possible to analyze experimental conditions not tested and understand more profoundly the kinetic reactions, thus determining the main experimental conditions for process optimization in future reactions (JOHNSON; KUNDU; BEERS, 2011). However, mathematical modelling studies of polymerization process of the PCL are quite scarce. There is only one work available in the literature, which is the work of Johnson, Kundu and Beers (2011) that proposed a mathematical model for the polymerization reactions of PCL by ring-opening via enzymatic catalysis at low pressure, using toluene as solvent.

For the application of the mathematical model developed by Johnson, Kundu and Beers (2011) in the polymerization system of PCL in high pressure is necessary to know first the thermodynamic behavior of the chemical species present in the reaction as CO_2, ε-CL, and PCL. Beyond water (H_2O), which is the initiator of the reaction of polymerization, the use of dichloromethane (CH_2Cl_2) as co-solvent can be added to improve the solubility of PCL in the reaction medium. The addition of a co-solvent substantially enhances the polymer solubility, because reduction of the free-volume difference between PCL and the CO_2 (BANG; LEE, 2019).

In the literature, there are a series of studies that evaluate the behavior of phases of binary systems (CO_2 + ε-CL) (BERGEOT et al., 2004; XU; WAGNER; DAHMEN, 2003; BENDER et al, 2010b) and (CO_2 + PCL) (BANG; LEE, 2019; de PAZ et al., 2010) and, ternary systems (CO_2 + CH_2Cl_2 + ε-CL) (MAYER et al., 2019) and (CO_2 + CH_2Cl_2 + PCL) (KALOGIANNIS; PANAYIOTOU, 2006; BENDER et al, 2010a), but there are not studies that evaluate the phases behavior of the quaternary system (CO_2 + CH_2Cl_2 + ε-CL + PCL). That is, the lack in the literature is concerning studies evaluating the interaction between the ε-CL and PCL.

The development of equations to describe behavior in polymeric systems is a difficult task, since the non-spherical molecular architecture of the polymer exerts great influence on the thermodynamic behavior of the solutions, and therefore, the phase

balance of the polymer solution depends strongly on the energy interactions and the size differences between the polymer and solvent molecules (SY-SIONG-KIAO; CARUTHERS; CHAO, 1966). In this sense, Gross and Sadowski (1990) proposed an equation of state called PC-SAFT (Perturbed-Chain Statistical Association Fluid Theory), which has been widely applied in polymer systems. This equation of state has been able to describe the phase behavior of systems with CO_2 and PCL (BANG; LEE, 2019; de PAZ et al., 2010).

In this context, the objective of this work was to evaluate the phase behavior in systems containing CO_2, CH_2Cl_2, ε-CL, and PCL, investigating the influence of molar mass effects and dispersion of PCL, as well obtaining the modelling of these effects through PC-SAFT EoS for application in a mathematical model of PCL polymerization.

3.2.2 Experimental

3.2.2.1 Materials

PCL ($\bar{M}_n$ (g.mol^{-1}) 10000 and dispersion 1.4), PCL ($\bar{M}_n$ (g.mol^{-1}) 80000 and dispersion < 2.0), ε-CL (6-hexanolactone) and CH_2Cl_2 were purchased from Sigma-Aldrich (USA). The CO_2 was purchased from White Martins S.A. (Brazil). The ε-CL was dried in a vacuum oven at 373.15 K and 0.01 MPa for 48 h, resulting in a H_2O content of 0.04 ± 0.001%. Karl Fischer Coulometric Titrator for moisture determination (HI-904 - HANNA® instruments) was used to measure the water content. The other chemicals were used without further purification. Table 13 presents the chemical name, molecular formula, CAS number (CASRN), supplier and minimum mass fraction purity of all components used in this work. The supplier reported the minimum mass fraction purity of all components.

Table 13 - Chemical name, molecular formula, CAS number, supplier and minimum mass fraction purity of the materials used (purity provided by suppliers).

Chemical Name	Molecular Formula	CASRN	Supplier	Minimum Mass Fraction Purity
Poly(ε-Caprolactone) [a]	$(C_6H_{10}O_2)_n$	24980-41-4	Sigma-Aldrich	not specified
Poly(ε-Caprolactone) [b]	$(C_6H_{10}O_2)_n$	24980-41-4	Sigma-Aldrich	> 0.995
ε-Caprolactone	$C_6H_{10}O_2$	502-44-3	Sigma-Aldrich	0.970
Dichloromethane	CH_2Cl_2	75-09-2	Sigma-Aldrich	0.998
Carbon dioxide	CO_2	124-38-9	White Martins S.A.	0.999

[a] $\bar{M}_n$ = 10,000 g.mol^{-1} and $\bar{M}_w$ = 14,000 g.mol^{-1}

[b] $\bar{M}_n$ = 80,000 g.mol^{-1} and $\bar{M}_w$ = 138,840 g.mol^{-1}

Source: Author himself.

3.2.3 Phase equilibrium apparatus and procedure

Phase equilibrium experiments were conducted employing the static synthetic method in a high pressure variable-volume view cell. Both the apparatus and the experimental procedure have been described in detail elsewhere (MAYER et al., 2019). Figure 12 and 13 shows the equilibrium cell and the schematic diagram of the experimental apparatus used in this work, respectively. Briefly, the experimental procedure is as follows. In the static synthetic method is necessary to know the overall composition. Thus, different mass of PCL, ε-CL, and CH_2Cl_2 were on a precision balance (Shimadzu, Model AY220 with accuracy 0.0001 g) and inserted quickly into the equilibrium cell together a magnetic bar. After the insertion of all components, the equilibrium cell was quickly closed and connected to the high pressure system.

Subsequently a known volume of CO_2 was added to the equilibrium cell by a syringe pump (Isco, Model 260D) which was maintained at 10.0 MPa and 280.15 K. During the CO_2 addition, no pressure was applied in the equilibrium system to allow that the experiment begins with the equilibrium cell in its maximum volume of the 27 cm^3. After the complete addition of CO_2, the stirring of the solution and the system heating has started. From the moment that the temperature of 353.15 K was achieved the pressure of the system was gradually increased until a single phase. After stabilization of the pressure and temperature, the phase equilibria (bubble point) measurements were initiated by reducing the pressure (0.15-0.3 $MPa \cdot min^{-1}$) until the appearance of a second phase. This procedure was repeated several times (at least 3) to evaluate the reproducibility of the experimental methodology. In this evaluated system, only vapor-liquid equilibrium at the bubble point (VLE–BP) was observed. In order to understand the effects of molar mass of PCL during a polymerization reaction, phase equilibrium experiments were carried out keeping the mass ratio between CO_2 and CH_2Cl_2 fixed and the mass of ε-CL was varied in relation the PCL with molar mass different in the temperature range from 323.15 to 353.15 K. The variation of the mass of ε-CL in relation of PCL was performed by simulating the monomer conversion in polymer during the polymerization reaction. In this study, experiments were carried out with PCL mass fractions (reaction conversion) of 0.0 to 15.0 wt%.

3.2.4 Thermodynamic modelling

Figure 21 shows the procedure for formation of a molecule according to the Perturbed Chain-Statistical Theory of Associative Fluids (PC-SAFT) development by Gross and Sadowski (2001).

The PC-SAFT is based on hard-chain theory and it can be applied a real chains systems with any size, both spheres and polymers. In this approach, the molecules are considered chains composed of spherical segments. The pair potential for the segment of a chain is given by a modified square-well potential, which was suggested by Chen and Kreglewski (1977), as shown in Eq. (24):

$$u(r)=\begin{cases}\infty & r<(\sigma-s_1)\\ 3\varepsilon & (\sigma-s_1)\le r<\sigma\\ -\varepsilon & \sigma\le r<\lambda\sigma\\ 0 & r\ge\lambda\sigma\end{cases} \tag{24}$$

where $u(r)$ is the pair potential (J), r is the radial distance between two segments (Å), σ is the segment diameter (Å), s_1 is the constant defining the pair potential (Å), ε is the depth of potential well (J) and λ is the reduced well width. This model takes in account an important aspect of real molecules behavior, the soft repulsion (GROSS; SADOWSKI, 2001).

Figure 21 - Formation of a PC-SAFT molecule according to Gross and Sadowski (2001).

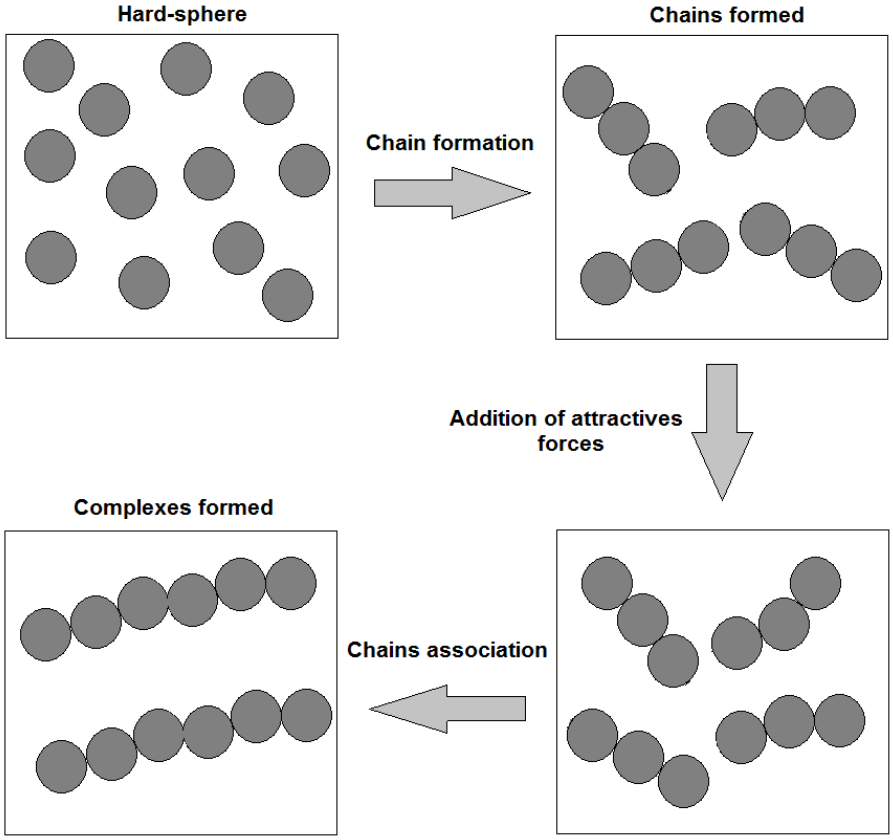

Source: Author himself.

According to the perturbed theories, the interaction between the molecules can be divided into a repulsive and perturbation parts. To calculate the first part, a reference fluid that does not generate attractions is used. The accuracy of this term indicates a good performance of the equation. For the second part, the theory of Bark and Henderson (CHEN; KREGLEWSKI, 1977; GROSS; SADOWSKI, 2001) is used.

In this case, as the reference fluid has a hard repulsion, the segment diameter is temperature-dependent and can be expressed as:

$$d_i(T) = \sigma_i \left[1 - 0.12 e^{\left(\frac{-3\varepsilon_i}{kT} \right)} \right] \tag{25}$$

The PC-SAFT Eos is given in terms of residual Helmholtz free energy ($\tilde{\boldsymbol{a}}^{\boldsymbol{res}}$), which can be calculated as the sum of three contributions:

$$\tilde{a}^{res} = \frac{A^{res}}{NkT} = \tilde{a}^{hc} + \tilde{a}^{disp} + \tilde{a}^{assoc} \tag{26}$$

where A^{res} is the Helmholtz free energy (J), N is the total number of molecules, k is the Boltzmann constant (J.K^{-1}), T is the temperature (K), $\tilde{a}^{hc}$ is the hard-chain reference contribution (J), $\tilde{a}^{disp}$ is the contribution due to dispersive attraction (J) and $\tilde{a}^{assoc}$ is the contribution due the associating interactions (J).

The $\tilde{a}^{hc}$ term was developed by Chapman et al. (1988) and it can be expressed by:

$$\tilde{a}^{hc} = \bar{m}\tilde{a}^{hs} - \sum_i x_i (m_i - 1) \ln\left(g_{ii}^{hs}\right) \tag{27}$$

where $\bar{m}$ is the mean segment number in the mixture, $\tilde{a}^{hs}$ is the Helmholtz free energy of the had-sphere (J), x_i is the mole fraction of component i, m_i is the number of segments in the mixture of component i and g_{ii}^{hs} is the radial distribution function of the hard-sphere fluid of component i. The terms $\tilde{a}^{hs}$ and g_{ii}^{hs} can be expressed as:

$$\tilde{a}^{hs} = \frac{1}{\zeta_0} \left[\frac{3\zeta_1\zeta_2}{(1-\zeta_3)} + \frac{\zeta_2^3}{\zeta_3(1-\zeta_3)^2} + \left(\frac{\zeta_2^3}{\zeta_3^3} - \zeta_0 \right) \ln(1-\zeta_3) \right] \tag{28}$$

$$g_{ii}^{hs} = \frac{1}{(1-\zeta_3)} + \frac{d_i d_j}{(d_i + d_j)} \frac{3\zeta_2}{(1-\zeta_3)} + \left(\frac{d_i d_j}{d_i + d_j} \right)^2 \frac{2\zeta_2^2}{(1-\zeta_3)^3} \tag{29}$$

As mentioned, the theory of Bark and Henderson (BARKER; HENDERSON, 1967a; BARKER; HENDERSON, 1967b) used by Gross and Sadoski (2001) to calculate the repulsive and perturbations parts between the chains, as shown in Eq. (30):

$$\frac{A^{dis}}{NkT} = \frac{A_1}{NkT} + \frac{A_2}{NkT} \tag{30}$$

where A_1 is the Helmholtz free energy of first-order perturbation term (J) and A_2 is the Helmholtz free energy of second-order perturbation term (J) and can be expressed as:

$$\frac{A_1}{NkT} = -2\pi\rho I_1(\eta, \overline{m}) \sum_i \sum_j x_i x_j m_i m_j \left(\frac{\varepsilon_{ij}}{kT} \right) \sigma_{ij}^3 \tag{31}$$

$$\frac{A_1}{NkT} = -\pi\rho\overline{m} \left(1 + Z^{hc} \rho \frac{\partial Z^{hc}}{\partial \rho} \right)^{-1} I_2(\eta, m) \sum_i \sum_j x_i x_j m_i m_j \left(\frac{\varepsilon_{ij}}{kT} \right)^2 \sigma_{ij}^3 \tag{32}$$

where ρ is the total number density molecules (Å^{-3}). The parameter $\overline{m}$ is calculated by linear mixing rule, while the ϵ_{ij}/k e σ_{ij} are calculated by Berthelot-Lorentz combining rules:

$$\sigma_{ij} = \frac{1}{2}(\sigma_i + \sigma_j) \tag{33}$$

$$\varepsilon_{ij} = \sqrt{\varepsilon_i \varepsilon_j}(1 - k_{ij}) \tag{34}$$

The Wertheim's thermodynamic perturbation theory of first-order (WERTHEIM, 1984a; WERTHEIM, 1984b; WERTHEIM, 1986a; WERTHEIM, 1986b) was used to compute the specific interactions between chains (association) by Chapman et al. (1988),

$$\widetilde{a}^{assoc} = \sum_i x_i \left[\sum_{A_i} \left(\ln X_{A_i} - \frac{X_{A_i}}{2} \right) + \frac{1}{2} M_i \right] \tag{35}$$

The key of association term is the X_{A_i}, which relates the sites fraction A of component i that are not linked to other active sites, being dependent on the strength of association between the sites, according to:

$$X_{A_i} = \left(1 + N_{AV} \sum_j \sum_{B_j} \rho_j X_{B_j} \Delta^{A_i B_j}\right)^{-1} \tag{36}$$

where N_{AV} is the Avogadro's Number (mol^{-1}) and the association force ($\Delta^{A_i B_j}$) is defined by:

$$\Delta^{A_i B_j} = d_{ij}^3 g_{ij}\left(d_{ij}\right)^{seg} \kappa^{A_i B_j}\left[e^{\left(\frac{\varepsilon^{A_i B_j}}{kT}\right)} - 1\right] \tag{37}$$

where $\varepsilon^{A_i B_j}$ and $\kappa^{A_i B_j}$ are energy and the volume of association between the site A of molecule i and the site B of molecule j, respectively.

The compressibility factor (Z) is derived from the thermodynamic relation:

$$Z = 1 + \eta\left(\frac{\partial \tilde{a}^{res}}{\partial \eta}\right)_{T,x_i} \tag{38}$$

The pressure can be calculated in units of *Pa* by applying the relation:

$$P = ZkT\rho\left(10^{10}\frac{\dot{A}}{m}\right)^3 \tag{39}$$

To the non-associated components, the parameters of PC-SAFT EoS are m_i, σ_i and ε_i/k. Already to associated components, there are two additional associated parameters $\varepsilon^{A_i B_i}/k$ and $\kappa^{A_i B_i}$. Table 14 presents the PC-SAFT EOS pure component parameters used in this work. The CO_2 and H_2O parameters were taken from literature (GROSS; SADOWSKI, 2001; GROSS; SADOWSKI, 2002) and the CH_2Cl_2, ε-CL and PCL parameters were estimated fitting the equation to density and vapor pressure.

Table 14 - PC-SAFT EOS pure component parameters used in this work.

Compound	M (g·mol^{-1})	m_i (-)	σ_i (Å)	ε_i/k (K)	$\varepsilon^{A_iB_i}/k$ (K)	$\kappa^{A_iB_i}$
Water	18.015	1.0656	3.0007	366.51	2500.7	0.034868
Carbon dioxide	44.010	2.0729	2.7852	169.21		
Dichloromethane	84.930	4.5620	3.1810	257.00		
ε-Caprolactone	114.140	6.2130	2.6020	268.80		
Poly(ε-Caprolactone)[a]	14,000	1483.6	2.7910	289.50		
Poly(ε-Caprolactone)[b]	138,840	1483.6	2.7910	289.50		

[a] $\bar{M}_n$ = 10,000 g.mol^{-1} and $\bar{M}_w$ = 14,000 g.mol^{-1}

[b] $\bar{M}_n$ = 80,000 g.mol^{-1} and $\bar{M}_w$ = 138,840 g.mol^{-1}

In order to calculated the saturation pressure of vapor-liquid bubble point and estimated the binary interaction parameters (k_{12}, k_{13}, k_{14}, k_{15}, k_{23}, k_{24}, k_{25}, k_{34}, k_{35} and k_{45}), a *PYTHON* computation code was implemented with the following objective function (OF):

$$OF = \sum_{i=1}^{nobs} (P_i^{cal} - P_i^{\exp})^2 \tag{40}$$

where P_i^{exp} represents the arithmetic mean of three measurements of transitions pressure, P_i^{cal} represents the calculated pressure by the PC-SAFT EoS, and $nobs$ denotes the number of observations. In this work, the results of the generated residues were presented by absolute deviation (AD) and root-mean-square deviation values ($rmsd$).

$$AD = \sum_{i=1}^{nobs} \frac{\left| P_i^{cal} - P_i^{\exp} \right|}{nobs} \tag{41}$$

$$rmsd = \sum_{i=1}^{nobs} \frac{\left(P_i^{cal} - P_i^{\exp} \right)^2}{nobs} \tag{42}$$

3.2.5 Results and Discussion

PCLs with number average molar mass of 10,000 and 80,000 g·mol^{-1} were used to understand the effect of the molar mass in the polymerization reactions. For this, phase equilibrium experiments were performed trying to imitate a polymerization reaction through the conversion of ε-CL to PCL. For this purpose, the mass fraction of the PCL for ε-CL was varied in 0.0, 1.0, 2.5, 5.0, 7.5, 10.0, 12.5 and 15.0 wt% and the mass ratio CO_2:CH_2Cl_2:(H_2O + ε-CL + PCL) was kept fixed in 1:0.5:1 and 1:1:1, respectively. In these experiments, there were evaluated mass fractions of PCL up to a maximum of 15.0%, mainly due to the difficulty to visualize the equilibrium point in the experimental apparatus.

Tables 16 to 19 show the experimental phase transition data measured for the quaternary system [CO_2 (1) + CH_2Cl_2 (2) + ε-CL(3) + PCL (4)], for the temperatures of 323.15, 333.15, 343.15 and 353.15 K, in CO_2 and CH_2Cl_2 free-basis, for mass ratios CO_2:CH_2Cl_2:(H_2O + ε-CL + PCL) of 1:0.5:1 and 1:1:1, respectively. Tables show the results in terms of pressure (*P*), experimental error for each conditions represented by the standard deviation of replicate pressure measurements ($\boldsymbol{sd}$) and the phase transition type of vapor-liquid equilibrium (VLE) with bubble point transition (BP). The molar fractions tables for the multicomponent system [CO_2 (1) + CH_2Cl_2 (2) + H_2O (3) + ε-CL (4) + PCL (5)] are present in 3.2.7 Supporting Information. In the molar fractions tables the water was considered as a component of the system, even though it is not added, but it is present in ε-CL and it is important in the e-ROP, because it acts as the initiator of the reaction. Thus, the knowledge of the water behavior in high pressure phase equilibrium data is important when the objective is to develop a mathematical model for e-ROP of the ε-CL in high pressure.

Table 15 - Phase equilibrium results for the quaternary system [CO_2 (1) + CH_2Cl_2 (2) + ε-CL (3) + PCL (4)] for the mass ratio CO_2: CH_2Cl_2: (H_2O + ε-CL + PCL) of 1:0.5:1. In this case the H_2O content in the ε-CL was 0.04 + 0.001 % and PCL had number average molar mass ($\overline{M}_n$) of 10000 g.mol^{-1} and dispersion (D) of 1.4.

T/K	*P*/MPa	*sd*/MPa	Transition type	*T*/K	*P*/MPa	*sd*/MPa	Transition type
w_3' = 100.00% (w_4' = 0.00%)				w_3' = 92.43% (w_4' = 7.57%)			
323.15	7.74	0.01	VLE-BP	323.15	8.17	0.03	VLE-BP
333.15	9.21	0.02	VLE-BP	333.15	9.90	0.01	VLE-BP
343.15	10.97	0.02	VLE-BP	343.15	11.81	0.01	VLE-BP
353.15	12.72	0.02	VLE-BP	353.15	14.05	0.02	VLE-BP
w_3' = 99.00% (w_4' = 1.00%)				w_3' = 90.03% (w_4' = 9.97%)			
323.15	7.85	0.02	VLE-BP	323.15	8.19	0.01	VLE-BP
333.15	9.33	0.02	VLE-BP	333.15	9.97	0.03	VLE-BP
343.15	11.12	0.01	VLE-BP	343.15	11.84	0.01	VLE-BP
353.15	12.87	0.01	VLE-BP	353.15	14.13	0.03	VLE-BP
w_3' = 97.52% (w_4' = 2.48%)				w_3' = 87.55% (w_4' = 12.45%)			
323.15	7.98	0.01	VLE-BP	323.15	8.21	0.01	VLE-BP
333.15	9.51	0.03	VLE-BP	333.15	10.01	0.03	VLE-BP
343.15	11.40	0.01	VLE-BP	343.15	11.99	0.01	VLE-BP
353.15	13.22	0.03	VLE-BP	353.15	14.27	0.03	VLE-BP
w_3' = 94.97% (w_4' = 5.03%)				w_3' = 85.00% (w_4' = 15.00%)			
323.15	8.15	0.01	VLE-BP	323.15	8.21	0.01	VLE-BP
333.15	9.86	0.02	VLE-BP	333.15	10.01	0.01	VLE-BP
343.15	11.79	0.03	VLE-BP	343.15	12.22	0.03	VLE-BP
353.15	13.91	0.02	VLE-BP	353.15	14.52	0.03	VLE-BP

w_3' denotes mass fraction of H_2O + ε-CL on in CH_2Cl_2 and CO_2 free-basis; w_4', denotes the mass fraction of PCL on in CO_2 and CH_2Cl_2 free-basis; VLE-BP, vapor-liquid-equilibrium type bubble point; *T*, system temperature; *P*, system pressure; sd, standard deviation.

Table 16 - Phase equilibrium results for the quaternary system [CO_2 (1) + CH_2Cl_2 (2) + ε-CL (3) + PCL (4)] for the mass ratio CO_2: CH_2Cl_2: (H_2O + ε-CL + PCL) of 1:1:1. In this case the H_2O content in the ε-CL was 0.040 + 0.001 % and PCL had number average molar mass ($\overline{M}_n$) of 10000 g.mol^{-1} and dispersion (D) of 1.4.

T/K	*P*/MPa	*sd*/MPa	Transition type	*T*/K	*P*/MPa	*sd*/MPa	Transition type
w_3' = 100.00% (w_4' = 0.00%)				w_3' = 92.54% (w_4' = 7.46%)			
323.15	6.43	0.02	VLE-BP	323.15	6.73	0.01	VLE-BP
333.15	7.53	0.02	VLE-BP	333.15	7.82	0.02	VLE-BP
343.15	8.80	0.01	VLE-BP	343.15	9.25	0.02	VLE-BP
353.15	10.24	0.03	VLE-BP	353.15	10.65	0.01	VLE-BP
w_3' = 99.00% (w_4' = 1.00%)				w_3' = 89.91% (w_4' = 10.09%)			
323.15	6.48	0.01	VLE-BP	323.15	6.67	0.01	VLE-BP
333.15	7.60	0.01	VLE-BP	333.15	7.73	0.02	VLE-BP
343.15	8.88	0.02	VLE-BP	343.15	9.18	0.01	VLE-BP
353.15	10.30	0.01	VLE-BP	353.15	10.52	0.01	VLE-BP
w_3' = 97.50% (w_4' = 2.50%)				w_3' = 87.38% (w_4' = 12.62%)			
323.15	6.55	0.01	VLE-BP	323.15	6.71	0.02	VLE-BP
333.15	7.65	0.01	VLE-BP	333.15	7.82	0.01	VLE-BP
343.15	8.98	0.03	VLE-BP	343.15	9.20	0.02	VLE-BP
353.15	10.37	0.02	VLE-BP	353.15	10.69	0.02	VLE-BP
w_3' = 94.97% (w_4' = 5.03%)				w_3' = 85.06% (w_4' = 14.94%)			
323.15	6.66	0.02	VLE-BP	323.15	6.80	0.02	VLE-BP
333.15	7.80	0.02	VLE-BP	333.15	8.01	0.01	VLE-BP
343.15	9.13	0.03	VLE-BP	343.15	9.36	0.01	VLE-BP
353.15	10.55	0.02	VLE-BP	353.15	10.87	0.02	VLE-BP

w_3' denotes mass fraction of H_2O + ε-CL on in CH_2Cl_2 and CO_2 free-basis; w_4', denotes the mass fraction of PCL on in CO_2 and CH_2Cl_2 free-basis; VLE-BP, vapor-liquid-equilibrium type bubble point; *T*, system temperature; *P*, system pressure; *sd*, standard deviation.

Table 17 - Phase equilibrium results for the quaternary system [CO_2 (1) + CH_2Cl_2 (2) + ε-CL (3) + PCL (4)] for the mass ratio CO_2: CH_2Cl_2: (H_2O + ε-CL + PCL) of 1:0.5:1. In this case the H_2O content in the ε-CL was 0.040 + 0.001 % and PCL had number average molar mass ($\overline{M}_n$) of 80,000 g.mol^{-1} and dispersion (D) of 1.74.

T/K	*P*/MPa	*sd*/MPa	Transition type	*T*/K	*P*/MPa	*sd*/MPa	Transition type
w_3' = 100.00% (w_4' = 0.00%)				w_3' = 92.38% (w_4' = 7.62%)			
323.15	7.74	0.01	VLE-BP	323.15	8.25	0.01	VLE-BP
333.15	9.21	0.02	VLE-BP	333.15	10.01	0.01	VLE-BP
343.15	10.97	0.02	VLE-BP	343.15	11.92	0.02	VLE-BP
353.15	12.72	0.02	VLE-BP	353.15	14.00	0.01	VLE-BP
w_3' = 99.00% (w_4' = 1.00%)				w_3' = 90.01% (w_4' = 9.99%)			
323.15	7.85	0.01	VLE-BP	323.15	8.28	0.01	VLE-BP
333.15	9.45	0.01	VLE-BP	333.15	10.05	0.01	VLE-BP
343.15	11.22	0.01	VLE-BP	343.15	11.99	0.01	VLE-BP
353.15	13.16	0.02	VLE-BP	353.15	14.22	0.03	VLE-BP
w_3' = 97.50% (w_4' = 2.50%)				w_3' = 87.51% (w_4' = 12.49%)			
323.15	7.91	0.01	VLE-BP	323.15	8.22	0.01	VLE-BP
333.15	9.51	0.01	VLE-BP	333.15	9.90	0.02	VLE-BP
343.15	11.44	0.03	VLE-BP	343.15	11.99	0.01	VLE-BP
353.15	13.47	0.02	VLE-BP	353.15	14.27	0.01	VLE-BP
w_3' = 95.00% (w_4' = 5.00%)				w_3' = 85.00% (w_4' = 15.00%)			
323.15	8.12	0.03	VLE-BP	323.15	8.22	0.01	VLE-BP
333.15	9.87	0.03	VLE-BP	333.15	9.82	0.01	VLE-BP
343.15	11.82	0.01	VLE-BP	343.15	12.00	0.02	VLE-BP
353.15	13.84	0.02	VLE-BP	353.15	14.31	0.03	VLE-BP

w_3' denotes mass fraction of H_2O + ε-CL on in CH_2Cl_2 and CO_2 free-basis; w_4', denotes the mass fraction of PCL on in CO_2 and CH_2Cl_2 free-basis; VLE-BP, vapor-liquid-equilibrium type bubble point; *T*, system temperature; *P*, system pressure; sd, standard deviation.

Table 18 - Phase equilibrium results for the quaternary system [CO_2 (1) + CH_2Cl_2 (2) + ε-CL (3) + PCL (4)] for the mass ratio CO_2: CH_2Cl_2: (H_2O + ε-CL + PCL) of 1:1:1. In this case the H_2O content in the ε-CL was 0.040 + 0.001 % and PCL had number average molar mass ($\overline{M}_n$) of 80,000 g.mol^{-1} and dispersion (D) of 1.74.

T/K	*P*/MPa	*sd*/MPa	Transition type	*T*/K	*P*/MPa	*sd*/MPa	Transition type
w_3' = 100.00% (w_4' = 0.00%)				w_3' = 92.51% (w_4' = 7.49%)			
323.15	6.43	0.02	VLE-BP	323.15	6.69	0.01	VLE-BP
333.15	7.53	0.02	VLE-BP	333.15	7.79	0.01	VLE-BP
343.15	8.80	0.01	VLE-BP	343.15	9.20	0.02	VLE-BP
353.15	10.24	0.03	VLE-BP	353.15	10.60	0.01	VLE-BP
w_3' = 98.98% (w_4' = 1.02%)				w_3' = 90.02% (w_4' = 9.98%)			
323.15	6.45	0.01	VLE-BP	323.15	6.69	0.01	VLE-BP
333.15	7.60	0.01	VLE-BP	333.15	7.79	0.01	VLE-BP
343.15	8.83	0.02	VLE-BP	343.15	9.20	0.02	VLE-BP
353.15	10.29	0.01	VLE-BP	353.15	10.60	0.01	VLE-BP
w_3' = 97.49% (w_4' = 2.51%)				w_3' = 87.48% (w_4' = 12.52%)			
323.15	6.45	0.02	VLE-BP	323.15	6.61	0.01	VLE-BP
333.15	7.60	0.03	VLE-BP	333.15	7.68	0.01	VLE-BP
343.15	8.89	0.02	VLE-BP	343.15	9.05	0.01	VLE-BP
353.15	10.33	0.02	VLE-BP	353.15	10.55	0.01	VLE-BP
w_3' = 95.00% (w_4' = 5.00%)				w_3' = 84.99% (w_4' = 15.01%)			
323.15	6.59	0.02	VLE-BP	323.15	6.73	0.02	VLE-BP
333.15	7.76	0.02	VLE-BP	333.15	7.85	0.01	VLE-BP
343.15	9.09	0.01	VLE-BP	343.15	9.29	0.03	VLE-BP
353.15	10.50	0.01	VLE-BP	353.15	10.74	0.03	VLE-BP

w_3' denotes mass fraction of H_2O + ε-CL on in CH_2Cl_2 and CO_2 free-basis; w_4', denotes the mass fraction of PCL on in CO_2 and CH_2Cl_2 free-basis; VLE-BP, vapor-liquid-equilibrium type bubble point; *T*, system temperature; *P*, system pressure; sd, standard deviation.

In Tables 15 to 18 it can be seen that only transition of vapor-liquid type were verified, characterized by the formation of vapor bubbles at the top of the equilibrium cell during the depressurization. This has already been expected, because Mayer et

al. (2019) for the ternary system [CO_2 (1) + CH_2Cl_2 (2) + ε-CL (3)] in the mass ratio CO_2: CH_2Cl_2: ε-CL of 1:0.5:1 and 1:1:1, also observed transition of vapor-liquid type. Another important point observed was that the substitution of up to 15.0% of ε-CL by PCL does not change the system transition type.

To improve visualization and interpretation of data from Tables 15 to 18, Figures 22 and 23 present the diagrams of pressure (*P*) vs. mass fraction of PCL (w_4') for the different CO_2: CH_2Cl_2: (H_2O + ε-CL + PCL) mass ratio, PCL molar mass and temperature.

Figure 22 - *P*-w_4' diagram for VLE-BP for the system [CO_2 (1) + CH_2Cl_2 (2) + ε-CL (3) + PCL (4)] for the mass ratio CO_2: CH_2Cl_2: (H_2O + ε-CL + PCL) of 1:0.5:1 in different number average molar mass ($\bar{M}_n$) of the PCL. Experimental data: 323:15 K: □ (10,000 g·mol^{-1}) and ■ (80,000 g·mol^{-1}); 333:15 K: ○ (10,000 g·mol^{-1}) and ● (80,000 g·mol^{-1}); 343:15 K: △ (10,000 g·mol^{-1}) and ▲ (80,000 g·mol^{-1}); 353:15 K: ▽ (10,000 g·mol^{-1}) and ▼ (80,000 g·mol^{-1}). Predicted data by PC-SAFT model: dashed line (10,000 g·mol^{-1}) and solid line (80,000 g·mol^{-1}).

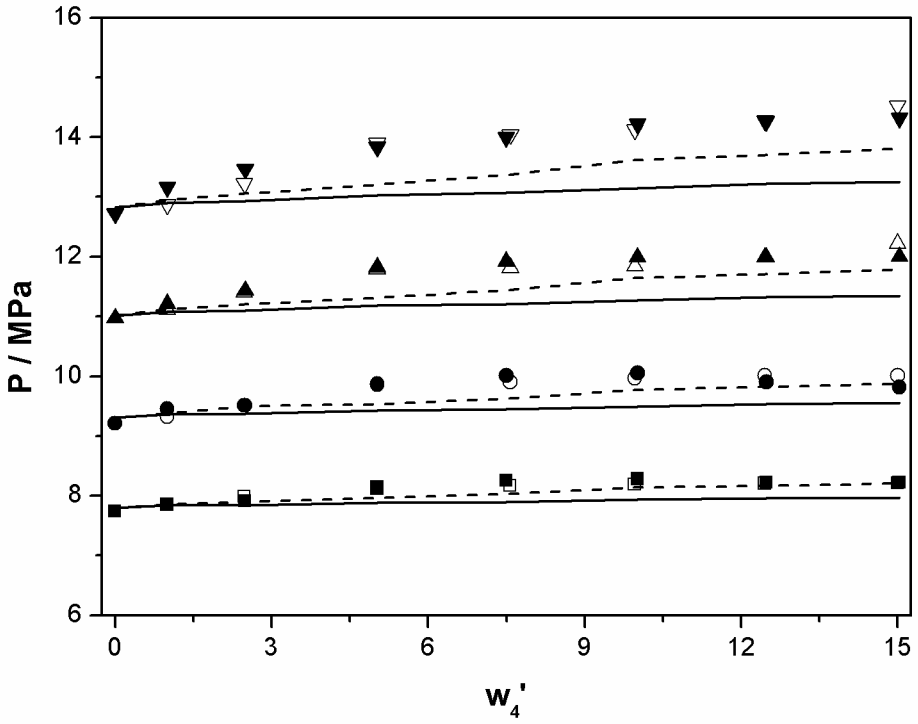

Source: Author himself.

Figure 23 - *P*-w_4' diagram for VLE-BP for the system [CO_2 (1) + CH_2Cl_2 (2) + ε-CL (3) + PCL (4)] for the mass ratio CO_2: CH_2Cl_2: (H_2O + ε-CL + PCL) of 1:1:1 in different number average molar mass ($\bar{M}_n$) of the PCL. Experimental data: 323:15 K: □ (10,000 g·mol^{-1}) and ■ (80,000 g·mol^{-1}); 333:15 K: ○ (10,000 g·mol^{-1}) and ● (80,000 g·mol^{-1}); 343:15 K: △ (10,000 g·mol^{-1}) and ▲ (80,000 g·mol^{-1}); 353:15 K: ▽ (10,000 g·mol^{-1}) and ▼ (80,000 g·mol^{-1}). Predicted data by PC-SAFT model: dashed line (10,000 g·mol^{-1}) and solid line (80,000 g·mol^{-1}).

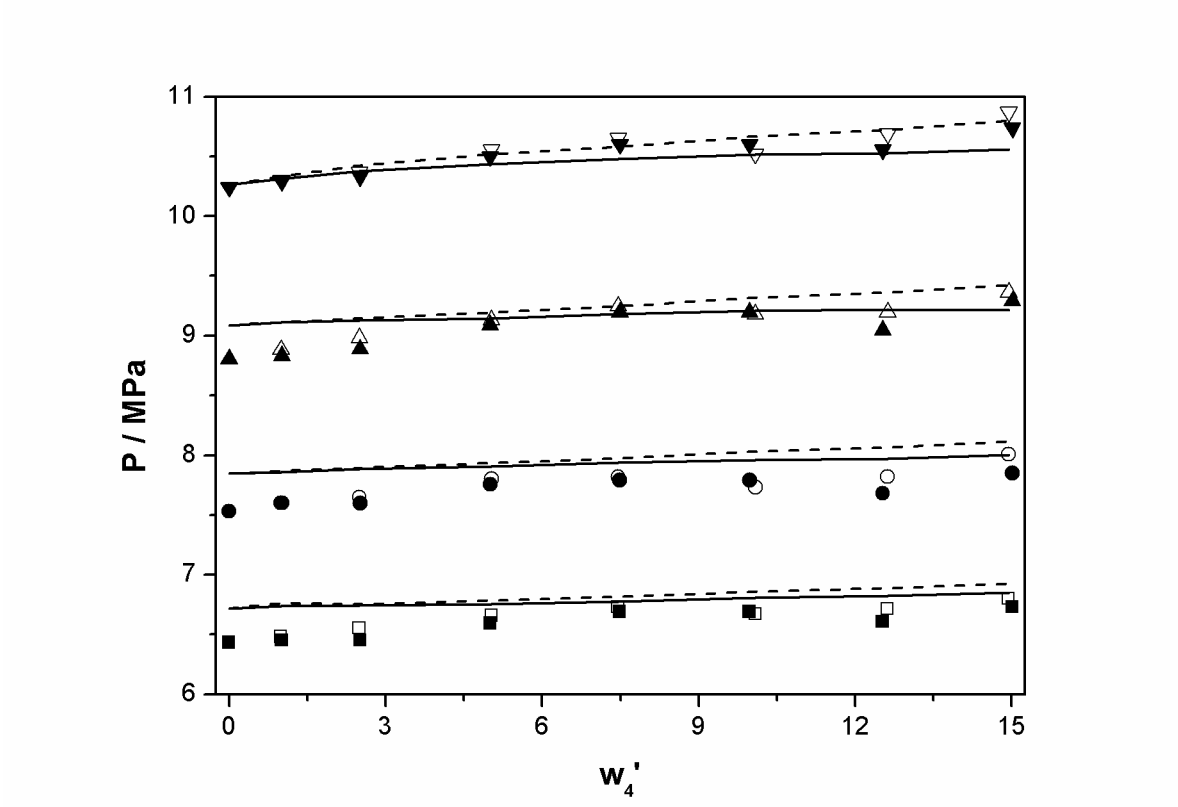

Source: Author himself.

In Figures 22 and 23, it is also possible to see that the molar mass does not change the pressure significantly for the temperatures and mass ratios analyzed. Similar results were also observed by Ndiaye et al. (2001) that evaluated the phase behavior of isotactic polypropylene with average molar mass of 245,000 and 197,000 g·mol^{-1} in 1-butene and *n*-butane. It is also observed in the diagrams that the substitution of ε-CL by PCL promoted a small increase in pressure. However, this small increase of pressure is not related with the increase of PCL fraction in the system, because according the work of Bang et al. (2019), that studied the behavior of phase equilibrium of systems chlorodifluoromethane + PCL and dimethyl ether + PCL, the increase of PCL fraction promote the decrease of pressure. Thus, this small increase

of pressure is due to the slight increase of CO_2 molar fraction in the system due to the substitution of ε-CL by PCL, as can be observed in molar fractions tables presented in 3.2.7 Supporting Information.

Figure 24 shows a *P-T* diagram for quaternary system CO_2 (1) + CH_2Cl_2 (2) + ε-CL(3) + PCL (4) for 0.0 and 15.0% of PCL with number average molar mass of 10,000 and 80,000 g·mol^{-1}. In this *P-T* diagram, it is possible to observe that with increasing temperature, there is an increase in system pressure. This behavior is characteristic of a lower critical solution temperature (LCST). According to Rebelatto et al. (2018a), an increase in the system temperature causes the more volatile compound (CO_2) to expand much more than compared to the ε-CL and the CH_2Cl_2, hence leading to a raise in the solution volume and greater pressure is needed to obtain an one-phase homogeneous system. This type of behavior has also been found in other works involving ε-CL, as the works of Bender et al. (2010b) and Mayer et al. (2019).

Note in the *P-T* diagram that for 15% PCL curves that the higher number average molar mass the lower the pressure is required to solubilize the system. This is due to the lower molar fraction of PCL present in the system and thus the contribution of PCL to the pressure is smaller. In addition, it has also been found that increasing the amount of CH_2Cl_2 helps in homogenizing the system, resulting in a reduction of the transition pressure.

The PC-SAFT EoS model was used to predict the phase equilibrium behavior for the multicomponent system [CO_2 (1) + CH_2Cl_2 (2) + H_2O (3) + ε-CL (4) + PCL (5)]. As we have commented previously, water was considered as a component of system for the phase equilibrium modelling, because it is present in ε-CL and it is important in the ROP. The binary interaction parameters (k_{12}, k_{13}, k_{14}, k_{15}, k_{23}, k_{24}, k_{25}, k_{34}, k_{35} and k_{45}) together with the absolute deviation (AD) and root-mean-square deviation values ($rmsd$) are presented in Table 19.

Figure 24 - *P-T* diagram for VLE-BP for the system [CO_2 (1) + CH_2Cl_2 (2) + ε-CL (3) + PCL (4)] for the different number average molar mass ($\bar{M}_n$) of the PCL to mass ratio CO_2: CH_2Cl_2: (H_2O + ε-Cl + PCL) of 1:0.5:1 and 1:1:1. Experimental data: 1:0.5:1: ◨ (w_4' = 0.00%), □ (w_4' = 15.00% - $\bar{M}_n$ = 10,000 g·mol^{-1}) and ■ (w_4' = 15.00% - $\bar{M}_n$ = 80,000 g·mol^{-1}); 1:1:1: ◭ (w_4' = 0.00%), △ (w_4' = 15.00% - $\bar{M}_n$ = 10,000 g·mol^{-1}) and ▲ (w_4' = 15.00% - $\bar{M}_n$ = 80,000 g·mol^{-1}). Predicted data by PC-SAFT model: dot line (0.00% PCL), dashed line (10,000 g·mol^{-1}) and solid line (80,000 g·mol^{-1}).

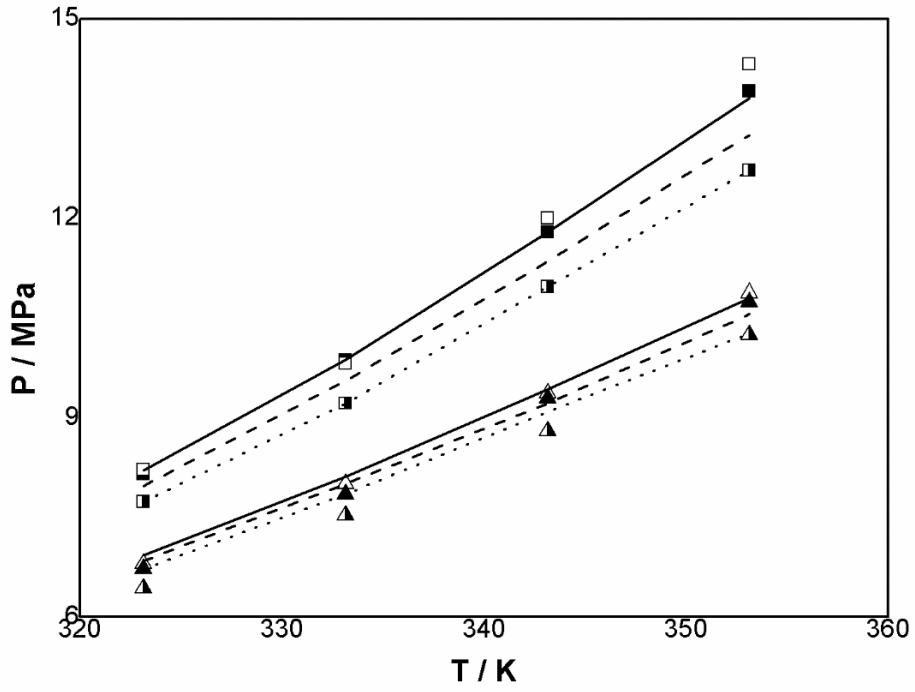

Source: Author himself.

Table 19 - Binary interaction parameters of PC-SAFT EOS in this work for the multicomponent system [CO_2 (1) + CH_2Cl_2 (2) + H_2O (3) + ε-CL (4) + PCL (5)].

T/K	k_{ij}		*AD/MPa*	*Rmsd/(MPa)²*
323.15 to 353.15	k_{12}	0.0150	0.9701	4.5104
	k_{13}	0.0000		
	k_{14}	-0.0380		
	k_{15}	0.0000		
	$k_{23} = k_{24} = k_{25}$	0.0000		
	$k_{34} = k_{35}$	0.0000		
	k_{45}	0.0000		

Through Table 19 it can be seen that using the PC-SAFT EoS only the binary interaction parameters between CO_2 and CH_2Cl_2 (k_{12} = 0.0150), and CO_2 and ε-CL (k_{14} = -0.0380) had to be adjusted. This shows the efficiency of PC-SAFT in predicting polymer systems, in others words shows the robustness of this model.

Another important point to highlight and that shows the robustness of PC-SAFT EoS is that binary interaction parameters were not considered temperature-dependent as it was performed by Mayer et al. (2019) that modeled the ternary system [CO_2 (1) + CH_2Cl_2 (2) + ε-CL (3)] with Peng-Robinson EoS with the van der Waals quadratic mixing rule considered the binary interaction parameter between CO_2 and ε-CL as temperature-dependent.

The good performance of PC-SAFT EoS becomes more evident comparison the experimental and calculated phase equilibrium values when Figures 22 to 24 are analyzed. The PC-SAFT EoS was able to represent the phase equilibrium for different number average molar masses of PCL (10,000 and 80,000 g·mol^{-1}), different mass ratio CO_2: CH_2Cl_2: ε-CL (1:0.5:1 and 1:1:1) and different temperatures (323.15 to 353.15 K).

3.2.6 Partial Conclusion

The phase behavior of the quaternary system [CO_2 (1) + CH_2CL_2 (2) + ε-CL (3) + PCL (4)] at different CO_2: CH_2CL_2: (H_2O + ε-CL + PCL) mass ratios (1:0.5:1 and 1:1:1) and two different molar mass of PCL was experimentally investigated in this work over the temperature range of 323.15 to 353.15 K in order to understand the polymerization reaction in a high pressure. In all systems, it was observed only VLE–BP, resulting in phase transition pressures up to 16.50 MPa. Through the *P-w* diagrams, it was observed that increasing the amount of CH_2CL_2 helps in homogenizing the system, resulting in a reduction of the transition pressure. In addition, it was found that the pressures increased as the temperature increased, characterizing an LCST behavior, where an increase in temperature results in the expansion of the system and thus higher pressures are required to solubilize the system in a single phase. The PC-SAFT EoS provided good performance of the experimental phase equilibrium results obtained when the global fitting was employed for data fitting. The data obtained in this work have great relevance, since they allow a better understanding of the polymerization reactions, serving as basis for the determination of the best conditions for the process performance.

3.2.7 Supporting Information

Table 20 - Molar fractions for the multicomponent system [CO_2 (1) + CH_2Cl_2 (2) + H_2O (3) + ε-CL (4) + PCL (5)] for the mass ratio CO_2: CH_2Cl_2: (H_2O + ε-CL + PCL) of 1:0.5:1. In this case, PCL had number average molar mass ($\bar{M}_n$) of 10,000 g·mol^{-1} and dispersion (D) of 1.40. Molar fractions related to the data presented in Table 15.

w_5'	x_1	x_2	x_3	x_4	x_5
0.00	0.607005	0.158489	0.000593	0.233913	0.000000
1.00	0.609302	0.157736	0.000589	0.232353	0.000019
2.48	0.611598	0.158241	0.000582	0.229532	0.000048
5.03	0.614971	0.159776	0.000569	0.224586	0.000097
7.57	0.618359	0.161004	0.000557	0.219932	0.000147
9.97	0.622974	0.160921	0.000546	0.215365	0.000194
12.45	0.625123	0.163473	0.000534	0.210626	0.000244
15.00	0.625918	0.165223	0.000527	0.208033	0.000299

w_5', denotes the mass fraction of PCL on in CO_2 and CH_2Cl_2 free-basis; x_1, molar fraction for the CO_2; x_2, molar fraction for the CH_2Cl_2; x_3, molar fraction for the H_2O; x_4, molar fraction for the ε-CL; x_5, molar fraction for the PCL.

Table 21 - Molar fractions for the multicomponent system [CO_2 (1) + CH_2Cl_2 (2) + H_2O (3) + ε-CL (4) + PCL (5)] for the mass ratio CO_2: CH_2Cl_2: (H_2O + ε-CL + PCL) of 1:1:1. In this case, PCL had number average molar mass ($\bar{M}_n$) of 10,000 g·mol^{-1} and dispersion (D) of 1.40. Molar fractions related to the data presented in Table 16.

w_5'	x_1	x_2	x_3	x_4	x_5
0.00	0.519195	0.272118	0.000512	0.202174	0.000000
1.02	0.526399	0.272508	0.000508	0.200567	0.000017
2.52	0.528095	0.273487	0.000502	0.197874	0.000042
5.00	0.530548	0.274940	0.000492	0.193937	0.000083
7.49	0.532939	0.276388	0.000482	0.190066	0.000126
9.98	0.536210	0.277503	0.000471	0.185648	0.000168
12.52	0.538680	0.279417	0.000459	0.181232	0.000212
15.01	0.541667	0.280561	0.000449	0.177069	0.000255

w_5', denotes the mass fraction of PCL on in CO_2 and CH_2Cl_2 free-basis; x_1, molar fraction for the CO_2; x_2, molar fraction for the CH_2Cl_2; x_3, molar fraction for the H_2O; x_4, molar fraction for the ε-CL; x_5, molar fraction for the PCL.

Table 22 - Molar fractions for the multicomponent system [CO_2 (1) + CH_2Cl_2 (2) + H_2O (3) + ε-CL (4) + PCL (5)] for the mass ratio CO_2: CH_2Cl_2: (H_2O + ε-CL + PCL) of 1:0.5:1. In this case, PCL had number average molar mass ($\bar{M}_n$) of 80,000 g·mol^{-1} and dispersion (D) of 1.74. Molar fractions related to the data presented in Table 17.

w_5'	x_1	x_2	x_3	x_4	x_5
0.00	0.607005	0.158489	0.000593	0.233913	0.000000
1.00	0.609203	0.157809	0.000589	0.232397	0.000002
2.49	0.611452	0.158754	0.000581	0.229209	0.000005
5.02	0.615517	0.159172	0.000570	0.224732	0.000010
7.50	0.618742	0.160350	0.000558	0.220334	0.000015
10.02	0.622501	0.161039	0.000547	0.215893	0.000020
12.48	0.626655	0.162139	0.000534	0.210647	0.000025
15.03	0.629928	0.163517	0.000522	0.206003	0.000030

w_5', denotes the mass fraction of PCL on in CO_2 and CH_2Cl_2 free-basis; x_1, molar fraction for the CO_2; x_2, molar fraction for the CH_2Cl_2; x_3, molar fraction for the H_2O; x_4, molar fraction for the ε-CL; x_5, molar fraction for the PCL.

Table 23 - Molar fractions for the multicomponent system [CO_2 (1) + CH_2Cl_2 (2) + H_2O (3) + ε-CL (4) + PCL (5)] for the mass ratio CO_2: CH_2Cl_2: (H_2O + ε-CL + PCL) of 1:1:1. In this case, PCL had number average molar mass ($\bar{M}_n$) of 80,000 g·mol^{-1} and dispersion (D) of 1.74. Molar fractions related to the data presented in Table 18.

w_5'	x_1	x_2	x_3	x_4	x_5
0.00	0.525195	0.272118	0.000512	0.202174	0.000000
1.00	0.527004	0.272111	0.000508	0.200376	0.000002
2.50	0.528332	0.273158	0.000502	0.198003	0.000004
5.03	0.530410	0.274818	0.000492	0.194172	0.000008
7.46	0.533517	0.275853	0.000482	0.190135	0.000013
10.09	0.536488	0.277355	0.000471	0.185669	0.000017
12.62	0.528690	0.279538	0.000460	0.181291	0.000022
14.94	0.542036	0.280320	0.000449	0.177169	0.000026

w_5', denotes the mass fraction of PCL on in CO_2 and CH_2Cl_2 free-basis; x_1, molar fraction for the CO_2; x_2, molar fraction for the CH_2Cl_2; x_3, molar fraction for the H_2O; x_4, molar fraction for the ε-CL; x_5, molar fraction for the PCL.

3.3 EFFECT OF WATER CONTENT ON THE HIGH PRESSURE CARBON DIOXIDE + ε-CAPROLACTONE + DICHLOROMETHANE + ε-CAPROLACTONE + POLY(ε-CAPROLACTONE) SYSTEM

Part of the results obtained in this chapter was presented in poster form at the **X Congresso Brasileiro de Termodinâmica Aplicada – CBTermo 2019**, (Nova Friburgo, RJ - 2019) Brazil and the other part was submitted in **The Journal of Chemical Thermodynamics** on November 27, 2019.

Abstract

Poly(ε-caprolactone) (PCL) is a biodegradable, bioresorbable and biocompatible polymer used in a wide variety of high-value biomedical, pharmaceutical, and food applications. This polymer can be produced by enzymatic ring-opening polymerization (e-ROP) of ε-caprolactone (ε-CL) in high pressure system. However, this process is strongly dependent on the amount of water (H_2O) initially present in ε-CL. High H_2O content in ε-CL provides the formation of polymers with low molar mass, whereas the opposite is noted for low H_2O concentrations. In this context, the aim of this work was to investigate the effect of H_2O content on the ε-CL at high pressure phase equilibrium data during the polymerization reaction of PCL for the multicomponent system [CO_2 (1) + CH_2CL_2 (2) + ε-CL (3) + PCL (4)]. The experiments were performed using a variable-volume view cell over the temperature range from 323.15 to 353.15 K, H_2O content in ε-CL of 0.04 and 0.18 wt% and mass ratios of CO_2:CH_2CL_2:(H_2O + ε-CL + PCL) of 1:0.5:1 and 1:1:1, and in order to understand the effect of H_2O content in the ROP of PCL it was performed trying to simulate the monomer conversion to polymer. In this study, experiments were carried out with PCL mass fractions (reaction conversion) of 0.0, 1.0, 2.5, 5.0, 7.5, 10.0, 12.5 and 15.0 wt%. Phase transitions of the type vapor-liquid type were verified, characterized by the formation of bubbles at the top of the equilibrium cell during the depressurizing of the system. Through the *P-T* diagram, the LCST behavior was observed and by *P-w* diagram, it was observed that higher water fraction in ε-CL required higher pressure to solubilize the system in a single phase.

Keywords: Biopolymer, lactones, phase equilibria, LCST

3.3.1 Introduction

PCL can be produced by enzymatic ring-opening polymerization (e-ROP) of ε-caprolactone (ε-CL) in supercritical carbon dioxide ($scCO_2$) medium. Literature shows that this process can be the same yield and molar mass that reactions were done in organic solvents and metallic catalysts (Comim et al., 2015; Thurecht et al., 2006). However, it is necessary to understand better the kinetic reactions and thermodynamic behavior of this process of polymerization. For example, an important point and understudied is the effect of H_2O initially content in ε-CL.

It is known that the H_2O is the initiator of the reaction of polymerization and it is directly connected with the molar mass of the final polymer, since high H_2O content in ε-CL provides the formation of polymers with low molar mass, whereas the opposite is noted for low H_2O concentrations

Analyzing literature, it is clear that there are only studies evaluating the simple systems as the binary systems (CO_2 + ε-CL) (Bergeot et al., 2004; Xu et al., 2003; Bender et al., 2010a) and (CO_2 + PCL) (Bang et al., 2019; de Paz et al., 2010), the ternary systems (CO_2 + CH_2CL_2 + ε-CL) (Mayer et al., 2019) and (CO_2 + CH_2CL_2 + PCL) (Kalogiannis and Panayiotou, 2006; Bender et al., 2010b), but there are no studies that evaluate the phase behavior of the multicomponent system (H_2O + CO_2 + CH_2CL_2 + ε-CL + PCL), with all chemical species presents during the polymerization reactions.

In this context, the objective of this work was to investigate the phase behavior in systems containing CO_2, CH_2CL_2, H_2O, ε-CL, and PCL investigating the influence of the H_2O content in the ε-CL in polymerization reactions of PCL for the mass relation of CO_2:CH_2CL_2:(H_2O + ε-CL + PCL) of 1:0.5:1 and 1:1:1, and temperature range from 323.15 to 353.15 K.

3.3.2 Experimental

3.3.2.1 Materials

PCL ($\overline{M}_n$ (g.mol^{-1}) 10000, dispersion 1.4), ε-CL (minimum purity of 97.0%) and CH_2CL_2 (minimum purity of 99.8%) were purchased from Sigma-Aldrich (United States of America). The CO_2 (minimum purity of 99.9%) was purchased from White Martins S.A. (Brazil). The ε-CL was dried by two different methods: (1) in a vacuum oven at 333.15 K and 0.01 MPa for 72 h, resulting in a H_2O content of 0.184 ± 0.030 %; (2) vacuum oven at 373.15 K and 0.01 MPa for 48 h, resulting in a H_2O content of 0.040 ± 0.001 %. The H_2O content was measured by the Karl Fischer Coulometric Titrator for moisture determination (HI-904 - HANNA® instruments). The other chemicals were used without further purification.

3.3.3 Phase equilibrium apparatus and procedure

The apparatus and the experimental procedure have been described in detail in the literature (Mayer et al., 2019). Figures 12 and 13 show the equilibrium cell and the schematic diagram of the experimental apparatus used in this work, respectively. Briefly, the experimental procedure is as follows. Initially a magnetic bar was inserted inside the equilibrium cell and precise quantities of the pure substances (CH_2CL_2, ε-CL and PCL) were weighed on an analytical balance (Shimadzu, Model AY220 with 0.0001 g accuracy) and inserted fast into the equilibrium cell that was quickly closed and connected to the high pressure system. Subsequently a known volume of CO_2 was added to the equilibrium cell by a syringe pump (Isco, Model 260D) which was maintained at 10.0 MPa and 280.15 K. After the addition of CO_2, the stirring of the solution was started with the help of the magnetic bar and the pressure of the system was gradually increased until a single phase. Finally the system heating has started. After complete stabilization of the system, the phase equilibrium (bubble point) measurements were initiated reducing the pressure, by programming in the syringe pump a pressure gradient, until the appearance of a second phase that was detected visually by the sapphire window. Each measure of the phase equilibrium point was repeated at least three times. In this evaluated system, only vapor–liquid equilibrium

(bubble point (VLE–BP)) was observed, characterized by the formation of a bubble at the top of the equilibrium cell during the depressurizing of the system.

In order to understand the effect of the H_2O initially contained in the ε-CL during a polymerization reaction equilibrium experiments were carried conducted maintaining the mass ratio between CO_2 and CH_2CL_2 fixed and the mass of ε-CL was varied in relation to PCL in the temperature range from 323.15 to 353.15 K. The variation of the mass of ε-CL in relation of PCL was performed trying to simulate the monomer conversion to polymer during the polymerization reaction. In this study, experiments were carried out PCL mass fractions (reaction conversion) of 0.0, 1.0, 2.5, 5.0, 7.5, 10.0, 12.5 and 15.0 wt%. This evaluation was performed with PCL of 10000 $g.mol^{-1}$ and ε-CL with 0.184% and 0.040% of H_2O.

3.3.4 Results and Discussion

Tables 15, 16, 24, and 25 show the experimental phase transition data measured for the multicomponent system [CO_2 (1) + CH_2CL_2 (2) + ε-CL (3) + PCL (4)] for the mass ratio CO_2: CH_2CL_2: (H_2O + ε-CL + PCL) of 1:0.5:1 and 1:1:1, at two different H_2O content in ε-CL, 0.040 and 0.184%, respectively. These tables show the equilibrium results in terms of temperature (*T*), pressure (*P*), experimental error for each condition measurements (*sd*) and the phase transition type (*TT*) of phase equilibrium (VL). In these tables, it can be seen that only transition of vapor–liquid type, characterized by the formation of vapor bubbles at the top of the equilibrium cell was observed. This same behavior was observed in the work of Mayer et al. (2019), which investigated the ternary system [CO_2(1) + CH_2CL_2(2) + ε-CL(3)] in the mass ratio CH_2CL_2: ε-CL of 0.5:1 and 1:1. In addition, it is observed that for this system phase transition pressures up to 16:50 MPa are verified. The molar fractions tables for the multicomponent system [CO_2 (1) + CH_2Cl_2 (2) + H_2O (3) + ε-CL (4) + PCL (5)] are present in 3.3.6 Supporting Information.

Table 24 - Phase equilibrium results for the quaternary system [CO_2 (1) + CH_2Cl_2 (2) + ε-CL (3) + PCL (4)] for the mass ratio CO_2: CH_2Cl_2: (H_2O + ε-CL + PCL) of 1:0.5:1. In this case the H_2O content in the ε-CL was 0.184 + 0.030 % and PCL had number average molar mass ($\overline{M}_n$) of 10000 g.mol^{-1} and dispersion (D) of 1.4.

T/K	*P*/MPa	*sd*/MPa	Transition type	*T*/K	*P*/MPa	*sd*/MPa	Transition type
w_3' = 100.00% (w_4' = 0.00%)				w_3' = 92.47% (w_4' = 7.53%)			
323.1	8.52	0.01	VLE-BP	323.15	8.95	0.02	VLE-BP
333.1	10.64	0.03	VLE-BP	333.15	10.98	0.02	VLE-BP
343.1	13.19	0.02	VLE-BP	343.15	13.57	0.03	VLE-BP
353.1	16.02	0.02	VLE-BP	353.15	16.27	0.03	VLE-BP
w_3' = 99.02% (w_4' = 0.98%)				w_3' = 89.87% (w_4' = 10.13%)			
323.1	8.71	0.02	VLE-BP	323.15	9.04	0.02	VLE-BP
333.1	10.80	0.01	VLE-BP	333.15	11.03	0.03	VLE-BP
343.1	13.35	0.03	VLE-BP	343.15	13.64	0.02	VLE-BP
353.1	16.12	0.02	VLE-BP	353.15	16.29	0.01	VLE-BP
w_3' = 97.50% (w_4' = 2.50%)				w_3' = 87.47% (w_4' = 12.53%)			
323.1	8.87	0.03	VLE-BP	323.15	9.13	0.01	VLE-BP
333.1	10.89	0.01	VLE-BP	333.15	11.10	0.03	VLE-BP
343.1	13.45	0.02	VLE-BP	343.15	13.69	0.01	VLE-BP
353.1	16.17	0.03	VLE-BP	353.15	16.39	0.01	VLE-BP
w_3' = 95.00% (w_4' = 5.00%)				w_3' = 84.90% (w_4' = 15.10%)			
323.1	8.91	0.02	VLE-BP	323.15	9.19	0.01	VLE-BP
333.1	10.95	0.02	VLE-BP	333.15	11.21	0.02	VLE-BP
343.1	13.51	0.03	VLE-BP	343.15	13.78	0.03	VLE-BP
353.1	16.21	0.03	VLE-BP	353.15	16.50	0.02	VLE-BP

w_3' denotes mass fraction of H_2O + ε-CL on in CH_2Cl_2 and CO_2 free-basis; w_4', denotes the mass fraction of PCL on in CO_2 and CH_2Cl_2 free-basis; VLE-BP, vapor-liquid-equilibrium type bubble point; *T*, system temperature; *P*, system pressure; sd, standard deviation.

Table 25 - Phase equilibrium results for the quaternary system [CO_2 (1) + CH_2Cl_2 (2) + ε-CL (3) + PCL (4)] for the mass ratio CO_2: CH_2Cl_2: (H_2O + ε-CL + PCL) of 1:1:1. In this case the H_2O content in the ε-CL was 0.184 + 0.030 % and PCL had number average molar mass ($\overline{M}_n$) of 10000 g.mol^{-1} and dispersion (D) of 1.4.

T/K	*P*/MPa	*sd*/MPa	Transition type	*T*/K	*P*/MPa	*sd*/MPa	Transition type
w_3' = 100.00% (w_4' = 0.00%)				w_3' = 92.52% (w_4' = 7.48%)			
323.1	7.02	0.03	VLE-BP	323.15	7.42	0.02	VLE-BP
333.1	8.09	0.01	VLE-BP	333.15	8.63	0.01	VLE-BP
343.1	9.50	0.01	VLE-BP	343.15	10.14	0.01	VLE-BP
353.1	10.93	0.02	VLE-BP	353.15	11.55	0.01	VLE-BP
w_3' = 99.00% (w_4' = 1.00%)				w_3' = 90.01% (w_4' = 9.99%)			
323.1	7.13	0.01	VLE-BP	323.15	7.47	0.01	VLE-BP
333.1	8.32	0.01	VLE-BP	333.15	8.77	0.02	VLE-BP
343.1	9.73	0.02	VLE-BP	343.15	10.32	0.01	VLE-BP
353.1	11.06	0.02	VLE-BP	353.15	11.68	0.02	VLE-BP
w_3' = 97.50% (w_4' = 2.50%)				w_3' = 87.52% (w_4' = 12.48%)			
323.1	7.23	0.02	VLE-BP	323.15	7.44	0.01	VLE-BP
333.1	8.46	0.01	VLE-BP	333.15	8.78	0.01	VLE-BP
343.1	9.85	0.01	VLE-BP	343.15	10.26	0.04	VLE-BP
353.1	11.33	0.02	VLE-BP	353.15	11.75	0.01	VLE-BP
w_3' = 94.95% (w_4' = 5.05%)				w_3' = 85.09% (w_4' = 14.91%)			
323.1	7.38	0.01	VLE-BP	323.15	7.43	0.01	VLE-BP
333.1	8.58	0.03	VLE-BP	333.15	8.75	0.01	VLE-BP
343.1	10.01	0.03	VLE-BP	343.15	10.25	0.01	VLE-BP
353.1	11.46	0.01	VLE-BP	353.15	11.69	0.01	VLE-BP

w_3' denotes mass fraction of H_2O + ε-CL on in CH_2Cl_2 and CO_2 free-basis; w_4', denotes the mass fraction of PCL on in CO_2 and CH_2Cl_2 free-basis; VLE-BP, vapor-liquid-equilibrium type bubble point; *T*, system temperature; *P*, system pressure; sd, standard deviation.

Figures 25 and 26 present the experimental phase equilibrium in *P-w* diagram forms. Through this diagram, it was observed that with the increase of H_2O content present in the ε-CL, higher pressures are required to solubilize the system. Moreover, the substitution of up to 15.0% of ε-CL by PCL does not change the system transition type. Another important point observed was that the variation of the fraction of PCL does not significantly change the system pressure and the highest-pressure variation occurred to 353.15 K and was of 0.50 and 0.56 MPa for ε-CL with 0.040 and 0.184% of H_2O, respectively.

Figure 25 - *P*-w_4' diagram for VLE-BP for the system [CO_2 (1) + CH_2Cl_2 (2) + ε-CL (3) + PCL (4)] for the mass ratio CO_2: CH_2Cl_2: (H_2O + ε-CL + PCL) of 1:0.5:1 in different H_2O content in ε-CL. Experimental data: 323:15 K: ■ (w_{H_2O}= 0.040) and □ (w_{H_2O}= 0.184); 333:15 K: ● (w_{H_2O}= 0.040) and ○ (w_{H_2O}= 0.184); 343:15 K: ▲ (w_{H_2O}= 0.040) and △ (w_{H_2O}= 0.184); 353:15 K: ▼ (w_{H_2O}= 0.040) and ▽ (w_{H_2O}= 0.184).

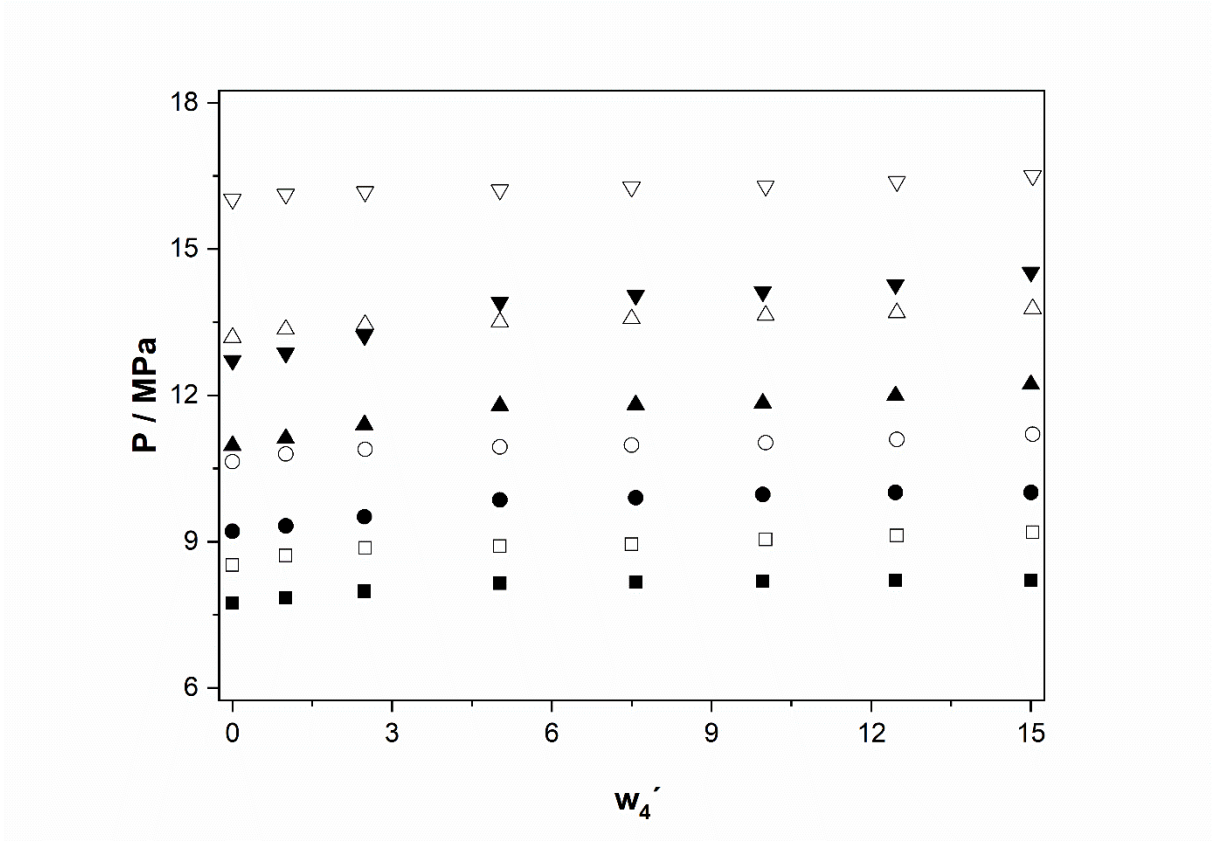

Source: Author himself.

Figure 26 - *P*-w_4' diagram for VLE-BP for the system [CO_2 (1) + CH_2Cl_2 (2) + ε-CL (3) + PCL (4)] for the mass ratio CO_2: CH_2Cl_2: (H_2O + ε-CL + PCL) of 1:0.5:1 in different H_2O content in ε-CL. Experimental data: 323:15 K: ■ (w_{H_2O}= 0.040) and □ (w_{H_2O}= 0.184); 333:15 K: ● (w_{H_2O}= 0.040) and ○ (w_{H_2O}= 0.184); 343:15 K: ▲ (w_{H_2O}= 0.040) and △ (w_{H_2O}= 0.184); 353:15 K: ▼ (w_{H_2O}= 0.040) and ▽ (w_{H_2O}= 0.184).

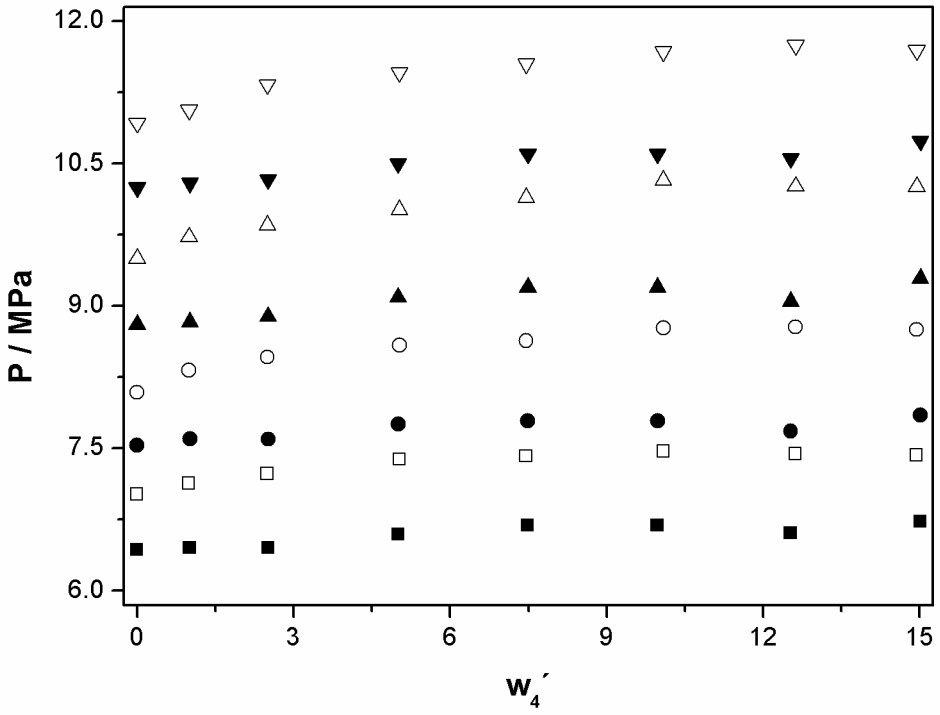

Source: Author himself.

Figure 27 shows a *P*-*T* diagram for multicomponent system [CO_2 (1) + CH_2CL_2 (2) + ε-CL (3) + PCL (4)] for 0.0% of the PCL to different H_2O content in ε-CL. In these diagrams, it is possible to observe again the effect of H_2O about the pressure of system, a higher amount of H_2O in the ε-CL, promote higher pressures to solubilize the system. Another important point observed in this diagram is the behavior Lower Critical Solution Temperature (LCST), where an increase in temperature results in the expansion of the system and thus higher pressures are required to solubilize the system in a single phase.

Figure 27 - *P-T* diagram for VLE-BP for the system [CO_2 (1) + CH_2Cl_2 (2) + ε-CL (3) + PCL (4)] for the mass ratio CO_2: CH_2Cl_2: (H_2O + ε-CL + PCL) of 1:0.5:1 and 1:1:1, and w_4' = 0.0%. Experimental data: 1:0.5:1: △ (w_{H_2O} = 0.040 %) and ▲ (w_{H_2O} = 0.184 %); 1:1:1: □ (w_{H_2O} = 0.040 %) and ■ (w_{H_2O} = 0.184).

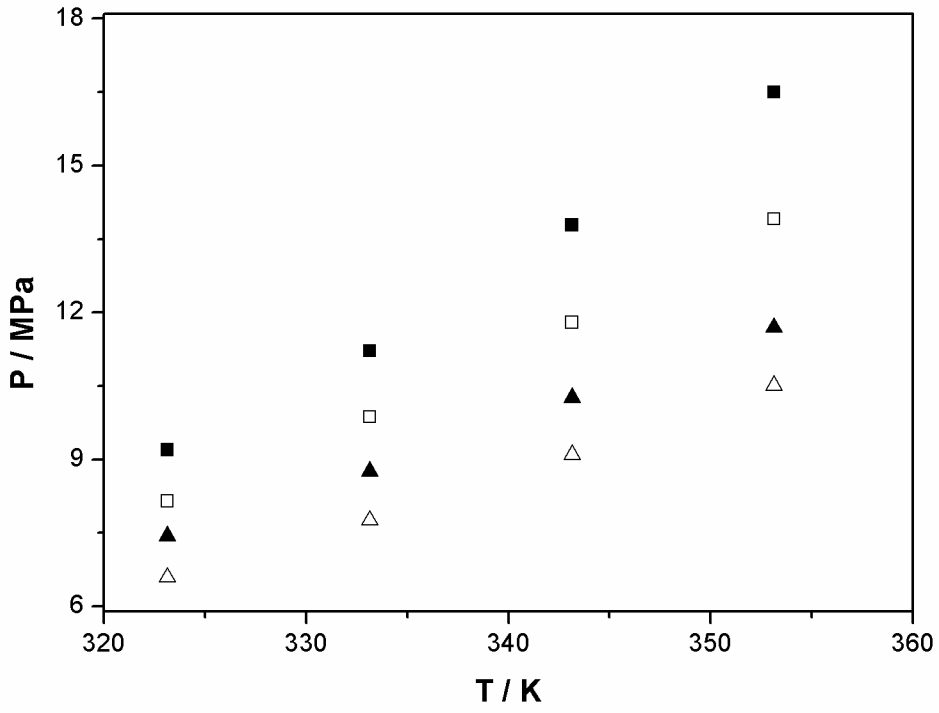

Source: Author himself.

Observing the data obtained in this work it is seen that water content in ε-CL affects considerably the system pressure, since the greater the amount of water in the ε-CL, greater the pressure required to solubilize a single-phase system. Thus, if the objective in the polymerization process is to achieve process optimization it is necessary to find the ideal amount of water, as besides affecting the final molar mass of the polymer it has a considerable effect on the system pressure.

3.3.5 Partial Conclusion

The phase behavior of the multicomponent system [CO_2 (1) + CH_2CL_2 (2) + ε-CL (3) + PCL (4)] was experimentally investigated in this work over the temperature range of 323.15 to 353.15 K in order to understand the effect of H_2O during the polymerization process by simulating various conversions (0.0 to 15.0 wt%). In all systems, there was observed only VLE–BP, resulting in phase transition pressures up to 11.69 MPa. Through the *P-w* diagrams, it was observed that how higher content of H_2O present in the ε-CL higher was the pressure required to solubilize the system. In addition, it was found that the pressures increased as the temperature increased, characterizing an LCST behavior, where an increase in temperature results in the expansion of the system and thus higher pressures are required to solubilize the system in a single phase. Lastly, the data reported in this work are important for the development and optimization of polymer synthesis in supercritical media, since it is through the understanding of the phenomena that occur at high pressures that the information necessary for the understanding of polymerization reaction systems.

3.3.6 Supporting Information

Table 26 - Molar fractions for the multicomponent system [CO_2 (1) + CH_2Cl_2 (2) + H_2O (3) + ε-CL (4) + PCL (5)] for the mass ratio CO_2: CH_2Cl_2: (H_2O + ε-CL + PCL) of 1:0.5:1. In this case, PCL had number average molar mass ($\overline{M}_n$) of 10,000 g·mol^{-1} and dispersion (D) of 1.40. . Molar fractions related to the data presented in Table 24.

w_5'	x_1	x_2	x_3	x_4	x_5
0.00	0.606740	0.157474	0.002721	0.233064	0.000000
0.98	0.607014	0.159902	0.002721	0.230376	0.000019
2.50	0.611070	0.157882	0.002666	0.228334	0.000048
5.00	0.614095	0.158965	0.002618	0.224225	0.000096
7.53	0.617792	0.159709	0.002566	0.219786	0.000146
10.13	0.619764	0.161399	0.002523	0.216114	0.000199
12.53	0.624665	0.162063	0.002459	0.210567	0.000246
15.10	0.628336	0.163215	0.002402	0.205749	0.000299

w_5', denotes the mass fraction of PCL on in CO_2 and CH_2Cl_2 free-basis; x_1, molar fraction for the CO_2; x_2, molar fraction for the CH_2Cl_2; x_3, molar fraction for the H_2O; x_4, molar fraction for the ε-CL; x_5, molar fraction for the PCL.

Table 27 - Molar fractions for the multicomponent system [CO_2 (1) + CH_2Cl_2 (2) + H_2O (3) + ε-CL (4) + PCL (5)] for the mass ratio CO_2: CH_2Cl_2: (H_2O + ε-CL + PCL) of 1:1:1. In this case, PCL had number average molar mass ($\overline{M}_n$) of 10,000 g·mol^{-1} and dispersion (D) of 1.40. . Molar fractions related to the data presented in Table 25.

w_5'	x_1	x_2	x_3	x_4	x_5
0.00	0.335144	0.332573	0.000611	0.331672	0.000000
1.00	0.333803	0.333353	0.000606	0.328916	0.003321
2.49	0.333803	0.333095	0.000598	0.324201	0.008304
5.05	0.332629	0.335699	0.000579	0.314355	0.016738
7.48	0.334147	0.333325	0.000566	0.307091	0.024872
9.99	0.333822	0.332938	0.000552	0.299958	0.033283
12.50	0.333462	0.333679	0.000536	0.290787	0.041536
14.90	0.333678	0.332136	0.000523	0.283846	0.049817

w_5', denotes the mass fraction of PCL on in CO_2 and CH_2Cl_2 free-basis; x_1, molar fraction for the CO_2; x_2, molar fraction for the CH_2Cl_2; x_3, molar fraction for the H_2O; x_4, molar fraction for the ε-CL; x_5, molar fraction for the PCL.

4 CONCLUSIONS

This work presented the study of the phase behavior of the ternary system [CO_2 + CH_2Cl_2 + ε-CL] at different CH_2Cl_2: ε-CL mass ratio (0.5:1, 1:1 and 2:1), and the study of the phase behavior of the quaternary system [CO_2 + CH_2Cl_2 + ε-CL + PCL] at different CO_2: CH_2CL_2: (H_2O + ε-CL + PCL) mass ratios (1:0.5:1 and 1:1:1), different molar mass of PCL, and different water contend in ε-CL. All phase equilibrium experiments were conducted employing the static synthetic method in a high pressure variable-volume view cell over the temperature range of 323.15 to 353.15 K.

Initially, it has been studied the ternary system [CO_2 + CH_2Cl_2 + ε-CL] in a wide overall composition range of CO_2, resulting in phase transition pressure up to 25.8 MPa. Experimental observations show that for all cases investigated an increase in CH_2Cl_2 to ε-CL mass ratio resulted in a decrease in pressure necessary to reach a single phase. Besides vapor-liquid equilibrium with bubble point transition presented for all systems, liquid-liquid, and vapor-liquid-liquid equilibrium transitions were observed for the system.

Subsequently, the quaternary system [CO_2 + CH_2Cl_2 + ε-CL + PCL] has been studied. In this system, the molar mass of PCL and water content in ε-CL were varied. In all system the phase transitions of vapor-liquid bubble point type were verified, in other words, the substitution of up to 15.0% of ε-CL by PCL does not change the system transition type. It was also noted that the molar mass of PCL does not change the pressure significantly for the temperatures and mass ratios analyzed, however, it was observed that with the increase of H_2O content present in the ε-CL, higher pressures are required to solubilize the system.

In all systems studied, it was observed the lower critical solution temperature (LCST) behavior phase, wherewith the increasing temperature, there is an increase in system pressure. This behavior is characteristic of the system involving lactones, solvents as $CHCl_3$ and CH_2Cl_2, and CO_2 as anti-solvent.

Regarding the thermodynamic modeling, it was observed that the PR EoS provided good performance for the ternary system, and the PC-SAFT EoS providing a good representation of the experimental phase equilibrium data for the system with polymers.

Finally, the data reported in this work are important for the development and optimization of polymer synthesis in supercritical fluid media, serving as the basis for the determination of the best conditions for the polymerization reactions, process optimization and, kinetic modeling.

4.1 SUGGESTIONS FOR FUTURE RESEARCH

- Investigate the phase behavior of the quaternary system [carbon dioxide + dichloromethane + ε-caprolactone + poly(ε-caprolactone)] in high pressure varying the mass ratio of dioxide carbon on the relation the dichloromethane and [ε-caprolactone + poly(ε-caprolactone)];
- Study the phase equilibrium for the ternary system [carbon dioxide + trichloromethane + ε-caprolactone] and the quaternary system [carbon dioxide + trichloromethane + ε-caprolactone + poly(ε-caprolactone)] in high pressure;
- Apply the mathematical model proposed by Johnson, Kundu and Beers (2011) for the polymerization reactions of poly(ε-caprolactone) by ring-opening via enzymatic catalysis to a high pressure system using the PC-SAFT EoS to model the thermodynamic behavior of the chemical species present in the reaction.

REFERENCES

AKCELRUD, L. **Fundamentos da ciência dos polímeros.** São Paulo: Malone, 2007. 308 p.

ALBUQUERQUE, M. C. C. et al. Aplicações de enzimas na síntese e na modificação de polímeros. **Química Nova**, v. 37, n. 4, p. 699-708, 2014.

ARAÚJO, C. B. K. et al. Phase behavior of Brazilian stock tank oil and carbon dioxide at reservoir conditions: experiments and thermodynamic modeling. **Journal of Petroleum Exploration and Production Technology**, v. 6, p. 39-44, 2016.

ATKINS, P; DE PAULA, J. **Físico-Química**. 8. ed. Rio de Janeiro: LTC, 2008. 589 p.

BANG, C.-H.; LEE, B.-S. Modeling phase behavior of poly(ε-caprolactone) solutions at high Pressure. **Fluid Phase Equilibria**, v. 483, p. 116-121, 2019.

BANKOVA, M. et al. Mass-selective lipase-catalyzed poly(ε-caprolactone) transesterification reactions. **Macromolecules, v. 35**, p. 6858-6866, 2002.

BARKER, J. A.; HENDERSON, D. Perturbation theory and equation of state for fluids: The square-well potential. **The Journal of Chemical Physics**, v. 47, p. 2856-2861, 1967a.

BARKER, J. A.; HENDERSON, D. Perturbation theory and equation of state for fluids. II. A successful theory of liquids, **The Journal of Chemical Physics**, v. 47, p. 4714-4721, 1967b.

BENDER, J. P. **Equilíbrio de fases de polímeros biocompatíveis e monômeros: dados experimentais e modelagem.** 2008. 131 f. Dissertação (Mestrado) – Curso Engenharia de Alimentos, Universidade Regional Integrada do Alto Uruguai e das Missões, Erechim, 2008.

BENDER, J. P. et al. Phase behavior of the ternary system [poly(ε-caprolactone) + carbon dioxide + dichloromethane]. **Journal of Chemical Thermodynamics**, v. 42, p. 229-233, 2010a.

BENDER, J. P. et al. Phase behavior of binary systems of lactones in carbon dioxide. **Journal of Chemical Thermodynamics**, v. 42, p. 48-53, 2010b.

BENDER, J. P. **Equilíbrio de fases do monômero L,L-lactídeo em altas pressões: dados experimentais e modelagem**. 2014. 201 f. Tese (Doutorado) – Curso Engenharia de Alimentos, Universidade Federal de Santa Catarina, 2014.

BERGEOT, V. et al. Anionic ring-opening polymerization of ε-caprolactone in supercritical carbon dioxide: parameters influencing the reactivity. **Journal of Supercritical Fluids**, v. 28, p. 249-261, 2004.

BISHT, K. S. et al. Enzyme-catalyzed ring-opening polymerization of ω-pentadecalactone. **Macromolecules**, v. 30, p. 2705-2711, 1997a.

BISHT, K. S. et al. Lipase-catalyzed ring-opening polymerization of trimethylene carbonate. **Macromolecules**, v. 30, p. 7735-7742, 1997b.

CANEVAROLO JÚNIOR, S. V. **Ciência dos polímeros: Um texto básico para tecnólogos e engenheiros.** 2. ed. São Paulo: Artliber Editora, 2002. 280 p.

CAROTHERS, W. H. Studies on polymerization and ring formation. I. An introduction to the general theory of condensation polymers. **Journal of the American Chemical Society**, v. 51, n. 8, p. 2548-2559, 1929.

CHAPMAN, W. G.; JACKSON, G.; GUBBINS, K. E. Phase equilibria of associating fluids Chain molecules with multiple bonding sites, **Molecular Physics**, v .65, n.5, p. 1057-1079, 1988.

CHAPMAN, W. G.; GUBBINS, K.E.; JACKSON, G.; RADOSZ, M. SAFT: Equation-of-state solution model for associating fluids. **Fluid phase Equilibria**, v. 52, p. 31-38, 1989.

CHAPMAN, W. G.; GUBBINS, K.E.; JACKSON, G.; RADOSZ, M. New reference equitation of state for associating liquids. **Industrial & Chemistry Engineering Research**, v. 29, p. 1709-1721, 1990.

CHEN, S.; RADOSZ, M. Density-tuned polyolefin phase equilibria. 1. Binary solutions of alternating poly(ethy1ene-propylene) in subcritical and supercritical propylene, 1-butene, and 1-hexene. Experiment and flory-patterson model. **Macromolecules**, v. 25, n. 12, p. 3089–3096, 1992.

CHEN, S. S.; KREGLEWSKI, A. Applications of the augmented van der Waals theory of fluids. I. **Berichte der Bunsengesellschaft für physikalische Chemie**, v. 81, p. 1048-1052, 1977.

COMIM, S. R. R. **Produção enzimática de poli(ε-caprolactona) em fluidos pressurizados**. 2012. 233 f. Tese (Doutorado) – Curso Engenharia de Alimentos, Universidade Federal de Santa Catarina, Florianópolis, 2012.

COMIM, S. R. R. et al. Enzymatic synthesis of poly(ε-caprolactone) in supercritical carbon dioxide medium by means of a variable-volume view reactor. **The Journal of Supercritical Fluids**, v. 79, p. 133-141, 2013.

COMIM, S. R. R. et al. Enzymatic synthesis of poly(ε-caprolactone) in liquefied petroleum gas and carbon dioxide. **Journal of Supercritical Fluids**, v. 96, p. 334-348, 2015.

COOPER, A. I. Polymer synthesis and processing using supercritical carbon dioxide. **Journal of Materials Chemistry**, v. 10, p. 207-234, 2000.

CORAZZA, M. L. et al. High pressure phase equilibria of the elated substances in the limonene oxidation in supercritical CO_2. **Journal of Chemical & Engineering Data**, v. 48, p. 354-358, 2003.

DARIVA, C. et al. Phase equilibria of polypropylene samples with hydrocarbon solvents at high pressures. **Journal of Applied Polymer Science**, v. 81, p. 3044-3055, 2001.

de PAZ, E. et al. Determination of phase equilibrium (solid-liquid-gas) in poly(ε-caprolactone)-carbon dioxide systems. **Journal of Chemical & Engineering Data**, v. 55, p. 2781-2785, 2010.

DENG, F.; GROSS, R. A. Ring-opening bulk polymerization of ε-caprolactone and trimethylene carbonate catalyzed by lipase Novozym 435. **International Journal of Biological Macromolecules**, v. 25, p. 153-159, 1999.

DOBRZYNSKI, P. Mechanism of ε-caprolactone polymerization and ε-caprolactone/trimethylene carbonate copolymerization carried out with $Zr(Acac)_4$. **Polymer**, v. 48, p. 2263-2279, 2007.

DONG, H. et al. Study on the enzymatic polymerization mechanism of lactone and the strategy for improving the degree of polymerization. **Journal of Polymer Science Part A: Polymer Chemistry**, v. 37, p. 1265-1275, 1999.

DOHRN, R.; BRUNNER, G. High pressure fluid-phase equilibria: Experimental methods and systems investigated (1988-1993). **Fluid Phase Equilibria**, v. 106, p. 213 – 282, 1995.

ESPINOSA, S. N. **Procesamiento supercrítico de produtos naturales modelado, análisis y optimización**. 2001. 312 f. Tese (Doutorado) – Curso Engenharia Química, Universidade Nacional del Sur, Buenos Aires, 2001.

FERNANDES, F. A. N.; LONA, L. M. F. **Introdução a modelagem de sistemas de polimerização.** São Carlos: Editora Booklink, 2004. 145 p.

FLORY, P. J. **Principles of polymer chemistry.** New York: Cornell University Press, 1953. 688 p.

FOENARI, R. E.; ALESSI, P.; KIKIC, I. High pressure fluid phase equilibria: Experimental methods and systems investigated (1978-1987). **Fluid Phase Equilibria**, v**.** 57, p. 1-33, 1990.

DOHRN, R.; BRUNNER, G. High pressure fluid-phase equilibria: Experimental methods and systems investigated (1988-1993). **Fluid Phase Equilibria**, v. 106, p. 213–282, 1995.

GIRARDI, D. G. L. et al. High pressure phase equilibrium data for the ternary system containing carbon dioxide, chloroform and ε-caprolactone. Unpublished work.

GONZALEZ, A. V.; TUFEU, V.; SUPRA, P. High pressure vapor−liquid equilibrium for the binary systems carbon dioxide + dimethyl sulfoxide and carbon dioxide + dichloromethane. **Journal of Chemical & Engineering Data**, v. 47, p. 492-495, 2002.

GROSS, J; SADOWSKI, G. Perturbed-chain SAFT: an equation of state based on a perturbation theory for chain molecules. **Industrial & Engineering Chemistry Research**, v. 40, p. 1244-1260, 2001.

GROSS, J; SADOWSKI, G. Application of the perturbed-chain SAFT equation of state to associating systems. **Industrial & Engineering Chemistry Research**, v. 41 p. 5510-5515, 2002.

HENDERSON, L. A. et al. Enzymatic-catalyzed polymerization of ε-caprolactone: Effects of initiator on product structure, propagation kinetics, and mechanism. **Macromolecules**, v. 29, p. 7759-7766, 1996.

HUANG, S. H.; RADOSZ, M. Equation of state for small, large, polydisperse, and associating molecules. . **Industrial & Engineering Chemistry Fundamentals**, v. 29, p. 2284-2294, 1990.

JOHNSON, P. M.; KUNDU, S.; BEERS, K. L. Modeling enzymatic kinetic pathways for ring-opening lactone polymerization. **Biomacromolecules**, v. 12, p. 3337-3343, 2011.

KALOGIANNIS, C. G.; PANAYIOTOU, C. G. Bubble and cloud points of the systems poly(ε-caprolactone) + carbon dioxide + dichloromethane or chloroform. **Journal of Chemical & Engineering Data**, v. 51, p. 107-111, 2006.

KHANSARY, M. A.; SANI, H. Using genetic algorithm (GA) and particle swarm optimization (PSO) methods for determination of interaction parameters in multicomponent systems of liquid–liquid equilibria. **Fluid Phase Equilibria**, v. 365, p. 141-145, 2014.

KIAO, R. S. S.; CARUTHERS, J. M.; CHAO, K. C. Polymer chain of rotators equation of state. **Industrial & Engineering Chemistry Research**, v. 35, p. 1446-1455, 1996.

KONTOGEORGIS, G. M. et al. Prediction of liquid-liquid equilibrium for binary polymer solutions with simple activity coefficient models. **Industrial & Engineering Chemistry Research**, v. 34, n. 5, p. 1823-1834, 1995.

KULPREECHANAN, N.; BUNAPRASERT, T.; RANGKUPAN, R. Electrospinning of polycaprolactone in dichloromethane/dimethylformamide solvent system. **Advanced Materials Research**, v. 849, p. 337-342, 2014.

KUMAR, A.; GROSS, R. A. Candida antarctica lipase B catalyzed polycaprolactone synthesis: Effects of organic media and temperature. **Biomacromolecules**, v.1, p. 133-138, 2000.

KUNDU, S. et al. Continuous flow enzyme-catalyzed polymerization in a microreactor. **Journal of the American Chemical Society**, v. 133, p. 6006-6011, 2011.

LABET, M.; THIELEMANS, W. Synthesis of polycaprolactone: a review. **Chemical Society Reviews**, v. 38, p. 3484-3504, 2009.

LAZZARONI, M. J. et al. High pressure vapor−liquid equilibria of some carbon dioxide + organic binary systems. **Journal of Chemical & Engineering Data**, v. 50, p. 60-65, 2005.

LAZZÚS, J. A. Optimization of activity coefficient models to describe vapor–liquid equilibrium of (alcohol + water) mixtures using a particle swarm algorithm. **Computes & Mathematics with Applications**, v. 60, p. 2260-2269, 2010.

LEE, C. S. et al. Multinuclear NMR study of enzyme hydration in an organic solvent. **Biotechnology and Bioengineering**, v. 57, n. 6, p. 686-693, 1998.

LICENCE, P. et al. Chemical reactions in supercritical carbon dioxide: from laboratory to commercial. **Green Chemistry**, v. 5, p. 99–104, 2003.

LINDVIG, T; MICHELSEN, M. L; KONTOGEORGIS, G. M. Liquid-liquid equilibria for binary and ternary polymer solutions with PC-SAFT. **Industrial & Engineering Chemistry Research**, v. 43, p. 1125-1132, 2004.

LOEKER, F. C. et al. Enzyme-catalyzed ring-opening polymerization of ε-caprolactone in supercritical carbon dioxide. **Macromolecules**, v. 37, p. 2450-2453, 2004.

MACDONALD, R. T. et al. Enzyme-catalyzed ε-caprolactone ring-opening polymerization. **Macromolecules,** v.28, p. 73-78, 1995.

MANDELA, N. **Lighting your way to a better future.** Planetarium. University of the Witwatersrand, Johannesburg, South Africa. 16th July 2003.

MAYER, D. A. et al. High pressure phase equilibrium data for the ternary system containing carbon dioxide, dichloromethane, and ε‑caprolactone. **Journal of Chemical & Engineering Data**, v. 64, p. 2036-2044, 2019.

MEI, Y.; KUMAR, A.; GROSS, R. A. Probing water-temperature relationships for lipase-catalyzed lactone ring-opening polymerizations. **Macromolecules,** v. 35, p. 5444-5448, 2002.

MEI, Y.; KUMAR, A.; GROSS, R. Kinetics and mechanism of Candida antarctica lipase B catalyzed solution polymerization of ε-caprolactone. **Macromolecules**, v. 36, p. 5530-5536, 2003.

NASCIMENTO, J. C. **Determinação experimental de dados de equilíbrio de fases da reação de polimerização da poli(ω-pentadecalactona) a alta pressões.** 2019. 79 f. Dissertação (Mestrado) – Curso Engenharia de Alimentos, Curso Engenharia de Alimentos, Universidade Federal de Santa Catarina, Florianópolis, 2019.

NDIAYE, P. M. et al. Phase behavior of isotactic polypropylene/C4-solvents at high pressure. Experimental data and SAFT modeling. **Journal of Supercritical Fluids**, v. 21, p. 93-103, 2001.

NDIAYE, P. M. **Equilíbrio de Fases de óleos vegetais e de biodiesel em CO_2 propano e n-butano.** 2004. 155 f. Tese (Doutorado) – Curso Engenharia Química, Universidade Federal do Rio de Janeiro, Rio de Janeiro, 2004.

NIST. National Institute of Standards and Technology. Disponível em: http://webbook.nist.gov/chemistry/fluid/. Acesso em: 13 dez. 2018.

NUNES DA PONTE, M. Phase equilibrium-controlled chemical reaction kinetics in high pressure carbon dioxide. **Journal of Supercritical Fluids**, v. 47, n. 3, p. 344-350, 2009.

ODIAN, G. **Principles of polymerization.** 4ª ed. New York: John Wiley & Sons, 2004. 832 p.

OLIVEIRA, J. V.; DARIVA, C.; PINTO, J. C. High pressure phase equilibria for polypropylene−hydrocarbon systems. **Industrial & Engineering Chemistry Research**, v. 39, p. 4627-4633, 2000.

PENG, D. Y.; ROBINSON, D. B. A new two-constant equation of state. **Industrial & Engineering Chemistry Fundamentals**, v. 15, p. 59-64, 1976.

POLING, B, E.; PRAUSNITZ, J. M.; O'CONNELL, J. P. **The properties of gases and liquids**. 5 ed. New York: McGraw-Hill Education, 2000.

PRAUSNITZ, J. M.; LICHTENTHALER, R. N.; AZEVEDO, E. G. **Molecular thermodynamics of fluid-phase equilibria.** New Jersey: Prentice-Hall, 1999.

REBELATTO, E. A. et al. High pressure phase equilibrium data for systems containing carbon dioxide, ω-pentadecalactone, chloroform and water. **Journal of Chemical Thermodynamics**, v. 122, p. 125-132, 2018a.

REBELATTO, E. A. et al. Phase behavior of pseudoternary system (carbon dioxide + ω-pentadecalactone + dichloromethane) at different dichloromethane to ω-pentadecalactone mass ratios. . **Journal of Chemical Thermodynamics**, v. 126, p. 55-62, 2018b.

REBELATTO, E. A. **Equilíbrio de fases de sistemas contendo dióxido de carbono, ω-pentadecalactona e cossolventes em altas pressões: dados experimentais e modelagem termodinâmica**. 2018. 165 f. Tese (Doutorado) – Curso Engenharia de Alimentos, Universidade Federal de Santa Catarina, Florianópolis, 2018.

REID, R C.; PRAUSNITZ, J. M. POLING, B. E. **The properties of gases and liquids,** 4 ed. Singapura: McGraw-Hill, 1987.

ROSSBERG, M. et al. **Choromethanes, in ulmann's encyclopedia of industrial**. 3 ed. Weinheim: Chemistry Wiley, 2012.

ROWLINSON, J. S.; SWINTON, F. L., **Liquids and Liquids Mixtures**. London: Butterworth Scientific, 1982.

SANTOS, T. M. M. et al. High pressure phase equilibrium data for carbon dioxide, methyl methacrylate and poly(dimethylsiloxane) systems. **Journal of Supercritical Fluids**, v. 143, p. 346-352, 2019.

SCOTT, R. L.; VAN KONYNENBURG, P. H. Static properties of solutions. van der Waals and related models for hydrocarbon mixtures. **Discussions of the Faraday Society**, v. 52, p. 87-97, 1970.

SHIN, M. S.; LEE, J. H.; KIM, H. Phase behavior of the poly(vinyl pyrrolidone) + dichloromethane + supercritical carbon dioxide system. **Fluid Phase Equilibria**, v. 272, p. 42-46, 2008.

SHIRONO, K.; MORIMATSU, T.; TAKEMURA, F. Gas solubilities (CO_2, O_2, Ar, N_2, H_2, and He) in liquid chlorinated methanes. **Journal of Chemical & Engineering Data**, v. 53, p. 1867-1871, 2008.

SMITH, J. M.; VAN NESS, H. C.; ABBOTT, M. M. **Introdução à Termodinâmica da Engenharia Química.** 7ª ed. Rio de Janeiro: LTC, 2007.

SY-SIONG-KIAO, R.; CARUTHERS, J. M.; CHAO, K. C. Polymer chain-of-rotators equation of state. **Industrial & Engineering Chemistry Fundamentals**, v. 35, p. 1446-1455, 1966.

THURECHT, K. J. et al. Kinetics of enzymatic ring-opening polymerization of ε-caprolactone in supercritical carbon dioxide. **Macromolecules**, v. 39, p. 7967-7972, 2006.

TSIVINTZELIS, I. et al. Phase compositions and saturated densities for the binary systems of carbon dioxide with ethanol and dichloromethane. **Fluid Phase Equilibria**, v. 224, p. 89-96, 2004.

UYAMA, H.; KOBAYASHI, S. Enzymatic ring-opening polymerization of lactones catalyzed by lipase. **Chemistry Letters**, v. 22, n. 7, p. 1149-1150, 1993.

UYAMA, H. et al. Lipase-catalyzed ring-opening polymerization of 12-dodecanolide. **Macromolecules**, v. 28, p. 7046-7050, 1995.

UYAMA, H.; TAKEYA, K.; KOBAYASHI, S. Enzymatic ring-opening polymerization of lactones to polyesters by lipase catalyst: Unusually high reactivity of macrolides. **Bulletin of the Chemical Society of Japan**, v. 68, p. 56-61, 1995.

VAN KONYNENBURG, P. H.; SCOTT, R. L. Critical lines and phase equilibria in binary van der Waals mixtures. **Philosophical Transactions of the Royal Society A: Mathematical, Physical and Engineering Sciences**, v. 298, n. 1442, p. 495-540, 1980.

VENERAL, J. G. et al. Continuous enzymatic synthesis of polycaprolactone in packed bed reactor using pressurized fluids. **Chemical Engineering Science**, v. 175, p. 139-147, 2018.

VIEIRA DE MELO, S. A. B. **Desterpenação do Óleo Essencial de Laranja Usando CO_2 Supercrítico**. 1997. Tese (Doutorado), - Curso de Engenharia Química, Universidade Federal do Rio de Janeiro, Rio de Janeiro, 1997.

VONDERHEIDEN, F. H.; ELDRIDGE, J. W. The system carbon dioxide-methylene chloride. Solubility, vapor pressure, liquid density, and activity coefficients. **Journal of Chemical & Engineering Data**, v. 48, p. 20-21, 1963.

XU, Q.; WAGNER, K. -D.; DAHMEN, N. Vapor–liquid equilibria of different lactones in supercritical carbon dioxide. **Journal of Supercritical Fluids**, v. 26, p. 83-93, 2003.

WERTHEIM, M. S. Fluids with highly directional attractive forces. I. Statistical thermodynamics. **Journal of Statistical Physics**, v. 35, p 19-34, 1984a.

WERTHEIM, M. S. Fluids with highly directional attractive forces. II. Thermodynamic perturbation theory and integral equations. **Journal of Statistical Physics**, v. 35 p. 35-47, 1984b.

WERTHEIM, M. S. Fluids with highly directional attractive forces. III. Multiple attraction sites. **Journal of Statistical Physics**, v. 42, p. 459-476, 1986a.

WERTHEIM, M. S. Fluids with highly directional attractive forces. IV. Equilibrium polymerization. **Journal of Statistical Physics**, v. 42, p. 477-492, 1986b.

WERTHEIN, M. S. Thermodynamic perturbation-theory of polymerization**. Journal of Chemical Physic,** v. 87, p. 7323-7331, 1987.